Glacial history of the Northeast Greenland continental shelf and adjacent waters revealed by hydro-acoustic data

Dissertation
zur Erlangung des akademischen Grades Dr. rer. nat.
vorgelegt dem Fachbereich Geowissenschaften
der Universität Bremen im Dezember 2015
von Jan Erik Arndt

1. Gutachter: Prof. Dr. Wilfried Jokat
2. Gutachter: Prof. Dr. Wolfgang Bach

Datum des Dissertationskolloquiums: 31. März 2016

Universität Bremen

ALFRED-WEGENER-INSTITUT
HELMHOLTZ-ZENTRUM FÜR POLAR-
UND MEERESFORSCHUNG

Erklärung

Hiermit versichere ich,

Jan Erik Arndt,

wohnhaft in der Bismarckstr. 35 in 27570 Bremerhaven,

dass ich

1. die Arbeit ohne unerlaubte fremde Hilfe angefertigt habe,

2. keine anderen als die von mir angegebenen Quellen und Hilfsmittel benutzt habe und

3. die den benutzten Werken wörtlich oder inhaltlich entnommenen Stellen als solche kenntlich gemacht habe.

_____________________, den ________

_ _ _ _ _ _ _ _ _ _ _ _ _ _ _

Zusammenfassung

Die großen Eisschilde in den Polarregionen reagieren auf ein sich wandelndes Klima durch Wachstum und Schmelze. Diese Eisschildveränderungen haben globalen Einfluss, wie zum Beispiel durch die Veränderungen des Meeresspiegels, und beschränken sich nicht nur auf die Polarregionen. Im letzten Jahrhundert hat sich die Durchschnittstemperatur der Erde kontinuierlich erhöht. Direkte präzise Beobachtungen der Eisschild-Massenbilanzen reichen in der Regel nur einige Jahrzehnte zurück. Dies erschwert es zwischen kurzfristigen Fluktuationen und langfristigen, vom Klimawandel verursachten Veränderungen der Eisschilde zu unterscheiden. Folglich ist es wichtig zu verstehen, wie die Eisschilde in der Vergangenheit auf ähnliche Klimaveränderungen reagiert haben, um dieses Wissen auf die Gegenwart und Zukunft übertragen zu können.

Zur Zeit der letzten maximalen Ausdehnung der Eisschilde, vor 26.500-19.000 Jahren, erstreckte sich der grönländische Eisschild bis auf den heute von Ozean bedeckten Kontinentalschelf. Die exakte Ausdehnung des Eisschildes auf dem Schelf ist jedoch bisher unbekannt. In der Bathymetrie des Schelfs sind morphologische Strukturen zurückgeblieben, die von diesem ausgedehnten Eisschild geformt wurden. Diese glazial erzeugten morphologischen Strukturen ermöglichen es aufschlußreiche Informationen über die ehemalige Eisausdehnung, die Struktur des Eisflusses, sowie dessen Rückzugsverhalten nach Ende der letzten Eiszeit abzuleiten. Für die Erfassung dieser Strukturen ist die Kenntnis der Bathymetrie in ausreichender Auflösung erforderlich, die mittels hydro-akustischer Systeme gewonnen werden kann.

Die meist dichte Meereisbedeckung in den Gewässern vor Nordostgrönland verhindert die Datenerfassung über weite Teile des Jahres und erfordert den Einsatz von Eisbrechern. Trotz dieser erschwerten Bedingungen zur Datenerfassung, ist es wichtig die glaziale Vergangenheit Nordostgrönlands zu rekonstruieren da etwa 20% des grönländischen Eisschildes über dieses Gebiet abfließen. Der Großteil hiervon fließt über den Nordostgrönlandeisstrom ab, der etwa 700 km in das Landesinnere hereinreicht und somit der größte Eisstroms Grönlands ist. Auch wenn der Kontinentalschelf in dieser Region der breiteste ganz Grönlands ist, gab es in diesem Gebiet bisher aufgrund der mangelnden Datengrundlage nur wenige Untersuchungen zur Eisschildkonstellation während des letzten glazialen Maximums.

In dieser Arbeit werden hydro-akustische Daten, die seit den 1980er Jahren in den Gewässern vor Nordostgrönland erfasst wurden, auf glaziale morphologische Strukturen untersucht um daraus die vergangene Eisschildkonstellation abzuleiten. Durch diese Untersuchung wird erstmalig die Ausdehnung des grönländischen Eisschildes über den Großteil des Kontinentalschelfs und in mindestens zwei Trögen bis hin zur Schelfkante direkt nachgewiesen. Die rekonstruierten Fließrichtungen der Eisströme legen den Schluß nahe, dass sich auf den flacheren Regionen des Kontinentalschelfs lokale marine Eisdome bildeten. Der anschließende Rückzug des Eises erfolgte unterschiedlich schnell in verschiedenen Teilen des Schelfs. In Phasen des Eisschildrückgangs trieben Eisberge mit einem Tiefgang von mehr als einem Kilometer vom Arktischen Ozean in den Nordatlantik. Diese Ergebnisse liefern neue Rahmenbedingungen, die unser Verständnis der vergangenen Eisschildkonstellation in der Arktis verbessern.

Abstract

Ice Sheet responses to a changing climate are not only effecting the polar regions but have global implications, i.e. sea level change. During the last century, a steady increase of average global temperatures has been observed. Accurate direct observations of ice sheet responses related to this increase are typically only available in timescales of decades. This results in difficulties to distinguish between short term ice mass fluctuations and long-term changes that may correspond to climate change. Subsequently, to understand ice sheet behavior in a changing climate and to enable us to predict future responses, it is necessary to understand how ice sheets have responded in the past.

During the last glacial maximum, 26,500-19,000 years before present, the entire Greenland Ice sheet extended onto the continental shelf that today is covered by the ocean. However, its extent on the shelf is still not resolved. The bathymetry of the shelf reveals morphologic remnants that have been created by this extensive ice sheet. These remnants, also referred to as submarine glacial landforms, allow us to infer the extent of the past Greenland Ice Sheet as well as giving information of its ice stream pathways and its retreat behavior in the succession of the last ice age. However, hydro-acoustic data acquisition is needed to reveal the bathymetry of the shelf in sufficient resolution to resolve submarine glacial landforms.

In Northeast Greenland, data acquisition is impeded by harsh sea-ice conditions during most parts of the year and icebreakers are required to operate in this region. Nevertheless, the reconstruction of Northeast Greenland’s glacial history is important as about 20% of the Greenland Ice Sheet is drained here. Most of this ice discharge is operated via the Northeast Greenland Ice Stream that reaches about 700 km inland and therefore is the largest ice stream of Greenland. The continental shelf of Northeast Greenland is the broadest shelf of Greenland but so far only few investigations shed light on the past ice sheet system, due to the limited availability of hydro-acoustic data.

In this thesis, I investigate hydro-acoustic data that have been acquired since the 1980s in the waters offshore Northeast Greenland for submarine glacial landforms that are used to derive the setting of the past ice sheet system. As a result, first direct marine evidence is provided that the Greenland Ice Sheet covered the majority of the continental shelf in Northeast Greenland and at least in two troughs extended to the shelf edge. Reconstruction of ice stream pathways suggests that local marine ice domes have resided on shallower parts of the shelf. The ice sheet retreat was spatially variable on the shelf during deglaciation. Large icebergs, reaching drafts of more than one kilometer, drifted from the Arctic Ocean to the North Atlantic continuously during deglaciation. These results deliver new constraints to improve our picture of the past Arctic ice sheet setting and development.

Contents

Abbreviations

AUV	autonomous undersea vehicle
AWI	Alfred Wegener Institute, Helmholtz Centre for Polar and Marine Research
B.P.	before present
BCFS	Bathymetric Chart of the Fram Strait
CTD	Conductivity-Temperature-Depth
DBM	digital bathymetric model
EGC	East Greenland Current
GIMP	Greenland Ice Mapping Project
GMT	Generic Mapping Tools
GZW	grounding zone wedge
HR	Hovgaard Ridge
IBCAO	International Bathymetric Chart of the Arctic Ocean
IBCSO	International Bathymetric Chart of the Southern Ocean
kHz	kilohertz
kyrs	kiloyears
LGM	Last Glacial Maximum
Ma	million ages
MIS	marine isotope stage
NADW	North Atlantic Deep-Water
NEG	Northeast Greenland
p.s.u.	practical salinity units
R/V	Research Vessel

List of Tables

List of Figures

1. Introduction

1.1 Motivation

The cryosphere, including the Greenland Ice Sheet, responds to changes of the global climate. The effects of these responses are not restricted to the polar regions, but have world-wide implications. Mass loss of the ice sheets is identified as a major contributor to sea level change [*Church et al.*, 2011]. By delivering an additional source of freshwater, ice discharge is influencing the deep water formation in polar regions, the main driver of the global thermohaline circulation which is essential for the global latitudinal heat exchange [*Broecker*, 2010]. The Greenland Ice Sheet experienced increased ice loss in a warming climate within the last two decades [*Vaughan et al.*, 2013]. However, these changes need to be examined in the context of past climate changes and their corresponding responses of the cryosphere [*Vaughan et al.*, 2013]. Reconstructing the past Greenland Ice Sheet extent and its development, hence, is crucial to understand past ice sheet responses and is needed to validate ice sheet models that estimate future responses.

Ice sheets are modulating the landscape by erosion and deposition of sediments. This altered landscape is left behind after ice sheet retreat. Probably the most impressive and well-known terrestrial example of such landscapes are fjords carved out by fast flowing outlet glaciers during long periods of glaciation. In the period of the last glacial maximum (LGM), 26,500-19,000 years before present, the Greenland Ice Sheet extended beyond the modern day coastline of Greenland [*Funder et al.*, 2011]. Subsequently, morphologic remnants produced by the LGM ice sheet are still present in the bathymetry of the Greenland continental shelves, where they are better protected against erosion compared to the terrestrial realm. These remnants, also referred to as submarine glacial landforms, can provide information on the glacial system that was active during their formation [e.g., *Jakobsson et al.*, 2014 and references therein; *Livingstone et al.*, 2012].

High resolution bathymetric data can be acquired with hydro-acoustic methods to assess these submarine glacial landforms. Despite modern icebreaker capabilities, the bathymetry of large areas in polar regions remain poorly resolved, due to their remoteness and inaccessibility caused by harsh sea-ice conditions. However, some of these regions are most relevant to deliver a comprehensive picture of the past glacial system and its responses to climate changes.

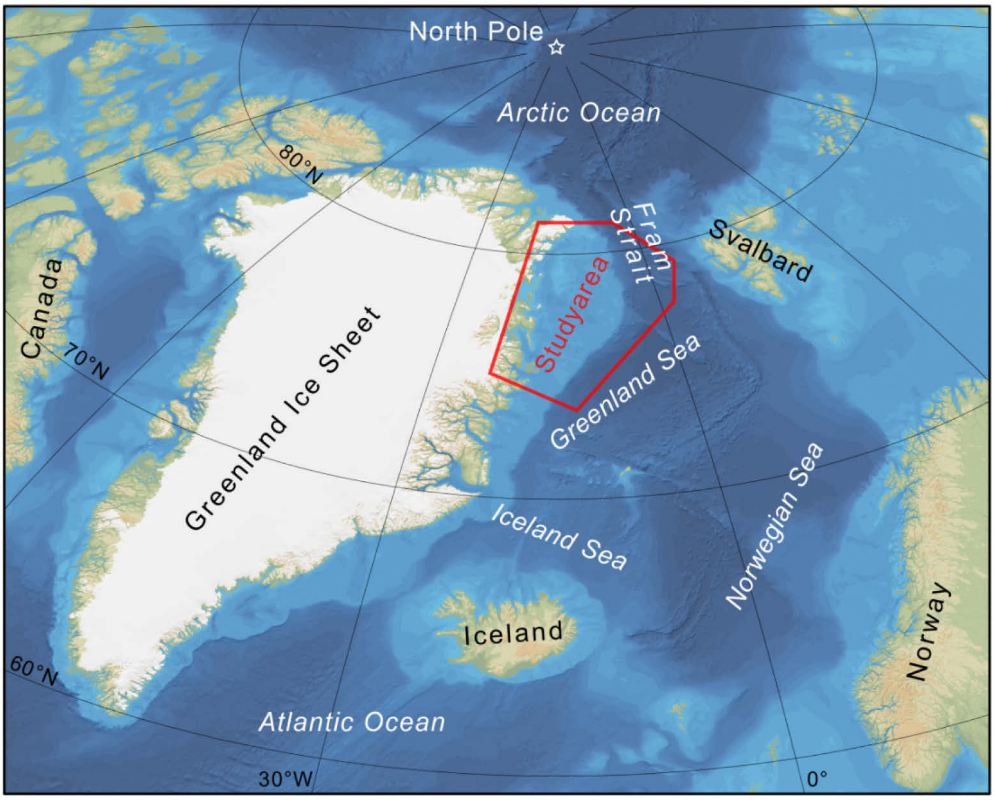

Figure 1.1: Location map of the study area and geographical locations, based on GEBCO_14 [*Weatherall et al.*, 2015]

The waters offshore Northeast Greenland (NEG) are such a remote and hardly accessible area which, nevertheless, is a key region to observe the past glacial system (Fig 1.1). High resolution bathymetric data have been acquired in this region predominantly with R/V Polarstern since the 1980s, but only few investigations on the submarine glacial landforms have been conducted on this data. In recent years, this data set has increased by a number of additional R/V Polarstern cruises. A joint investigation of the available data promised to significantly increase the understanding on the past glacial system that has been active in this region.

1.2 The Northeast Greenland continental shelf and adjacent waters

The study area covers the NEG continental shelf and parts of the Fram Strait between the latitudes 74°N and 81°N (Fig. 1.1). Bathymetric compilations, created before this thesis, model the continental shelf with irregular undulating topography, pre-dominantly in a depth range between 400 to 100 m, and show coarsely defined cross-shelf troughs (Fig. 1.2) [*Jakobsson et al.*, 2012b]. Here, the Greenland continental shelf reaches its maximum width of more than 300 km. Subsequently, this broad shelf represents the largest possible area for oscillation of the Greenland Ice Sheet. The continental shelf consists of sediments that in parts are more than 13 km thick [*Hamann et al.*, 2005]. These sediments filled basins and covered ridges that where formed during the complex breakup of the North Atlantic Ocean and the Fram Strait including various oblique spreading processes [*Engen et al.*, 2008]. The sediment transport since ~7 Ma is assumed to be pre-dominantly facilitated by ice streams [*Berger and Jokat*, 2009].

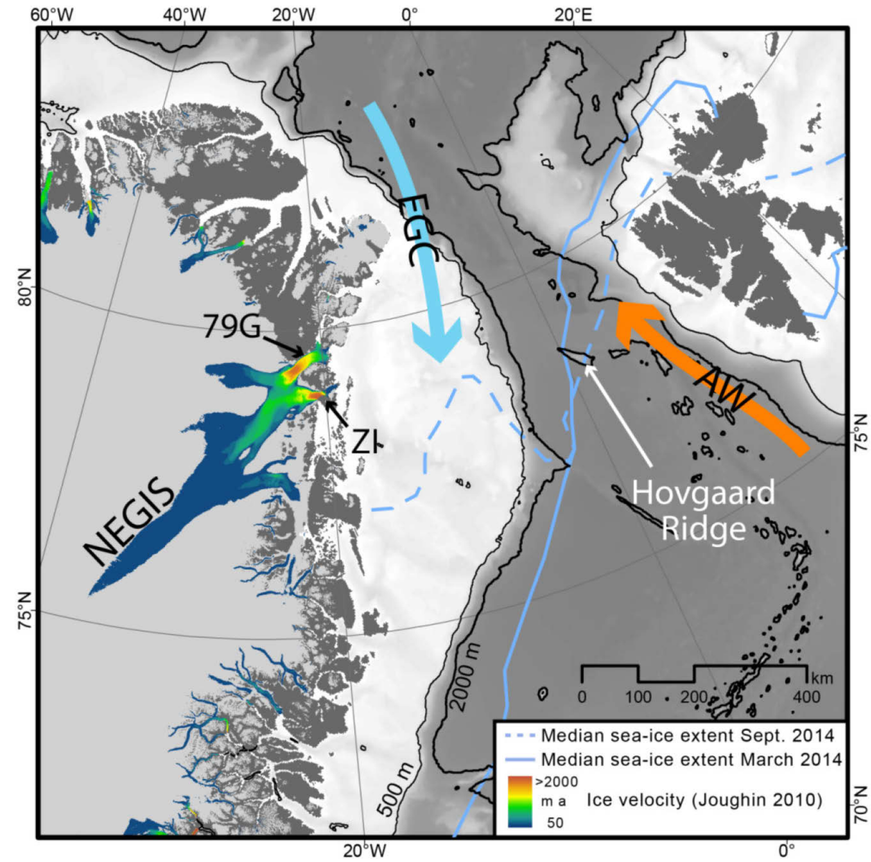

Figure 1.2: Map of the study area with glacial setting, major oceanographic currents, median sea-ice extent and geographical locations; Bathymetry from IBCAO V3.0 [*Jakobsson et al.*, 2012b]; AW=Atlantic Water, EGC=East Greenland Current, NEGIS=Northeast Greenland Ice Stream, 79G=79°-Glacier, ZI=Zachariae Isstrøm

The Fram Strait, located between NEG and Svalbard, has an average depth of about 2500 m. In the center of Fram Strait, Hovgaard Ridge is the shallowest undersea feature with its crest reaching 1180 m depth. The Fram Strait is the only deep-water connection of the Arctic Ocean to the world's oceans. In the eastern part of Fram Strait, warm Atlantic water flows into the Arctic Ocean and keeps the waters west of Svalbard free of sea ice for longer periods (Fig. 1.2). In contrast, on its western side cold Arctic water, including sea ice from the Arctic Ocean, is exported southward within the East Greenland Current (EGC) [*Aagaard and Coachman*, 1968]. This results in year-round harsh sea-ice conditions for the western Fram Strait (Fig. 1.2), as well as regular formation of fast ice close to the NEG coast [*Hughes et al.*, 2011]. Despite this inflow of cold Arctic water, relatively warm Atlantic water (1°C) has been observed close to the coast near a marine terminating outlet glacier [*Straneo et al.*, 2012]. This Atlantic water must have crossed the continental shelf from the east to the west through bathymetric pathways and could enhance basal melting at the of the outlet glacier.

The largest outlet glaciers in the study area are Nioghalvfjerdsfjorden Glacier (also referred to as 79°-Glacier) and Zachariae Isstrøm. These are fed by the NEG ice stream (Fig. 1.2). This ice stream is the largest of the Greenland Ice Sheet, reaching approximately 700 km inland [*Joughin et al.*, 2001]. The drainage area of all outlet glaciers terminating in the study area cover approximately 20% of the Greenland Ice Sheet [*Zwally et al.*, 2012]. This highlights their importance for the entire ice sheet. While the northeastern part of the ice sheet has been thought to be relatively stable compared to other regions of Greenland [Rignot and Kanagaratnam 2006; Joughin et al. 2010], recent studies based on satellite observations showed increased ice sheet thinning [*Helm et al.*, 2014; *Khan et al.*, 2014].

1.3 Research Questions

1.3.1 Ice extent of the Greenland Ice Sheet during the Last Glacial Maximum

The LGM extent of the Greenland Ice Sheet on the NEG continental shelf is still predominantly based on conceptual models [*Funder et al.*, 2011]. These models estimate the minimum LGM ice extent to be located close to the coastline south of 79°N. North of 79°N, observations of submarine glacial landforms in swath bathymetric data gave evidence for the existence of an ice stream on the middle shelf but did not map its maximum extent [*Evans et al.*, 2009; *Winkelmann et al.*, 2010]. Based on relative late deglaciation dates at the coastline, Bennike and Björck [2002] suggested that the Greenland Ice Sheet reached further offshore NEG, possibly until the shelf break. However, marine geophysical evidence for this more extensive LGM ice sheet is missing so far.

- ***What was the LGM ice extent on the NEG continental shelf?***
- ***Can the larger LGM ice extent suggested by Bennike and Björck [2002] be verified by marine geophysical data?***

1.3.2 Retreat dynamics of the Greenland Ice Sheet after the Last Glacial Maximum

Submarine glacial landforms, formed underneath and at the margin of an ice stream, can provide indications for the retreat dynamics during deglaciation [*Dowdeswell et al.*, 2008]. Studies of submarine glacial landforms in the northernmost trough on the NEG continental shelf demonstrate that the retreat dynamics varied between different parts of the trough [*Evans et al.*, 2009; *Winkelmann et al.*, 2010]. Landforms indicative of slow stepwise retreat as well as landforms indicative of rapid retreat have been mapped. Due to the relatively small spatial coverage of the so far studied high resolution swath bathymetric data, these observations are restricted to a small portions of the trough. The retreat dynamics in other parts of the trough and on the remaining shelf are unresolved.

- ***How are submarine glacial landforms that are indicative of retreat dynamics distributed on the NEG continental shelf?***
- ***Is there a systematic pattern of ice retreat?***

1.3.3 Paleo-ice stream pathways in Northeast Greenland

Paleo-ice stream pathways can be inferred from observations of submarine glacial landforms formed by palaeo-ice streams [e.g. *Lavoie et al.*, 2015; *Ottesen et al.*, 2005]. The limited bathymetric data coverage on the shelf and the usage of ice topography instead of under-ice topography for Greenland in recent bathymetric models [*Jakobsson* *et al.*, 2012b], has impeded detailed reconstructions of palaeo-ice stream pathways in NEG. Ice stream pathways, however, are crucial to reconstruct the past ice sheet system and the drainage areas. Fast flowing marine based ice streams typically have a relatively little slope and are close to floatation [*Lavoie et al.*, 2015]. Subsequently, they have only small potential for sea level rise after deglaciation. Pathways redirected around shallower bathymetric areas, however, can indicate locations where local marine ice domes were present. These ice domes potentially stored more ice above floatation, with corresponding higher potential to change the sea level after deglaciation.

- ***Which pathways have been used by the ice streams that drained the Greenland Ice Sheet?***
- ***Did local marine ice domes exist on the continental shelf?***
- ***If local marine ice domes existed, how large were they and what was their contribution to sea-level change?***

1.3.4 Ice export from the Arctic Ocean through Fram Strait

Ice from the Arctic Ocean drifts within the EGC through the Fram Strait and delivers freshwater to the Greenland-Iceland-Norwegian Sea. Increased freshwater inflow, i.e. during deglaciations, can relocate or even shut down the formation of North Atlantic Deep Water (NADW) [*Aagaard and Carmack*, 1989], one of the main drivers of the global thermohaline circulation [*Broecker*, 2010]. It remains under debate, whether thick sea-ice or large icebergs were responsible for NADW shut-downs in the past [*Bradley and England*, 2008; *Moore*, 2005]. For this reason, Moore [2005] suggested to investigate the shallower parts in Fram Strait for traces of grounded very large icebergs that could have been exported from the Arctic Ocean. These would indicate that icebergs played an important role in the formation of NADW by exporting a significant amount of freshwater. Evidence for very deep drafted icebergs, furthermore, would provide an estimate for ice shelf thickness as an additional constraint for the complex and debated glacial history of the Arctic Ocean [*Jakobsson et al.*, 2014].

- ***Have there been deep drafted icebergs exported from the Arctic Ocean through Fram Strait and what was their maximum draft?***

2. Material and Methods

The results of this thesis are based on data acquired by hydro-acoustic surveys from R/V Polarstern that have been recorded and processed in-house by the bathymetry and geodesy group of the Alfred Wegener Institute, Helmholtz Centre for Polar and Marine Research (AWI) including myself. Occasionally, additional hydro-acoustic data from other vessels are used that have been acquired and processed by collaborators or contributors. Seismic and topographic data sets have been integrated for the production of the NEG digital bathymetric model (DBM) (for further details see Chapter 7.3). In this chapter, a short introduction of hydro-acoustic measuring principles, the acquisition systems (Fig. 2.1) and the processing steps is given. A more comprehensive description of hydro-acoustics can be found in the literature [e.g. *de Jong et al.*, 2002; *Lurton*, 2004]. For more specific information on the data and methods used in each publication, please refer to the data and method chapters of the contributions to scientific journals and books (Chapters 4.2, 7.2, 7.3 and 8.2).

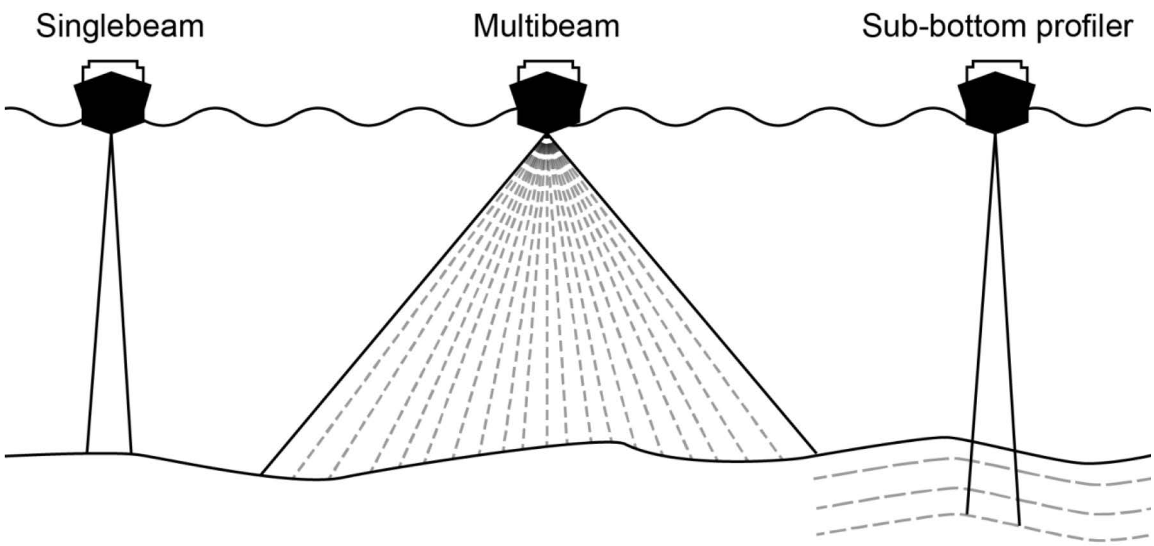

Figure 2.1: Different types of hydro-acoustic seafloor mapping systems that have been used in this thesis.

2.1 Hydro-acoustic measuring principles

The basic principle of hydro-acoustically surveying the water depth is to measure the time between the transmission of an acoustic signal and the arrival of the received signal that was reflected from the seafloor. Given this time interval (t) and a water sound velocity (c) it is possible to calculate the depth (d) of the reflector by:

$$d = t \times c / 2$$

The water sound velocity is typically about 1500 m/s but varies with density. Density again depends on temperature, salinity and depth. Temperature and salinity are laterally, vertically, and temporally variable. The highest variation in temperature usually is present in the upper 1000 m of the water column caused by surface mixing, solar heating, currents and external inputs. The salinity is given as the percentage of dissolved salts in pure water (p.s.u. = practical salinity units). In average, the oceans salinity is about 35 p.s.u., but can vary significantly in different areas. The water masses of the NEG continental shelf for example can vary from 35 to 30 p.s.u., due to freshwater input [Rabe et al. 2009]. With depth, the increased hydrostatic pressure results in higher sound velocities. A typical sound velocity profile from central Fram Strait is shown in Figure 2.2. While hydro-acoustic waves that travel perpendicular to the water layers are only experiencing a velocity change, waves that travel through stratified water layers at an oblique angle are refracted by the change in sound velocity (Fig. 2.3b).

In model conditions, the transmitted acoustic signal will only reflect from the targeted seabed. In the real world, however, the received signal will include reflections that can interfere with the target signal, i.e. reflections at obstacles in the water column. In addition, the strength of the returning targeted signal depends on seafloor composition and its ability to backscatter the transmitted signal, i.e. rough seafloor has a higher backscatter than smooth seafloor. Furthermore, the receiver not only records the reflected signal but also records noise from other acoustic sources, i.e. from the vessel itself, other acoustic systems, or especially in ice covered areas noise from ice breaking activities. These factors have to be considered and treated during post-processing to obtain the targeted reflected signal.

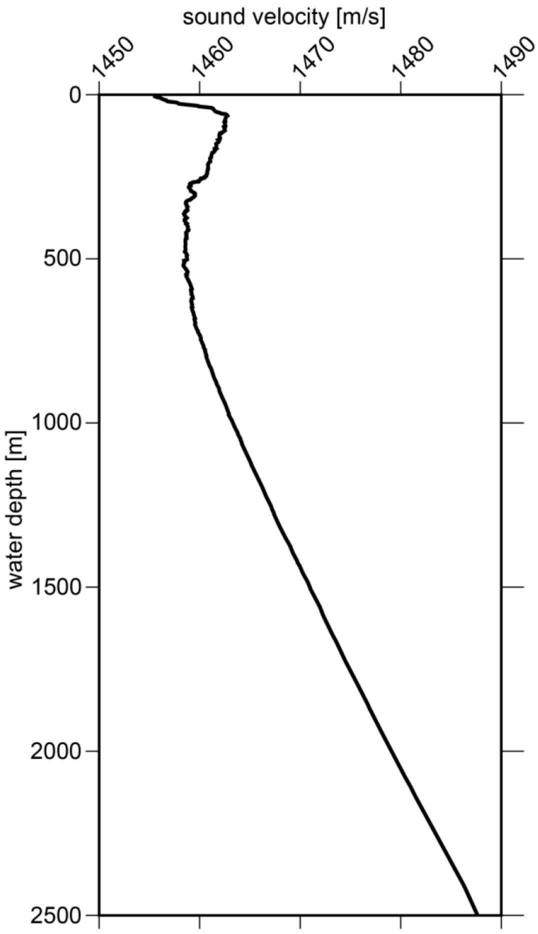

Figure 2.2: Example sound velocity profile, measured in central Fram Strait (PS85/0460-1)

2.2 Hydro-acoustic data acquisition systems and processing

2.2.1. Bathymetric data

Since the early 20th century, singlebeam echosounding systems have been used to measure the ocean depth. An acoustic signal, also called ping, is transmitted vertically into the water column below the vessel (Fig. 2.1) and the return echo is recorded. Knowing the speed of water, the measured two-way travel time of the seafloor backscattered signal is used to determine the water depth. Typically these systems have an opening angle of 5-15° and operate with 12 kHz frequency for deep water systems [*Lurton*, 2004].

Multibeam echosounding systems have been established in the 1970s. Multibeam systems not only receive depth information of one point per ping, but receive multiple depth measurements simultaneously (Fig. 2.1). This is achieved by transmitting and receiving several beams, with small individual beam widths of 1-3°, in different angles perpendicular to the axis of the vessel at once. This results in a swath of depth measurements underneath the vessel, from port to starboard. The width of this swath is depending on the swath angle and the water depth. Hence, the swath angle is a key parameter for determining the size of the surveyed area. The number of beams in one swath and their beam angle is determining the resolution of the system. Over the last decades these parameters of multibeam acquisition systems have improved continuously. The systems installed onboard R/V Polarstern over time for example have underwent a change in swath angle from 90° to 150° and the number of beams has increased from 16 to 345 (Table 2.1). These improvements have doubled the size of the surveyed area and improved the resolution perpendicular to the vessel by more than an order of magnitude.

Table 2.1: Multibeam echosounding systems installed on R/V Polarstern over time

System	Installation date	Transmitting frequency [kHz]	Beams	Swath angle	A-priori depth accuracy center beam (outer beam)
Seabeam (L3 ELAC Nautik)	1983	12.3	16	<90°	0.5% (1%)
Hydrosweep DS1 (ATLAS Hydrographic)	1989	15.5	59	<120°	0.5% (1%)
Hydrosweep DS2 (ATLAS Hydrographic)	1997	15.5	59 (240)	<120°	0.5% (1%)
Hydrosweep DS3 (ATLAS Hydrographic)	2010	15.5	345	<150°	0.2% (0.5%)

Due to the more complex survey setting of multibeam systems compared to singlebeam systems, more parameters are needed for data processing. Apart from the geographical position of the vessel from global positioning system (GPS) measurements, information is needed for the motion of the vessel given by the parameters roll, pitch, heading, and heave, to calculate the orientation of the beam vectors (Fig. 2.3a). On R/V Polarstern, this information is gathered by the Marine Inertial Navigation System (MINS) and is subsequently sent to the multibeam system. The geometry of the transmitted beams in a multibeam system results in oblique observation rays relative to the sea surface that are refracted when they cross the stratified water layers of varying sound velocity in an oblique angle (Fig. 2.3b). This has to be assigned in the data processing by including a sound velocity profile, which, in addition to calculate the traveled distance of the sound signal, is used to calculate the refracted true ray. Due to the variability of the sound velocity, in situ measurements either of the variables temperature, salinity, and depth or the sound velocity directly are needed for data processing. During most research expeditions Conductivity-Temperature-Depth (CTD) sensor measurements are conducted regularly, pre-dominantly for oceanographic investigations. These measurements deliver information on temperature and salinity in different depths. With this information the sound velocity can be calculated (Fig 2.2) [e.g. *Chen and Millero*, 1977; *Medwin*, 1975]. Another option to obtain the sound velocity profile on board is the Valeport Limited MIDAS SVP instrument. This instrument can directly measure the sound velocity by measuring the time of a signal that is sent over a very short but precisely measured distance. This instrument has been used as often as possible in areas where no CTD measurements have been made.

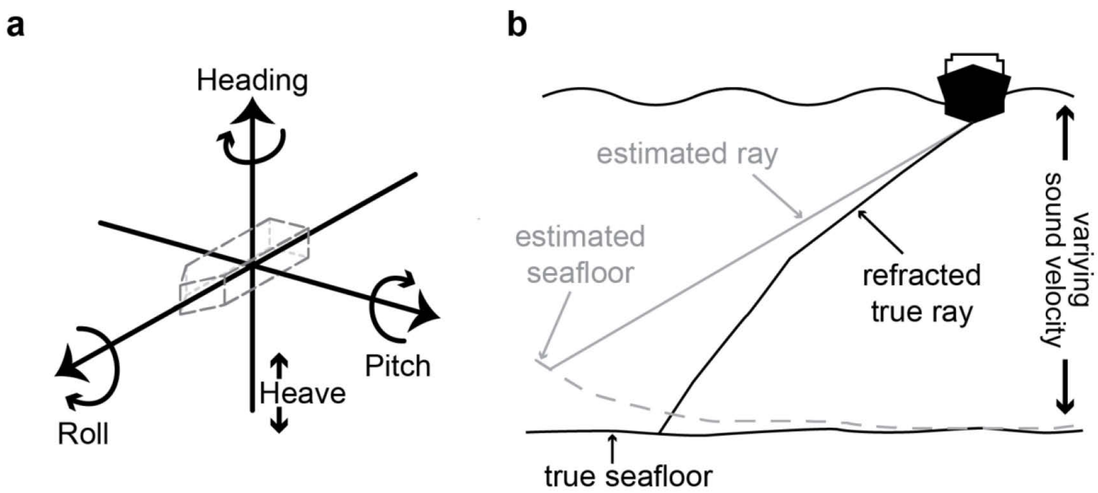

Figure 2.3: Sketch of a) the vessel motion parameters and b) the geometry of refracted observation rays

Bathymetric data acquired by R/V Polarstern has been processed and cleaned manually with CARIS HIPS&SIPS. Cleaning of the data is necessary due to the challenges in data acquisition mentioned above, e.g. reflectors in the water column, vessel motion errors, noise from ice breaking activities, and so forth. Additional cleaning has partly been carried out with QPS Fledermaus. For visualization and interpretation purposes, gridded bathymetric models have been derived from the data. Detailed high resolution models of multibeam data have been gridded either with QPS Fledermaus or the Generic Mapping

Tools (GMT) [*Wessel and Smith*, 1995]. The larger scale DBM of the NEG continental shelf, with interpolated surface in data gaps, has been gridded using a two-resolution gridding technique (see chapter 7.3.3). This technique is a modified version of the gridding techniques used for the mapping projects International Bathymetric Chart of the Arctic Ocean (IBCAO) [*Jakobsson et al.*, 2012b] and International Bathymetric Chart of the Southern Ocean (IBCSO) [*Arndt et al.*, 2013] and combined tools of QPS Fledermaus, ESRI ArcGIS and GMT.

2.2.2. Subbottom profiler data

Subbottom profiler systems are similarly set up as singlebeam echosounders and transmit an acoustic signal vertically from the vessel to the ocean floor (Fig 2.1). In contrast to the singlebeam system that surveys the water depth, the subbottom profiler system is designed to survey reflections of the first sedimentary layers of the seafloor. To achieve this, it operates with lower frequencies, typically 3.5 kHz, that can penetrate into the sediment. Besides the frequency, the penetration depth is depending on the type of seafloor. In clay-like sediment the signal penetration can reach down to 50-200 m to resolve its inner structure [*Lurton*, 2004]. On formerly glaciated shelves however the penetration usually is much less due to sediments that were over-consolidated by the presence of an ice sheet.

On R/V Polarstern currently the ATLAS Parasound P-70 system is installed. This system utilizes the parametric effect of two transmitted acoustic signals, usually set to 18 kHz and 22 kHz, to create a transmitted carrier wave of 20 kHz and a beat frequency of 4 kHz that is used for the measurement. This setting of transmitting acoustic signals with higher frequencies makes it possible to use a relatively small transducer and to achieve a narrow beam of 4 x 4.5° that minimizes the footprint of the signal and, hence, increases the lateral accuracy of the signal. The recorded signal today is stored by the acquisition system in ASD files. These can be exported to files in SGY format, which have been used to visualize the data in IHS Kingdom.

3. Contributions to scientific journals and books

My work on this PhD thesis comprises three contributions to ISI-peer reviewed journals and two contributions to a peer-reviewed book as first author:

Deep water paleo-iceberg scouring on top of Hovgaard Ridge – Arctic Ocean

Arndt, J. E., F. Niessen, W. Jokat, and B. Dorschel (2014)

Geophysical Research Letters, 41(14), p. 5068-5074, doi: 10.1002/2014gl060267.

In this article, we investigated hydro-acoustic data from Hovgaard Ridge, located in the center of the Fram Strait. On the top of the ridge, we found iceberg ploughmarks (scours) in a modern day water depth of >1200 m. We discuss source regions of these giant icebergs and their drift direction. Based on this discussion we infer that a significant amount of freshwater was supplied to the Greenland-Iceland-Norwegian Sea by icebergs during phases of deglaciation.

I reprocessed and investigated the hydro-acoustic data and wrote the manuscript. Frank Niessen gave valuable support for the discussion chapter and in the method chapter for the subbottom profiler data section. Wilfried Jokat and Boris Dorschel provided scientific input and supervised the work.

Deep-water iceberg ploughmarks on Hovgaard Ridge, Fram Strait

Arndt, J. E., and M. Forwick (accepted)

in *Atlas of Submarine Glacial Landforms: Modern, Quaternary and Ancient*, edited by J. A. Dowdeswell, M. Canals, M. Jakobsson, B. J. Todd, E. K. Dowdeswell and K. A. Hogan, Geological Society, London.

In this book chapter, we described the iceberg ploughmarks on Hovgaard Ridge, as described in the article above, with newer and higher resolution hydro-acoustic data. These data give a more accurate picture of the ploughmarks.

I wrote the manuscript. Matthias Forwick provided the hydro-acoustic data.

Glacial lineations and recessional moraines on the continental shelf of Northeast Greenland

Arndt, J. E., and J. Evans (accepted)

in *Atlas of Submarine Glacial Landforms: Modern, Quaternary and Ancient*, edited by J. A. Dowdeswell, M. Canals, M. Jakobsson, B. J. Todd, E. K. Dowdeswell and K. A. Hogan, Geological Society, London.

In this book chapter, we reviewed the findings of two studies that investigated hydro-acoustic data from the northernmost trough of the NEG continental shelf. Submarine glacial landforms are described that reveal the presence of a palaeo-ice stream in the trough and indicate that it had variable retreat dynamics during deglaciation.

I wrote the generic part of the chapter and the section on recessional moraines of the manuscript. Jeffrey Evans wrote the section on glacial lineations.

A new bathymetry of the Northeast Greenland continental shelf: Constraints on glacial and other processes

Arndt, J. E., W. Jokat, B. Dorschel, R. Mykelbust, J. A. Dowdeswell, and J. Evans (2015),

Geochemistry Geophysics Geosystems, 16(10), p. 3733-3753, doi: 10.1002/2015GC005931.

In this article, we have compiled a new digital bathymetric model of the NEG continental shelf. The model is based on all available bathymetric data and up-to-date continental topography data sets. The bathymetric data have been reprocessed or, respectively, quality controlled for this compilation. We have investigated the morphology of the new bathymetric model to infer glacial, halokinetic, and volcanic processes active during its formation. In addition, the new model provides constraints on recent oceanographic processes that are depending on the continental shelf morphology.

I acquired and processed the bathymetric data from R/V Polarstern cruise PS85, obtained bathymetric data from other resources, supervised reprocessing and partly reprocessed the remaining bathymetric base data sets including a final quality control, wrote and conducted the gridding routines, and prepared the manuscript. Wilfried Jokat provided the seismic data from AWI, scientific input and supervised the work. Boris Dorschel provided scientific input and supervised the work. Reidun Myklebust provided first reflector data from TGS seismic surveys. Julian A. Dowdeswell and Jeffrey Evans provided swath bathymetric data of cruise JR106.

Ice sheet limits and retreat dynamics on the Northeast Greenland continental shelf during the last full-glacial period

Arndt, J. E., W. Jokat, and B. Dorschel (submitted)

Quaternary Science Reviews.

In this article, we investigated all high resolution swath bathymetric data acquired with R/V Polarstern in the two northernmost troughs of the NEG continental shelf and the inter-trough area. We mapped small-scale submarine glacial landforms and used these to reconstruct the last full-glacial ice extent of the Greenland Ice Sheet, its successive retreat dynamics, and the distribution and orientations of iceberg ploughmarks after deglaciation in this region.

I acquired and processed the bathymetric data from R/V Polarstern cruise PS85, supervised reprocessing and partly reprocessed the remaining bathymetric base data sets including a final quality control, mapped the submarine glacial landforms, and wrote the manuscript. Wilfried Jokat and Boris Dorschel provided scientific input and supervised the work.

4. Deep water paleo-iceberg scouring on top of Hovgaard Ridge–Arctic Ocean

Jan Erik Arndt[1], Frank Niessen[1], Wilfried Jokat[1], and Boris Dorschel[1]

[1]*Alfred Wegener Institute Helmholtz Centre for Polar and Marine Research, Bremerhaven, Germany*

Published in *Geophysical Research Letters, Vol. 41(14), p. 5068-5074, doi: 10.1002/2014GL060267*

Abstract

In multibeam echosounder and subbottom profiler data acquired during R/V Polarstern cruise ARK-VII/3a from the Hovgaard Ridge (Fram Strait), we found evidence for very deep (>1200 m) iceberg scouring. Five elongated seafloor features have been detected that are interpreted to be iceberg scours. The scours are oriented in north-south/south-north direction and are about 15m deep, 300m wide, and 4 km long crossing the entire width of the ridge. They are attributed to multiple giant paleo-icebergs that most probably left the Arctic Ocean southward through Fram Strait. The huge keel depths are indicative of ice sheets extending into the Arctic Ocean being at least 1200m thick at the calving front during glacial maxima. The deep St. Anna Trough or grounded ice observed at the East Siberian Continental Margin are likely source regions of these icebergs that delivered freshwater to the Nordic Seas.

4.1 Introduction

The Fram Strait (FS) is the only deep water connection of the Arctic Ocean to the world oceans and for this reason plays an important role in water and heat exchange [*Fieg et al.*, 2010; *Rabe et al.*, 2013; *Schauer et al.*, 2004]. The Greenland-Iceland-Norwegian Sea south of the Fram Strait is an important area for North Atlantic Deep Water (NADW) formation, one of the main drivers of the global oceanic thermohaline circulation [*Broecker*, 2010]. NADW formation in this area is most vulnerable to freshwater discharges out of the Arctic Ocean [*Aagaard and Carmack*, 1989; *Bradley and England*, 2008]. Isotopic evidence from a sediment record in the Fram Strait (ODP Site 910) suggests strong imprint of Arctic Freshwater pulses on Earth's climate system throughout the last 0.8 Ma [*Knies et al.*, 2007]. Predominantly, the freshwater was exported at major glacial terminations, when continental ice sheets in the circum-Arctic collapsed and large amounts of ice were released into the Arctic Ocean [*Darby et al.*, 2002; *Knies et al.*, 2007]. The amount of ice exported from the Arctic Ocean then can be sufficient to shut down the NADW production south of Fram Strait [*Bradley and England*, 2008; *Moore*, 2005]. The question arose whether mainly large icebergs released from ice shelves in the Arctic Ocean or sea ice of more than 50m in thickness were exported during glacial terminations [*Bradley and England*, 2008; *Moore*, 2005]. It has been suggested to investigate the ridges and plateaus in the Arctic gateway region including the Hovgaard Ridge (HR) (see Figure 4.1a) in order to explore the possibility of deep draft icebergs invading the Nordic Sea from the north [*Moore*, 2005].

Between the years 1984 and 1997, the German research vessel Polarstern collected swath bathymetry data in this area during nine research cruises. These data were compiled in the Bathymetric Chart of the Fram Strait (BCFS) [*Klenke and Schenke*, 2002] providing information on the geometry of large-scale topographic features in Fram Strait. Here we focus on small-scale features on top of HR (Figures 4.1b and 4.1c). Five linear features are located at about 1200 m. We interpret these features to be scours of giant paleo-icebergs. Our study strongly supports the hypothesis that icebergs calved off ice shelves in the Arctic Ocean and drifted through the Fram Strait into the Nordic Sea.

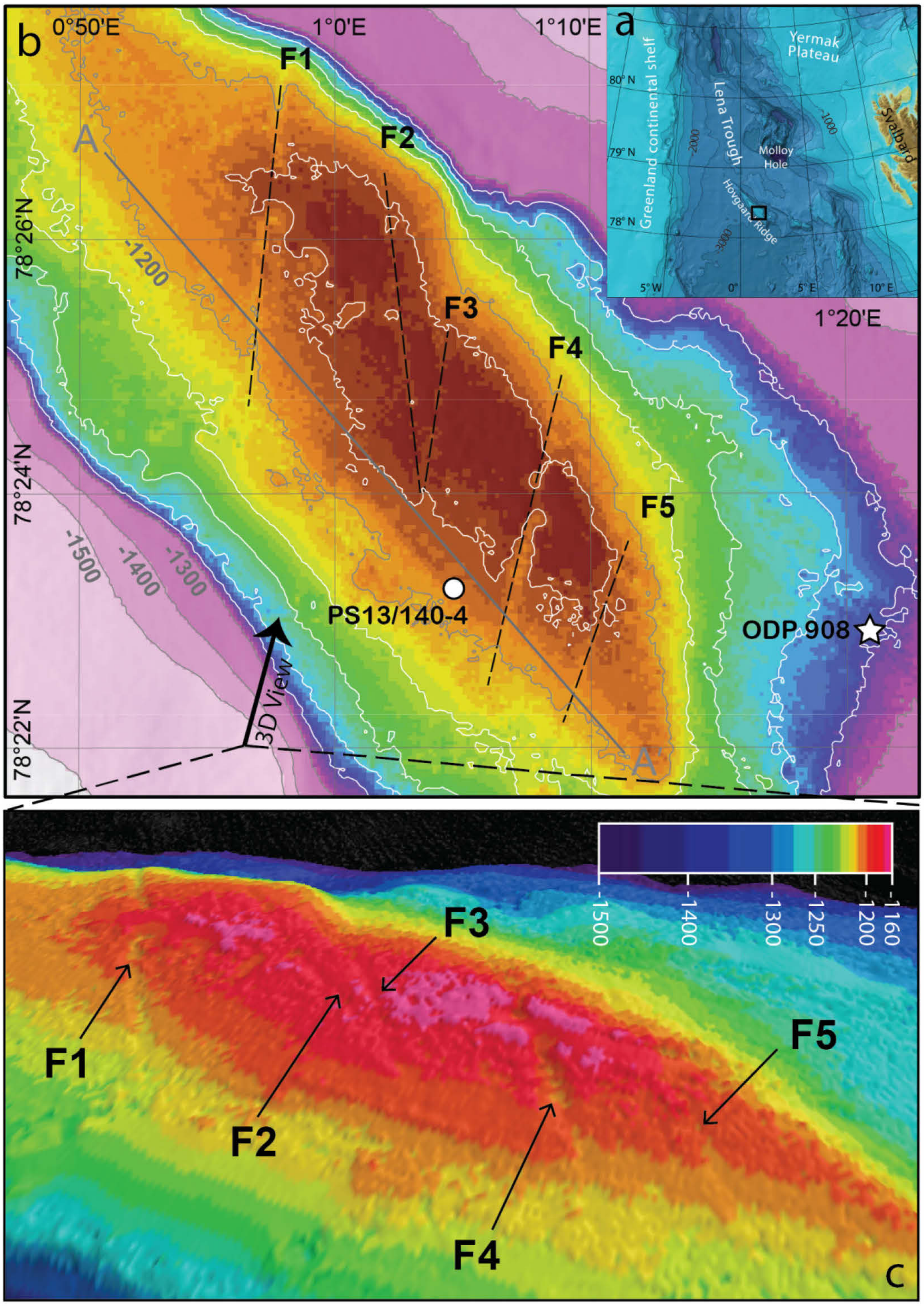

Figure 4.1: (a) Bathymetric overview map of Fram Strait based on International Bathymetric Chart of the Arctic Ocean (IBCAO) 3.0 [*Jakobsson et al.*, 2012b]. (b) Planar view of gridded ARK-VII/3a bathymetric data on Hovgaard Ridge with identified scours (black dashed lines) and the location of dated cores (star) and undated cores (circle). (c) Three-dimensional view of the bathymetry.

Bathymetric studies carried out in the Arctic Ocean during the last decades demonstrated that ice shelves have extended north into the Arctic Ocean [*Jakobsson et* *al.*, 2010; *Jakobsson et al.*, 2013; *Mercer*, 1970; *Niessen et al.*, 2013] and that the common view of Quaternary Arctic ice sheets that terminated at the shelf edges [*Ehlers and Gibbard*, 2007; *Svendsen et al.*, 2004] is too simple. In places, evidence of grounded ice can be found in the seafloor morphology of the entire Arctic Ocean and are so far detected up to a maximum depth of 1200m [e.g., *Dowdeswell et al.*, 2010b; *Gebhardt et al.*, 2011; *Jakobsson et al.*, 2008b; *Jakobsson et al.*, 2005; *Niessen et al.*, 2013] (see Figure 3). Traces of single grounded megascale icebergs from the Arctic have been found at about 1000m depth [e.g., *Dowdeswell et al.*, 2010b; *Jakobsson et al.*, 2010; *Kuijpers and Werner*, 2007], with the deepest at about 1085 m in Baffin Bay, West Greenland [*Kuijpers et al.*, 2007]. Thus, the scours discussed in this paper also underlines the existence of huge ice sheets and are so far the deepest traces of giant icebergs.

4.2 Data and Methods

All bathymetric and subbottom profiler data were acquired during cruise ARK-VII/3a in August 1990. Subbottom profiler data were measured with the Atlas Parasound system and were recorded on paper only (Atlas Deso-25). Parasound is a parametric system using 18 and 22 kHz as primary and 4 kHz as secondary (subbottom) frequencies, respectively. The footprint of Parasound is given with about 7% of the water depth (84m lateral resolution at 1200m water depth). Due to its age and former acquisition setup, the data quality is rather poor compared to modern parametric systems but still significantly better than that of conventional 3.5 kHz subbottom systems.

Swath bathymetry was surveyed with an Atlas Hydrosweep DS1 multibeam system with 59 beams and a transmitting frequency of 15.5 kHz. The bathymetric data were cleaned with Caris HIPS software for the BCFS [*Klenke and Schenke*, 2002]. In 2013 the data were again checked with Caris HIPS and additionally with QPS Fledermaus. For this study, a bathymetric grid was calculated using the remove-restore method [*Jakobsson et al.*, 2012b] applying 60 m resolution where data were available and 180m resolution in the data gaps.

Table 4.1: Properties of Identified Seafloor Features

ID	Relative Depth	Width (m)	Length (m)	Grid Bearing (deg)
F1	10	200	4000	185
F2	5	200	4000	173
F3	5	100	2000	187
F4	15	300	4000	193
F5	10	150	2000	199

4.3 Results

In total, five elongated features were identified in the bathymetric data on the crest of HR at about 1200 m (Figures 4.1b and 4.1c). All structures are straight. The most prominent features are F1 and F4 and are clearly visible in the bathymetric grid (Figures 4.1b and 4.1c). Table 4.1 lists the properties of each identified feature. The scours only appear at the very top of HR in a fixed range between 1180 m and 1210 m depth (Figures 4.1b and 4.1c). In general, they are oriented in a north-south/south-north direction with grid bearing ranging by 26° and less (Table 4.1). All five lineaments are verified by transects of subbottom profiler data (Figure 4.2 and Appendix A). To a depth of approximately 40 m below the sea floor, three acoustic units can be distinguished. Unit 1 is a spotted but otherwise featureless drape with a thickness of about 5 m. Unit 2 consists of sediments with discontinuous reflectors intercalated with more massive or semitransparent deposits, underlain by well stratified sediments (Unit 3, Figure 4.2). Lineaments F2/F3 and F5 are clearly draped by Unit 1 sediments. For lineaments F1 and F4 such a drape is not, or not clearly, visible (Figure 4.2), which may be the result of the limited lateral resolution of the system (84m on top of the HR). The sediments of Unit 3 are undisturbed (Figure 4.2).

4.4 Discussion

Lineaments on the sea floor can have different origins, such as induced by active faulting (e.g., caused by differential compaction of underlying sediments [*Chopra and Marfurt*, 2012]) or by erosion (e.g., by grounding of ice [e.g., *Dowdeswell et al.*, 2010b]). The undisturbed character of the sediments of Unit 3 (Figure 4.2) shows that the features are caused by erosion rather than by processes active within the formation. Elongated features of a moving grounded ice sheet generally occur in groups as parallel bed form sets [e.g., *Graham et al.*, 2009]. The features observed here are not streamlined parallel but show grid bearing differences of up to 26° (Table 4.1 and Figure 4.1). Thus, we suggest that these features were produced by giant icebergs scouring the ridge crest at some time in the past. The differences in grid bearing also indicate that the scours were created by several icebergs rather than by a single multikeeled iceberg.

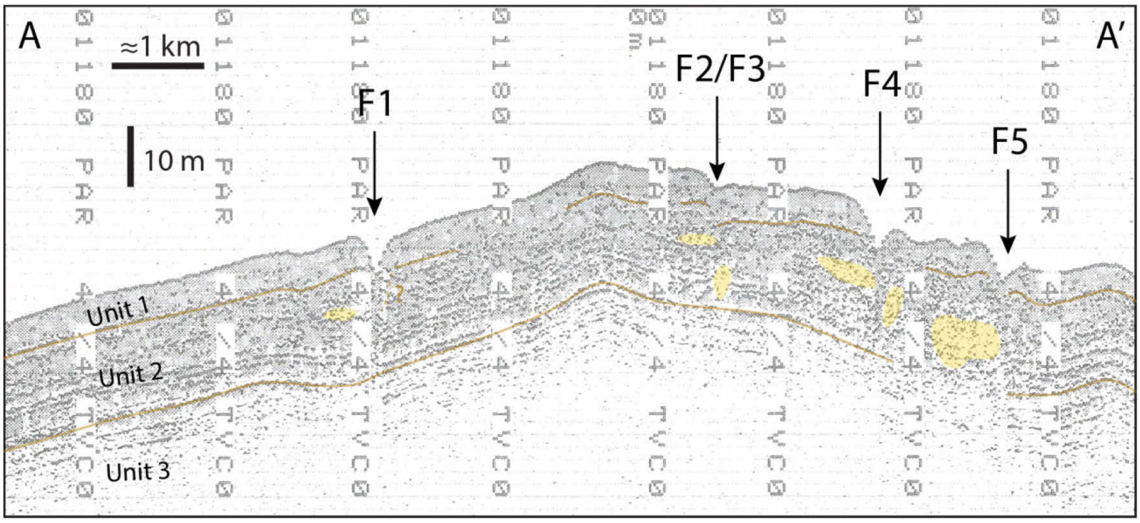

Figure 4.2: Subbottom profiler data (for location see grey line in Figure 4.1b) showing the acoustic units (separated by orange lines). Note massive sediments with discontinuous reflectors in Unit 2 (yellow areas).

The basic question is: Where did these icebergs come from? Iceberg trajectories are mainly steered by ocean currents and additionally by wind, waves, and sea ice that are variable in time and space [*Death et al.*, 2006]. Modern day oceanographic observations show that the water current direction at HR to more than 1000m depth is strongly influenced by the East Greenland Current (EGC) having a north to south flow direction. The more easterly West Spitsbergen Current, transporting relative warm Atlantic water to the north, has only a marginal influence on HR [*Schauer et al.*, 2004]. Moreover, the flux of Atlantic water into the Arctic Ocean via Fram Strait has a relatively large indirect effect on currents at HR, because the major part of water masses transported by the West Spitsbergen Current are recycled into the EGC intermediate water in the central Fram Strait [*Johannessen*, 1986]. This component is suggested to be reduced with a reduction of the West Spitsbergen Current during phases of glacial maxima

[*Jakobsson et al.*, 2010] and a more southerly overturning circulation in the North Atlantic [*Hu et al.*, 2010]. However, even with a weaker EGC during glacial times the drift direction at HR is suggested to be north to south. Consistently, Darby et al. [2002] showed that icebergs from the Laurentide and Innuitian Ice Sheet left the Arctic Ocean through Fram Strait based on drop stone investigations. In addition, core PS13/140-4, a 4.3 m long sediment core retrieved from the top of the HR in 1988 (Figure 1b), has a variable lithology including abundant ice-rafted debris and coal fragments [*Wollenburg*, 2012]. Bischof et al. [1990] reconstructed the ice drift pattern of the Nordic Seas based on coal fragments and concluded that they most probably originate from coal exposures in northern Siberia eroded by ice and then transported through Fram Strait by icebergs into the North Atlantic. Furthermore, scour and lineation directions observed on Morris Jesup Rise [*Jakobsson et al.*, 2010] and Yermak Plateau [*Gebhardt et al.*, 2011], respectively, are also indicating that Arctic ice was drifting in the direction of Fram Strait (see Figure 4.3). Thus, the scours on HR most likely are caused by icebergs produced in the Arctic Ocean drifting southward trough Fram Strait and less likely originate from ice streams farther south such as those entering the Nordic Sea from Greenland or Scandinavia. Subsequently, the scours give evidence that several megascale icebergs left the Arctic Ocean trough Fram Strait, with only the deepest leaving a trace on HR. This is indicating that iceberg export to lower latitudes was larger than currently though. The icebergs were an additional source of fresh water. Therefore, they likely influenced the formation areas of polar deep water and thus the meridional overturning circulation [*Knies et al.*, 2007].

The icebergs are estimated to have keel depths of at least up to 1090 m assuming a 120 m lower sea level during maximum glaciations [*Rohling et al.*, 2009]. No similar features are visible in the deeper, also relatively flat, parts of HR. Therefore, we suggest that 1090 m keel depth was the maximum size limit of paleo-icebergs passing Fram Strait. Modern day observations of icebergs in the Antarctic show a maximum draft of less than 700 m [*Dowdeswell and Bamber*, 2007]. Thus, today we have no equivalent of the processes producing giant icebergs during glacial times. However, Dowdeswell and Bamber [2007] conclude that deep-keeled icebergs originate from fast-flowing ice, which in our case had to be thicker than 1200m at the grounding line to produce icebergs of sufficient size. Furthermore, the pathway to HR had to be free of shallower bathymetric obstacles, e.g., ridges or continental shelf edges.

Batchelor and Dowdeswell [2013] analyzed Arctic cross shelf troughs that could have facilitated fast ice flow. They found that Arctic troughs are up to 1000 m deep. Southern Greenland and the Baffin Bay area can be excluded as source areas of icebergs on the HR due to shallow bathymetric obstacles in the North Atlantic (<700 m at Denmark Strait). The remaining troughs are up to 900 m deep (M'Clintock Inlet). This depth is reached at the inner continental shelf with a shallower shelf edge further offshore, preventing the release of giant icebergs into the Arctic Ocean. Thus, icebergs had to be calved offshore the continental shelf in order to travel to HR. St. Anna Trough is the deepest Arctic trough at the shelf edge (800 m) [*Jakobsson et al.*, 2012b]. Polyak et al. [1997] suggested that the St. Anna ice stream has reached the shelf edge. The ice in St. Anna Trough was at least ≈ 900 m thick to stay grounded at the shelf edge. Therefore, we can conclude that the ice sheet had to be at least 300 m thicker at the St. Anna Trough grounding line than the currently estimated minimum ice thickness, in order to calve icebergs of sufficient size. Other slightly shallower major Arctic troughs are located in the Amerasian Basin. The Laurentide Ice Sheet, however, was too thin reaching up only to <100 m above sea level close the north Canadian coast during glacial maxima [*England et al.*, 2009]. In contrast, the central Innuitian Ice Sheet is suggested to be thicker than 1000 m for the last glacial maximum [*England et al.*, 2006] and supplied the M'Clintock Inlet Ice Stream (700 m trough depth at shelf edge). In order to travel from the Amerasian Basin to Fram Strait, icebergs had to cross the Lomonosov Ridge. This ridge only has a few gateways deep enough for giant icebergs (See Figure 4.3). In addition, Polyak et al. [2001] showed that the central crest of Lomonosov Ridge was eroded by ice originating most likely from the Eurasia Basin. Thus, giant iceberg source areas in the Eurasian Basin are more likely responsible for the HR scours.

The only traces of grounded ice in similar depths as the iceberg scours we describe here are observed on the formerly glaciated East Siberian Continental Margin [*Niessen et al.*, 2013] of which the former glaciations and ice flow dynamics are still mostly unknown. The East Siberian Continental Margin, however, is also located in the Amerasian Basin. A regional ice advance documented on Yermak Plateau before 790 kyrs B.P. is only about 400 km northeast of HR [e.g., *Flower*, 1997; *Gebhardt et al.*, 2011; *Knies et al.*, 2007; *O'Regan et al.*, 2010]. This, however, unlikely was the source of the giant icebergs due to the observed depth of less than 850 m, and the lack of evidence for fast-flowing ice since no troughs are present on Yermak Plateau. A determination of the source of the icebergs is not possible within this study. Nevertheless, St. Anna Trough, showing the smallest difference to its estimated minimum ice thickness and located in the Eurasian Basin, and the East Siberian Continental Margin, with grounded ice at similar depths, are likely sources.

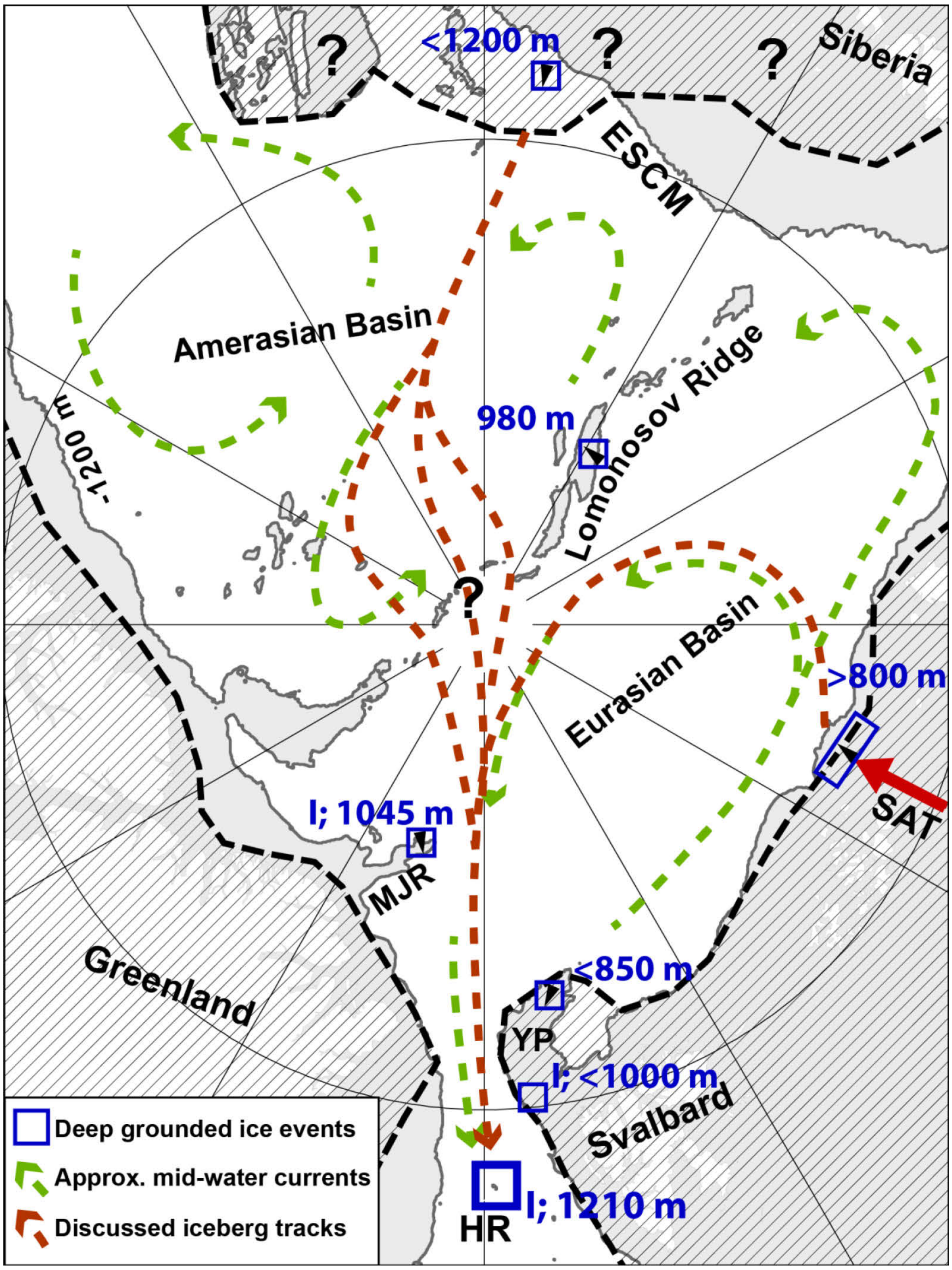

Figure 4.3: Deep grounded ice events (I = produced by single icebergs) in the central Arctic Ocean with depths and if known direction (black arrow). The maximumice extent [after *Niessen et al.*, 2013] is shown as black dashed line; red arrow shows St. Anna Trough (SAT) ice stream; grey shows areas shallower than 1200m based on IBCAO 3.0 [*Jakobsson et al.*, 2012b]; generalized current directions between 200m and 1700m depth are from Rudels et al. [1994]; MJR = Morris JesupRise; SAT = St. Anna Trough; YP = Yermak Plateau.

According to our interpretation of acoustic subbottom data, icebergs grounded on the HR during and at the end of the deposition of Unit 2, because all elongated grooves were cut into Unit 2 sediments. In places, grounding leads to alteration of well-stratified sediments into massive or transparent deposits. The iceberg keels were subsequently draped by hemipelagic mud of Unit 1. However, the limited resolution of the subbottom images does not exclude the possibility that some features (F1, F4) were eroded into Unit 1.

The chronology of the scours remains undetermined until well-dated cores from the top of the HR become available. Core PS13/140-4 from the top of HR (Figure 4.1b) has no chronology [*Wollenburg*, 2012]. However, ODP Site 908, located on the eastern flank of HR (Figure 4.1b), has an age model and subbottom structures similar to those described here for the top area of the HR [*Knies et al.*, 2009]. Unit 1 is approximately 2m thicker close to ODP Site 908 than adjacent to the scours suggesting sedimentation rates are about 35% lower on top of HR compared to the drill site (see Appendix A). For the top 35 m of Site 908 the linear sedimentation rate is 4.4 cm kyr1, which is calculated from one chronological point of 780 kyrs at 34.45 m below seafloor [*Knies et al.*, 2009]. Assuming a linear sedimentation rate of 2.9 cm kyr^{-1} on top of the HR (35% lower than 4.4 cm kyr^{-1}) the base of Unit 2 and Unit 1 has an estimated age of 700 kyrs and 170 kyrs B.P., respectively. Taking into account the low resolution in the age model of the Quaternary sediments of site 908 including the uncertainty in the correlation of acoustic Units 1 and 2 to the top of the HR, it seems reasonable to assume that ice grounding took place since about 600 to 800 kyrs B.P. (marine isotope stage (MIS) 15 to MIS 20). Since this time the global ice volume has increased significantly [*Gebhardt et al.*, 2011; *Tiedemann et al.*, 1994]. Abundant ice-rafted debris is found in sediment cores from the Arctic Ocean indicative of drifting icebergs since MIS 16 [*Stein et al.*, 2010]. Increased export of ice to the HR is also recorded at Site 908 where the sand content shifts above 30 wt % after approximately 700 kyrs B.P. [*Knies et al.*, 2009]. We suggest that icebergs grounded on HR for several times during this period. The scours visible in our bathymetric data were eroded into the upper sediments of Unit 2 possibly during MIS 6 (190 to 130 kyrs B.P.) when the maximum glacial coverage of the circum-Arctic area is thought to have occurred [*Jakobsson et al.*, 2010]. With only the present data at hand, we cannot exclude post-MIS-6 erosion by grounded ice.

4.5 Conclusions

1. The five seafloor features on top of HR at depths down to 1210 m are erosional and best explained as scours of giant paleo-icebergs (draft of ≈ 1090 m), which has occurred several times during the last 800 kyrs. These are, so far, the deepest observed iceberg scours and thus are an important constraint for paleo-ice sheet thickness at the former calving line.
2. Based on past and modern oceanic conditions megascale icebergs most probably left the Arctic Ocean through Fram Strait and scoured the HR in a north to south direction. Accordingly, a significant amount of freshwater was likely exported to lower latitudes by icebergs, of which the largest (giant icebergs) grounded at the HR. Likely, giant iceberg source areas are the St. Anna Trough or the East Siberian Continental Margin.

4.6 Acknowledgements

Thanks to Hans Werner Schenke, who was chief scientist of R/V Polarstern cruise ARK-VII/3a. Thanks to captain and crew of this research cruise. We thank two anonymous reviewers for commenting and improving the previous version of this manuscript.

The Editor thanks two anonymous reviewers for their assistance in evaluating this paper.

5. Deep-water iceberg ploughmarks on Hovgaard Ridge, Fram Strait

Jan Erik Arndt[1] and Matthias Forwick[2]

[1]Alfred Wegener Institute Helmholtz Centre for Polar and Marine Research, Bremerhaven, Germany

[2]Department of Geology, University of Tromsø, Tromsø, Norway

Accepted for publication in the *Atlas of Submarine Glacial Landforms: Modern, Quaternary and Ancient*, edited by J. A. Dowdeswell, M. Canals, M. Jakobsson, B. J. Todd, E. K. Dowdeswell and K. A. Hogan, Geological Society, London.

5.1 Introduction

The drift of partially grounded icebergs leads to the formation of ploughmarks on the sedimentary seafloor of high-latitude continental shelves, bathymetric ridges and plateaus. Ploughmarks of various dimensions have been identified at several locations in the Arctic Ocean, suggesting that the icebergs produced during past glaciations were of different sizes and configurations [*Jakobsson et al.*, 2014]. According to Jakobsson et al. [2014], giant icebergs with drafts of more than 1000 m were present in the Arctic Ocean, most probably during the Saalian glaciation of Marine Isotope Stage 6. Very deep iceberg ploughmarks have been mapped on Morris Jesup Rise at 1045 m water depth [*Jakobsson et al.*, 2010] and offshore of central West Greenland at 1085 m of modern water depth [*Kuijpers et al.*, 2007]. The iceberg ploughmarks illustrated here, from Hovgaard Ridge in central Fram Strait (Figure 5.1a), are the deepest features mapped to date where they occur to water depths of 1210 m [*Arndt et al.*, 2014].

5.2 Description

Hovgaard Ridge is an approximately 110-km long, southeast-northwest orientated ridge representing the shallowest bathymetric obstacle in the central Fram Strait, the only deep-water gateway of the Arctic Ocean (Figure 5.1a). Its summit is at about 1180 m water depth (78°25'N, 1°E). The very top of the ridge is relatively flat, whereas its flanks are steep (>10°). Six elongate shallow depressions with raised rims have been identified on swath-bathymetric imagery from the shallow parts of Hovgaard Ridge (1-6, Figures 5.1b and c). The depressions are almost straight and strike north-south, with their bearings ranging over 26°. They are up to 4 km long and cross the shallowest part of Hovgaard Ridge (1180 m to 1210 m water depth). The depressions have a relative depth of 5 to 15 m and are between about 100 and 300 m wide. A single elliptical depression has been identified between depressions 1 and 2 (P, Figures 5.1b and c). This depression is about 400-500 m in diameter and 10 m deep.

The subbottom stratigraphy contains three seismostratigraphic units (Figure 5.1d): an approx. 8 m thick acoustically stratified Unit 1; an up to 5 m thick, acoustically semi-transparent Unit 2 with acoustically transparent bodies (marked in red; Figure 5.1d); an acoustically stratified Unit 3. The data reveal that the linear depressions and rims on the seafloor mimic the irregularities in Unit 2.

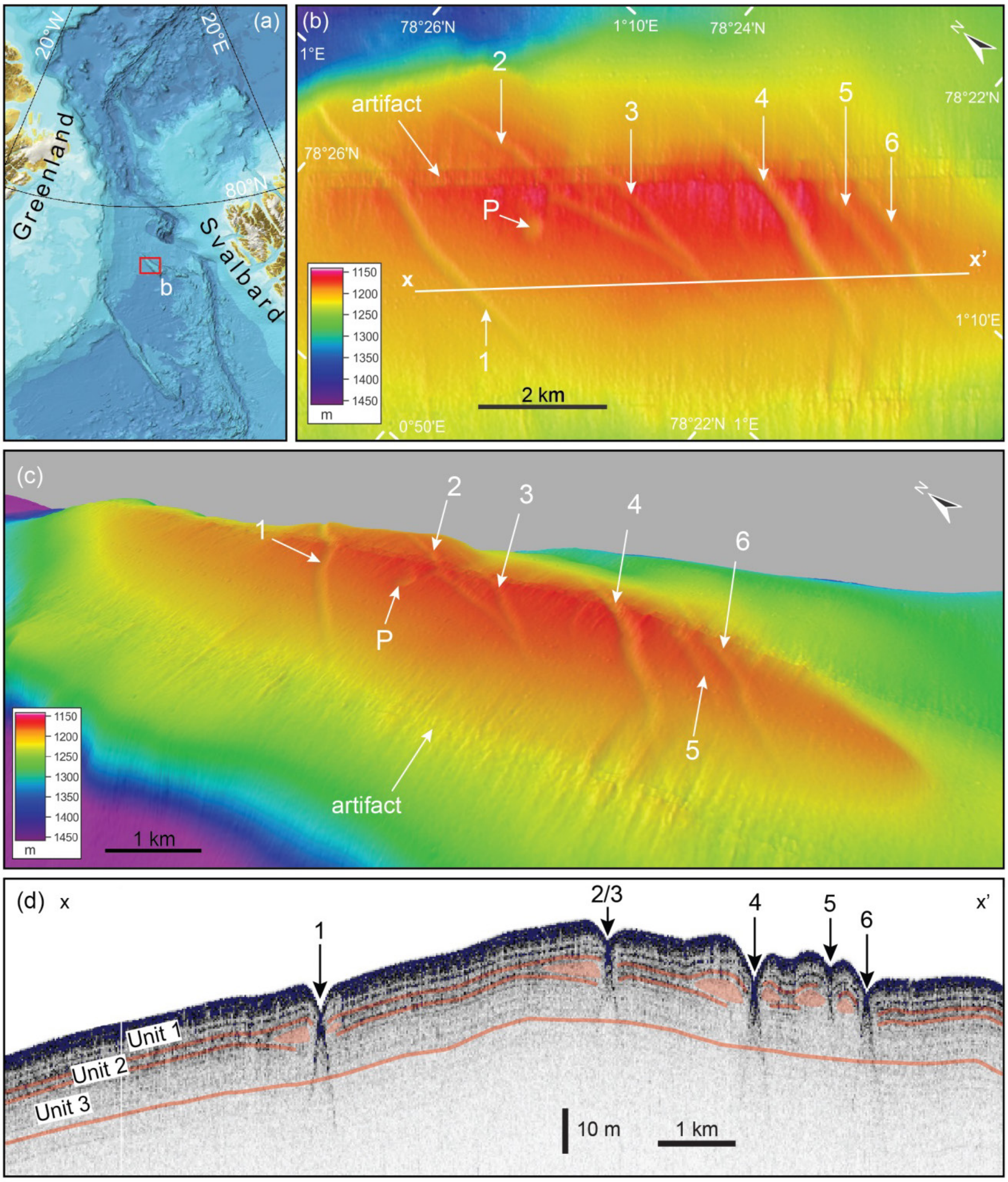

Figure 5.1: Multibeam bathymetry and subbottom profiler data of iceberg ploughmarks on Hovgaard Ridge. (a) Location of the study area (red box; map from IBCAO v. 3.0). (b) Swath-bathymetric image of iceberg ploughmarks on Hovgaard Ridge, orientated in a north-south direction and the pit hole (P). Acquisition System Kongsberg EM300. Frequency 30-34 kHz. Grid-cell size 25 m. (c) 3D oblique view of iceberg ploughmarks looking from the north-east. (d) Subbottom profile crossing the iceberg ploughmarks. The ploughmarks are formed in the upper sedimentary units, whereas Unit 3 is undisturbed. Shaded red areas show semi-transparent deposits. Acquisition system Edgetech 3300-HM subbottom profiler, pulse mode 1.5-9 kHz, pulse-length 40 ms.

5.3 Interpretation

The elongated depressions on the relatively flat upper surface of Hovgaard Ridge are interpreted as ploughmarks formed from the grounding of giant icebergs with very deep keels. The undisturbed character of acoustic Unit 3 implies that the depressions were formed by an erosive process. The slightly varying orientations of the ploughmarks suggest that they were produced by several individual icebergs rather than by one multi-keeled iceberg; a phenomenon observed on Yermak Plateau [*Dowdeswell et al.*, 2010b]. Assuming a sea-level lowering of approximately 120 m during past full-glacial periods, the iceberg drafts reached water depths of 1090 m. The transparent deposits in acoustic Unit 2 are suggested to be iceberg turbates that formed during iceberg grounding [*T. O. Vorren et al.*, 1983]. The elliptical depression is interpreted as a grounding pit produced by a single hit of a turning giant iceberg.

Modern and reconstructed past oceanographic observations suggest a southward drift of icebergs through Fram Strait into the North Atlantic [e.g., *Darby et al.*, 2002]. The southward iceberg drift in the past is also supported by ice-rafted debris found in a sediment core on Hovgaard Ridge, which consists of coal fragments that can be linked to source areas in the Arctic Ocean [*Bischof et al.*, 1990], and by the orientations of iceberg ploughmarks in the central Arctic Ocean that indicate a drift direction towards Fram Strait [*Jakobsson et al.*, 2014]. Thus, the icebergs leading to the formation of the ploughmarks on the crest of Hovgaard Ridge most likely derived from ice sheets with grounding lines at water depths of 1200 m or more surrounding the Arctic Ocean. An additional pre-requisite is that the pathway between the calving front and Hovgaard Ridge was free of shallower bathymetric obstacles. St. Anna Trough, located at about 70°E between Russian Franz Josef Land and Severnaya Zemlya, is the deepest trough at the shelf edge in the Arctic Ocean. It has been demonstrated that grounded ice streams extended repeatedly to the shelf break in this trough [*Polyak et al.*, 1997]. Further east, the East Siberian continental margin is the only other place in the Arctic Ocean where traces of grounded ice at a similar depth (about 1200 m) have been found [*Niessen et al.*, 2013]. Consequently, the iceberg ploughmarks on the crest of Hovgaard Ridge are suggested to have their origin from grounded giant icebergs calving from ice sheets terminating in the St. Anna Trough or on the East Siberian continental margin [*Arndt et al.*, 2014].

6. Glacial lineations and recessional moraines on the continental shelf of Northeast Greenland

Jan Erik Arndt[1] and Jeffrey Evans[2]

[1]*Alfred Wegener Institute Helmholtz Centre for Polar and Marine Research, Bremerhaven, Germany*

[2]*Department of Geography, Loughborough University, Loughborough, United Kingdom*

Accepted for publication in the *Atlas of Submarine Glacial Landforms: Modern, Quaternary and Ancient*, edited by J. A. Dowdeswell, M. Canals, M. Jakobsson, B. J. Todd, E. K. Dowdeswell and K. A. Hogan, Geological Society, London.

6.1 Introduction

The Northeast Greenland (NEG) continental shelf is only sparsely mapped due to its remoteness and harsh year-round sea-ice conditions. Mapping the distribution of submarine glacial landforms relies mainly on single track lines of multibeam echo sounder bathymetric data with only occasional systematic surveys. Ice streams drain the modern Greenland Ice Sheet to its northeastern margin in several fjords near the head of the Westwind Trough (Figure 6.1a). The presence of glacial lineations and recessional moraines in the inner to middle trough indicates that the Greenland Ice Sheet extended onto the continental shelf probably during the Last Glacial Maximum [*Evans et al.*, 2009; *Winkelmann et al.*, 2010].

6.2 Description

Multibeam bathymetry and subbottom profiler data showing glacial landforms were acquired along several transects transverse to the orientation of Westwind Trough (Figure 6.1a) [*Evans et al.*, 2009]. The multibeam bathymetry reveals the presence of numerous, parallel to sub-parallel and elongated ridges or lineations forming positive relief relative to the surrounding seafloor (Figure 6.1b). The orientation of the lineations is sub-parallel to the long-axis of Westwind Trough. The lineations are well-defined in some areas of the trough but are more subtle elsewhere. Lineations often exceed 2.5 km in length and can approach 10 km. They are up to 10 m in height, about 350 m in width, with elongation ratios of 12:1 to 33:1 (Figures 6.1c and d).

Subbottom profiles show that the lineations are sedimentary, and comprise acoustically transparent and homogenous sediment with a distinct, flat to undulating basal reflector (Figures 6.1c and d). The thickness of this uppermost sedimentary unit is up to 30 m but, in some areas of the trough, the unit is <10 m thick or appears to be absent or below the vertical resolution of the TOPAS system. The acoustically-transparent sediment is either: (a) confined to the lineations; or (b) occurs as a semi-continuous layer in which lineations are formed in the surface and sediment extends beneath the intervening grooves.

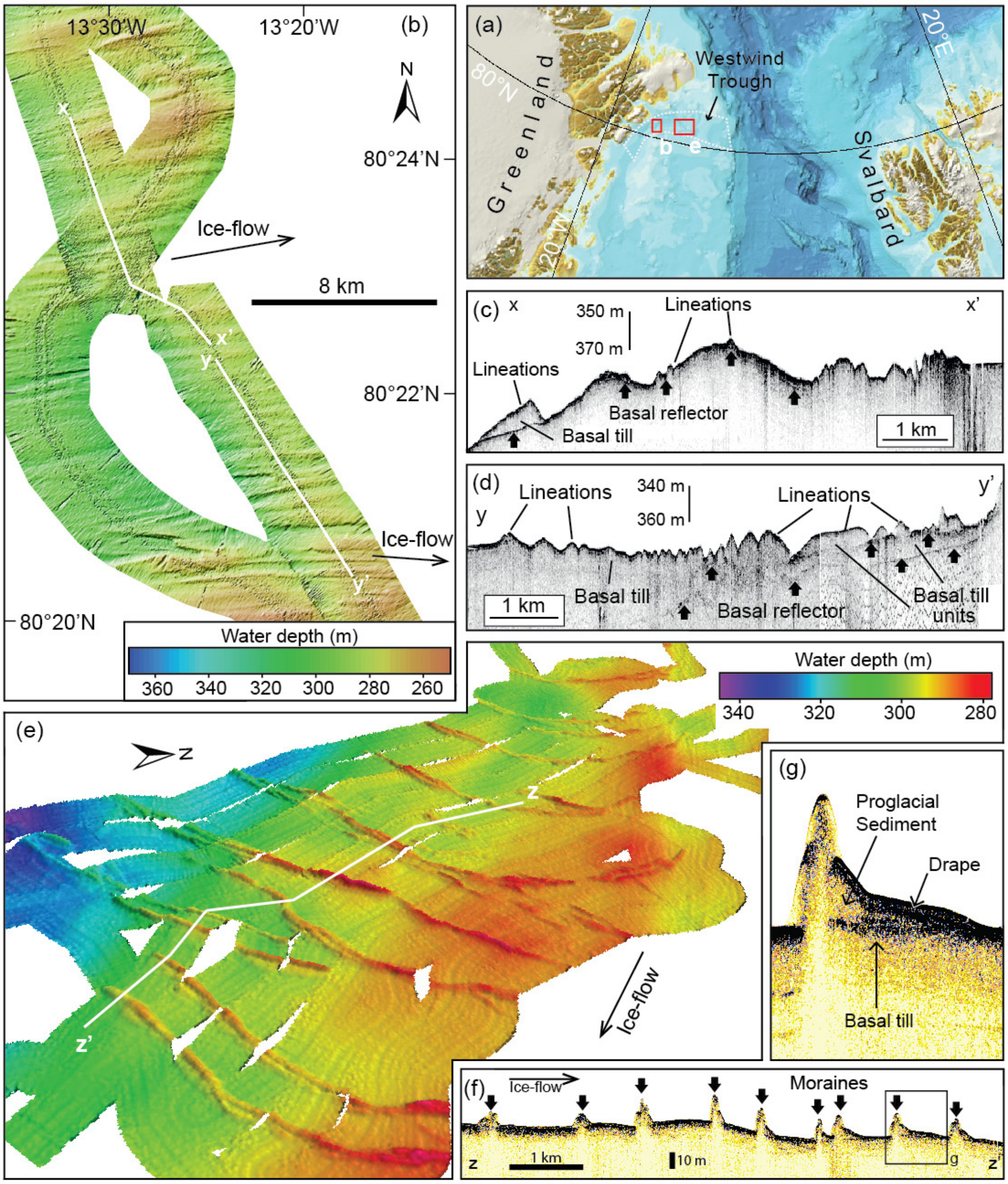

Figure 6.1: Multibeam bathymetry and cross-profiles of glacial lineations and recessional moraines in middle to outer Westwind Trough on the NE Greenland continental shelf. (a) Location map showing the study area (red boxes) (map from IBCAO Version 3.0). (b) Image showing glacial lineations indicating the past expansion of the Greenland Ice Sheet onto the continental shelf [modified from *Evans et al.*, 2009]. Acquisition system Kongsberg EM120. Frequency 12 kHz. Grid-cell size 15 m. (c) and (d) 3.5 kHz subbottom profiles transverse to the trough long-axis (x-x' and y-y' in Fig. 1b) showing glacial lineations formed in an acoustically transparent sedimentary unit consistent with spatially discontinuous to semi-continuous soft basal till. Acquisition system Kongsberg TOPAS PS 018, secondary beam frequency 0.5-6 kHz. (e) 3D oblique view of swath bathymetry showing arcuate to elongate recessional moraines produced along a retreating ice sheet margin. Acquisition system ATLAS Hydrosweep DS2. Frequency 15,5 kHz. Grid-cell size 20 m. (f) and (g) 4 kHz subbottom profiles trough recessional moraines (z-z' in Fig. 1e). The moraines are asymmetric in profile, with steeper west-facing slopes and comprise acoustically transparent sediment consistent with soft basal till. Acquisition system ATLAS PARASOUND, 18 kHz and 22 kHz transmission frequencies. Images in (e), (f) and (g) modified from Winkelmann et al. [2010].

A 160 km² area of the central Westwind Trough (Figure 6.1a) was surveyed systematically by Winkelmann et al. [2010]. A number of ridges are visible in water depths between 270 to 350 m (Figure 6.1e), and are generally oriented roughly orthogonal to the lineations mapped further west in the trough (Figure 6.1b). They are between 10 to 25 m high relative to the surrounding seafloor and up to 7 km long. Most of the ridges are arcuate, a few are more elongated and smaller in height (< 10m). Further, most ridges are asymmetrical in cross-section with the majority having a steeper west-facing slope (Figures 6.1f and g). Subbottom profiler data shows a rather flat surface representing the surface of an acoustic unit extending underneath the ridges (Figure 6.1g). The internal structure of the ridges consists of an acoustically-transparent unit, and both the ridges and intervening flat seafloor are draped by a thin upper acoustic unit.

6.3 Interpretation

The elongated, streamlined sedimentary lineations in inner Westwind Trough (Figure 6.1b) are interpreted as subglacial bedforms produced at the base of an active ice sheet. Comparison with sediments of similar acoustic character, found in close association with subglacial lineations on other polar continental shelves [*Ó Cofaigh et al.*, 2002], indicates that the lineations are formed in the surface of a homogenous soft or dilatant till [*Dowdeswell et al.*, 2004]. The distribution of lineations within a cross-shelf trough are often used as indicators of the former presence of ice streams where fast-ice flow is facilitated by substrate deformation [e.g., *Dowdeswell et al.*, 2004; *Ó Cofaigh et al.*, 2002]. The fresh appearance of the lineations in Westwind Trough suggest an advance of the Greenland Ice Sheet onto the adjacent NEG shelf most probably during the last glacial cycle, and that a fast-flowing ice stream was active in Westwind Trough [*Evans et al.*, 2009]. The apparent lack of retreat moraines and the presence of only a very thin drape of deglacial/postglacial sediments overlying the subglacial lineations on geophysical records from the inner shelf suggest that ice recession through this part of Westwind Trough was relatively rapid [*Dowdeswell et al.*, 2008].

In contrast, transverse-to-flow moraines imply a stepwise deglaciation with multiple halts and minor readvances of the ice-stream grounding-zone [*Dowdeswell et al.*, 2008]. The ridges located further east on the middle shelf (Figures 6.1a and e), based on their asymmetric morphology and their inner structure, are probably recessional push moraines formed during episodic still-stands that punctuated the retreat of a Westwind Trough palaeo-ice stream [*Winkelmann et al.*, 2010]. These recessional moraines are formed at the ice-sheet terminus by bulldozing sediment during minor re-advances of a grounded ice front or by deposition during significant halts [*Golledge et al.*, 2008]. The thin drape of sediments overlying the moraines and adjacent seafloor is probably of Holocene age.

The distribution of lineations on the inner shelf and recessional push moraines on the middle shelf indicate that the speed of the palaeo-ice stream retreat in Westwind Trough was highly variable. In the initial phase of deglaciation, ice retreat was stepwise forming moraines. In a later stage, ice retreat accelerated leaving undisturbed sub-ice stream lineations.

7. A new bathymetry of the Northeast Greenland continental shelf: Constraints on glacial and other processes

Jan Erik Arndt[1], Wilfried Jokat[1], Boris Dorschel[1], Reidun Myklebust[2], Julian A. Dowdeswell[3], and Jeffrey Evans[4]

[1]*Alfred Wegener Institute Helmholtz Centre for Polar and Marine Research, Bremerhaven, Germany*

[2]*TGS-NOPEC Geophysical Company ASA, Asker, Norway*

[3]*Scott Polar Research Institute, University of Cambridge, Cambridge, UK,*

[4]*Department of Geography, Loughborough University, Loughborough, UK*

Published in *Geochemistry, Geophysics, Geosystems, Vol. 16(10), p. 3733-3753, doi: 10.1002/2015GC005931*

Abstract

A new digital bathymetric model (DBM) for the Northeast Greenland (NEG) continental shelf (74°N–81°N) is presented. The DBM has a grid cell size of 250 m 3 250 m and incorporates bathymetric data from 30 multibeam cruises, more than 20 single-beam cruises and first reflector depths from industrial seismic lines. The new DBM substantially improves the bathymetry compared to older models. The DBM not only allows a better delineation of previously known seafloor morphology but, in addition, reveals the presence of previously unmapped morphological features including glacially derived troughs, fjords, grounding-zone wedges, and lateral moraines. These submarine landforms are used to infer the past extent and ice-flow dynamics of the Greenland Ice Sheet during the last full-glacial period of the Quaternary and subsequent ice retreat across the continental shelf. The DBM reveals cross-shelf bathymetric troughs that may enable the inflow of warm Atlantic water masses across the shelf,

driving enhanced basal melting of the marine-terminating outlet glaciers draining the ice sheet to the coast in Northeast Greenland. Knolls, sinks, and hummocky seafloor on the middle shelf are also suggested to be related to salt diapirism. North-south orientated elongate depressions are identified that probably relate to ice-marginal processes in combination with erosion caused by the East Greenland Current. A single guyot-like peak has been discovered and is interpreted to have been produced during a volcanic event approximately 55 Ma ago.

7.1 Introduction

The Northeast Greenland (NEG) continental shelf (20°W–5°W and 74°N–81°N) is the broadest shelf along the Greenland margin, extending more than 300 km from the coastline (Figure 7.1). It is bounded to the east by the Fram Strait, the only deep water connection between Arctic Ocean and lower-latitude seas, and to the west by the East Greenland coastline that consists of fjords, islands, and marine-terminating glaciers. Nioghalvfjerdsfjorden Glacier (also referred to as 79°-Glacier), Zachariae Isstrøm, Storstrømmen, and L. Bistrup Bræ (Figure 7.1b) are the major ice streams of the Greenland Ice Sheet in our study area, of which the former three are part of the NEG ice stream (Figure 7.1; NEGIS) that extends up to ~700 km inland [*Joughin et al.*, 2001]. In total, these ice streams drain about 20% of the Greenland Ice Sheet [*Zwally et al.*, 2012]. Over the past few decades, the NEG area of the ice sheet has been thought to be relatively stable compared to other parts of Greenland [*Joughin et al.*, 2010; *Rignot and Kanagaratnam*, 2006]. Recent studies, however, have shown increased ice-sheet thinning in this area [*Helm et al.*, 2014; *Khan et al.*, 2014]. During the late Quaternary, the extent of the NEG glaciers has experienced great variability. For example, 79°-Glacier today has a fringing ice shelf approximately 80 km long and 20 km wide [*Mayer et al.*, 2000]. In the early-mid Holocene, from 7.7 to 4.5 kyrs, this ice shelf was not present [*Bennike and Weidick*, 2001]. In contrast, high-resolution bathymetric observations of submarine glacial features demonstrate that the ice sheet extended onto the continental shelf [*Evans et al.*, 2009; *Winkelmann et al.*, 2010] and possibly reached the shelf edge 300 km to the east during the Last Glacial Maximum (LGM) [*Bennike and Weidick*, 2001]. However, the glacial history of the NEG continental shelf remains poorly known because few records of glacial geomorphology and sediments are available and more constraints on past ice-sheet dynamics are required to understand ice-sheet response in a changing climate. With its exceptional width, the NEG continental shelf represents the largest possible oscillation of the Greenland Ice Sheet and thus is a key region to study past ice-sheet behavior and assess its possible contribution to full-glacial sea level fall. For several other formerly glaciated continental shelves, new regional digital bathymetric models (DBM) have been produced recently [*Dickens et al.*, 2014; *Graham et al.*, 2011; *Nitsche et al.*, 2007], providing new insights on past ice-sheet extent and ice-stream activity through the identification and regional mapping of large-scale glacial features, such as cross-shelf troughs and grounding-zone wedges (GZWs) [e.g. *Batchelor and Dowdeswell*, 2014; *Batchelor and Dowdeswell*, 2015].

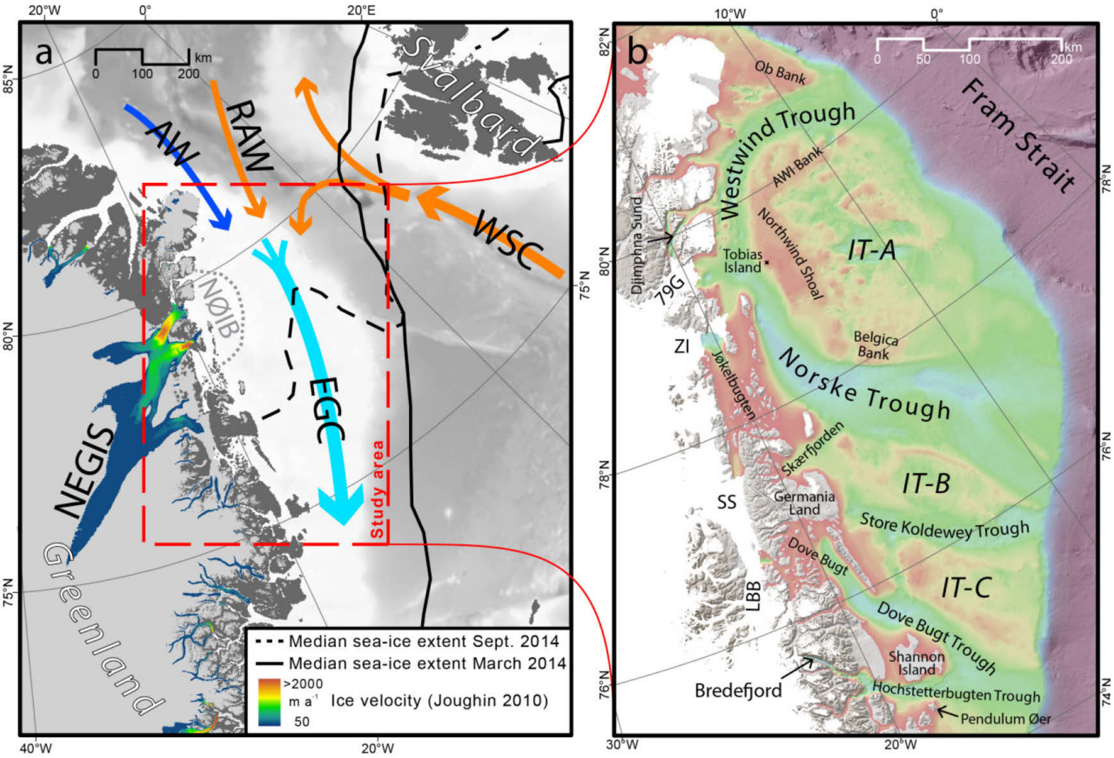

Figure 7.1: (a) Location map of the study area showing sea ice, glaciological, and oceanographic conditions. Ice-sheet velocities are from Joughin et al. [2010]. NEGIS = Northeast Greenland Ice Stream, NØIB=Norske Øer Ice Barrier, AW=Arctic Water, RAW=Return Atlantic Water, WSC=West Spitsbergen Current, and EGC=East Greenland Current. (b) Geographical names mentioned in the text; 79G=79°-Glacier, ZI=Zachariae Isstrøm, SS=Storstrømmen, LBB=L. Bistrup Bræ, and IT=inter-trough areas.

The extend and dynamics of marine-terminating glaciers or ice-streams draining the Greenland Ice Sheet are strongly dependent not only on atmospheric forcing but, additionally, on ocean circulation, which can transport relatively warm water masses to or below the ice front that enhance submarine melting at the grounding-line or underside of the floating margins [*Christoffersen et al.*, 2011; *Hellmer et al.*, 2012; *Holland et al.*, 2008]. The western part of Fram Strait and the NEG outer shelf are influenced strongly by the cold southward-flowing East Greenland Current (Figure 7.1a; EGC) [*Aagaard and Coachman*, 1968]. The currents on the inner shelf are still only poorly understood, with conflicting interpretations suggesting clockwise or counterclockwise water circulation [*Bourke et al.*, 1987; *Budéus and Schneider*, 1995; *Wadhams et al.*, 2006]. Nevertheless, relatively warm Atlantic water (1°C) has been observed at 79°-Glacier [*Straneo et al.*, 2012] that must have crossed the continental shelf from the east. The movement of water masses on the continental shelf is dependent, in part, on bathymetric pathways that allow the density-driven exchange of water masses. Accordingly, modeling of such systems relies on accurate knowledge of shelf bathymetry.

The geology of the NEG continental shelf is related to the highly variable and complex breakup of the North Atlantic Ocean and Fram Strait, linked to various oblique spreading processes [*Engen et al.*, 2008]. Hamann et al. [2005] showed that the northern part of the NEG shelf consists predominantly of deep sedimentary basins, including areas with salt diapirism and faulting. South of 75°N, the NEG Volcanic Province is present [*Hamann et al.*, 2005]. Occasionally, these processes leave imprints in the form of unique morphological features on the seafloor. Mapping these features allows a greater horizontal resolution for geological interpretations that have previously relied on limited seismic data coverage.

The EGC continuously transports sea ice from the Arctic Ocean, resulting in year-round harsh sea ice conditions on the NEG shelf. In addition, a large area of land-fast sea ice, named Norske Øer Ice Barrier (Figure 7.1a), was present for decades and has recently started to break up more regularly in late summer [*Hughes et al.*, 2011]. Therefore, the NEG shelf is typically inaccessible to research vessels collecting bathymetric data. This situation has changed dramatically in the last decade with periodically light sea-ice conditions even in the northern parts of NEG enabling seafloor bathymetric data to be acquired during a number of geoscience cruises.

Bathymetry data for the NEG continental shelf were first described by Johnson and Eckhoff [1966], indicating the wide extent of the shelf. Later, bathymetric models described trough structures on the shelf [*Perry et al.*, 1980]. The most recent regional compilation was published in 1994 [*Cherkis and Vogt*]. Today, the bathymetry of the NEG shelf is best described by the International Bathymetric Chart of the Arctic Ocean (IBCAO) Version 3.0 [*Jakobsson et al.*, 2012b]. These data sets, however, are outdated or, in case of IBCAO, are part of larger pan-Arctic compilations that cannot focus on relatively small regions and, thus, have more artifacts and/or missing data in comparison to a designated regional compilation.

Here we present a new regional digital bathymetric model (DBM) for the NEG continental shelf. This DBM was produced using both new and reprocessed bathymetric data. The core of the database consists of 30 cruises with multibeam echo sounder data and more than 20 cruises with single-beam echo sounder data from 1985 until the present. In addition, seismic first reflector data, echo-sounding data from an autonomous undersea vehicle (AUV), CTD maximum depths, as well as topographic under-ice data have been integrated in the database. The database was gridded at a cell size of 250 m 3 250 m, which is twice as high as older models. These improvements make it possible to reveal for the first time previously unmapped seafloor landforms and to improve the resolution and description of the morphology of the NEG continental shelf. Based on the new DBM, we have mapped and described various morphological seafloor features on the NEG shelf. These provide information on the extent, pathways, and behavior of past ice streams draining the NE sector of the Greenland Ice Sheet and the location of active salt diapirism. Furthermore, the DBM serves as an important boundary condition for future oceanographic and biological research in the region.

7.2 Data

7.2.1 DBM Base Data

The compilation of the NEG DBM is based on bathymetric, topographic, and under-ice bedrock elevation data (Table 7.1 and Figure 7.2). In addition to echo-sounding data from research vessels, first reflector depth data from systematic seismic surveys have been made available by TGS and Autosub-II AUV data from mission M365 underneath Norske Øer Ice Barrier (Figure 7.1) [*Wadhams et al.*, 2006] have been integrated.

For areas without any acoustic soundings, alternate data sets were used to constrain the water depth. Maximum depths of CTD casts were used as minimum depth information in areas where the resulting gridded depths were otherwise shallower. Furthermore, the bathymetric map of Cherkis and Vogt [1994] was used to infer contours close to the coast. In addition, we added inferred contours at 5 m above sea level for islands that were not represented by the topographic data sets. Some of these islands were identified offshore of the Nioghalvfjerdfjorden ice shelf edge from satellite imagery [*NASA Landsat Program*, 2000]. Tuppiap Qeqertaa (Tobias Island) on Northwind Shoal was described by Bennike et al. [2006] (Figure 7.1b). The locations of inferred contours are shown in the source identifier grid that accompanies the DBM (Figure 7.2 and Appendix B).

Table 7.1: Data Sets used in the Digital Bathymetric Model[a]

Type	ID	Year	Vessel	Source	Reference
Multibeam	ARK-III/2	1985	FS Polarstern	AWI	Klenke and Schenke 2002
	ARK-III/3	1985	FS Polarstern	AWI	Klenke and Schenke 2002
	ARK-IV/1	1987	FS Polarstern	AWI	Klenke and Schenke 2002
	ARK_IV/3	1987	FS Polarstern	AWI	Klenke and Schenke 2002
	ARK-VII/1	1990	FS Polarstern	AWI	
	ARK-VII/3a	1990	FS Polarstern	AWI	Klenke and Schenke 2002
	ARK-VII/3b	1990	FS Polarstern	AWI	
	ARK-VIII/3	1991	FS Polarstern	AWI	Klenke and Schenke 2002
	ARK-X/1	1994	FS Polarstern	AWI	
	ARK-X/2	1994	FS Polarstern	AWI	
	ARK-XI/2	1995	FS Polarstern	AWI	Klenke and Schenke 2002
	ARK-XIII/2	1997	FS Polarstern	AWI	
	ARK-XIII/3	1997	FS Polarstern	AWI	Klenke and Schenke 2002
	ARK-XV/2	1999	FS Polarstern	AWI	
	ARK-XVI/1	2000	FS Polarstern	AWI	
	ARK-XVII/1	2001	FS Polarstern	AWI	
	ARK-XVIII/1	2002	FS Polarstern	AWI	
	ARK-XVIII/2	2002	FS Polarstern	AWI	
	ARK-XIX/4a	2003	FS Polarstern	AWI	
	ARK-XIX/4b	2003	FS Polarstern	AWI	
	ARK-XX/2	2004	FS Polarstern	AWI	
	ARK-XX/3	2004	FS Polarstern	AWI	
	ARK-XXIV/3	2009	FS Polarstern	AWI	Winkelmann et al. 2010
	ARK-XXVII/1	2012	FS Polarstern	AWI	
	ARK-XXVIII/2	2014	FS Polarstern	AWI	
	ARK-XXVIII/3	2014	FS Polarstern	AWI	
	ARK-XXVIII/4	2014	FS Polarstern	AWI	
	LOMROG	2007	RV Oden	SU	Jakobsson et al. 2008a, 2010
	NEGC2008	2008	RV Oden	SU	
	JR106	2004	RRS JC Ross	SPRI	Evans et al. 2009
Singlebeam	ARK-IX/2	1993	FS Polarstern	AWI	
	ARK-IX/3	1993	FS Polarstern	AWI	
	ARK-XIII/1	1997	FS Polarstern	AWI	
	ARK-XIV/2	1998	FS Polarstern	AWI	
	ARK-XV/1	1999	FS Polarstern	AWI	
	ARK-XV/3	1999	FS Polarstern	AWI	
	ARK-XVI/2	2000	FS Polarstern	AWI	
	ARK-XIX/2	2003	FS Polarstern	AWI	
	ARK-XX/1	2004	FS Polarstern	AWI	
	ARK-XXI/1	2005	FS Polarstern	AWI	
	ARK-XXIII/1	2008	FS Polarstern	AWI	
	ARK-XXIII/2	2008	FS Polarstern	AWI	
	ARK-XXIV/1	2009	FS Polarstern	AWI	
	ARK-XXV/1	2010	FS Polarstern	AWI	
	ARK-XXV/2	2010	FS Polarstern	AWI	
	ARK-XXVI/1	2011	FS Polarstern	AWI	
	various cruises	2008-14		NPI	
	1 cruise	2009	MV Arctic Sunrise	WHOI	
	PLRSEA90	1990	USCGC Polar Sea	USN	
Seismic first reflector	NEG08	2008		TGS	
	NEG09	2009		TGS	
	NEG10	2010		TGS	
	NEG11	2011		TGS	
	NEG12	2012		TGS	
	NEG13	2013		TGS	
	NEG14	2014		TGS	
	64 single shots	1998-99		AWI	Mayer et al. 2000
AUV-Singlebeam	M365	2004	Autosub-II	SPRI	Wadhams et al. 2006
CTD (max depths)	25 casts	-		NODC	
	9 casts	1998-99		AWI	Mayer et al. 2000
	3 casts	-		NPI	
Topography	GIMP	2014		BPRC	Howat et al. 2014
Bedrock topography	-	2014		UCI	Morlighem et al. 2014

[a]AWI = Alfred Wegner Institute; BAS = British Antarctic Survey; BPRC = Byrd Polar Research Center; NODC = National Oceanographic Data Center; NPI = Norske Polar Institute; UCI = University of California, Irvine; USN = U.S. Naval Research Laboratory; SPRI = Scott Polar Research Institute; SU = Stockholm University; WHOI = Woods Hole Oceanographic Institute.

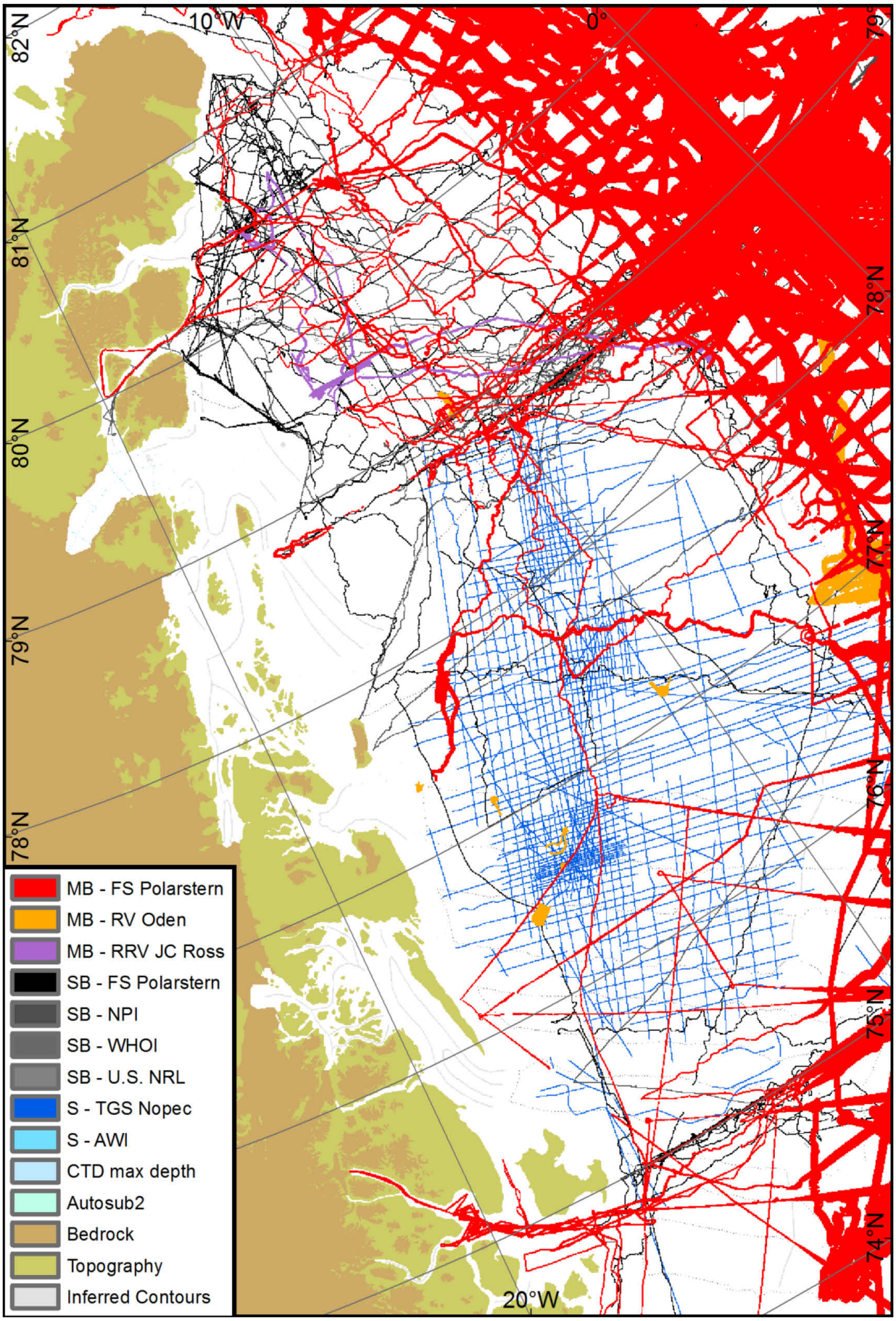

Figure 7.2: Bathymetric data coverage map for the Northeast Greenland shelf and deeper water showing the locations of different data sources. MB = Multibeam echo-sounding; SB = Single-beam echo-sounding; S = First reflector picked from seismic data.

7.2.2 Seismic Data for Interpretation

Multichannel seismic data were used from FS Polarstern cruise ARK-XV/2 (for location see Figure 7.4). The data were acquired in heavy ice with a 1600 m long 64-channel streamer using a tuned air gun cluster with a total volume of 24l (8VLF air guns). In addition, 14 sonobuoys were deployed during this cruise to better determine the seismic velocities of the subsurface.

7.3 Methods

7.3.1 Bathymetric Data Processing

All Polarstern multibeam and single-beam data were edited with CARIS HIPS and SIPS software and, finally, extracted as XYZ ASCII data. Multibeam and single-beam data from other vessels were available as partly cleaned XYZ ASCII data. All bathymetric points were checked and further cleaned with QPS Fledermaus software using the PFM file format. Single-beam data were acquired using 1500 m/s as the standard sound velocity through water. At crossing points between single-beam data and multibeam data surveys, we were able to estimate a reasonable sound velocity from the depth differences and to correct the single-beam measurements to a common depth reference.

7.3.2 Topographic Data Processing

In glaciated regions, bedrock topography underneath the ice sheet is the continuation of shelf bathymetry. The onshore part of the study area comprises of ice-covered and ice-free landscapes. The Greenland Ice Mapping Project (GIMP) DEM [*Howat et al.*, 2014] describes the ice sheet surface and the ice-free topography, and this was used for ice-free areas in the NEG DBM. For ice-covered areas, we used the icepenetrating radar-derived under-ice bedrock data set from Morlighem et al. [2014].

The GIMP DEM showed erroneous data leading to artifacts in the surface representation in some areas (e.g., spikes or holes). Therefore, we exported the DEM as a XYZ ASCII point cloud and removed these errors using a QPS Fledermaus PFM file. The cleaned point cloud was then gridded at 200 m resolution with a spline under tension algorithm [*W H F Smith and Wessel*, 1990] to fill the data gaps that resulted from the data editing.

The GIMP DEM and the data set from Morlighem et al. [2014] used ellipsoidal WGS84 altitude as the vertical reference. All bathymetric data are referenced to mean sea level. In NEG, the difference between ellipsoidal and mean sea level is approximately 30–50 m. When combining the bathymetric and land-topographic data sets, their vertical datum has to be the same. Accordingly, we transformed the vertical reference of the topographic data to the EGM2008 geoid that approximately matches mean sea level.

The elevation data sets were clipped and integrated into the DBM by applying masks on the bedrock and topographic elevation data sets. These masks were derived from the ice-covered and ice-free terrain classification masks of GIMP [*Howat et al.*, 2014]. Where the GIMP DEM had erroneous areas, as mentioned above, the masks misleadingly indicated ocean grid cells. Both masks where manually cross checked for errors by comparison to satellite imagery and the adjacent topography. In the area of 79°-Glacier, and particularly on the floating ice shelf at its margin, the ice mask was modified to use the seismic measurements of Mayer et al. [2000] as under-ice bedrock elevation instead of the data set of Morlighem et al. [2014]. Finally, the masked topographic and under-ice bedrock elevation data sets were converted to XYZ ASCII. Figure 7.2 shows ice-free and ice-covered areas where bedrock elevation data have been used.

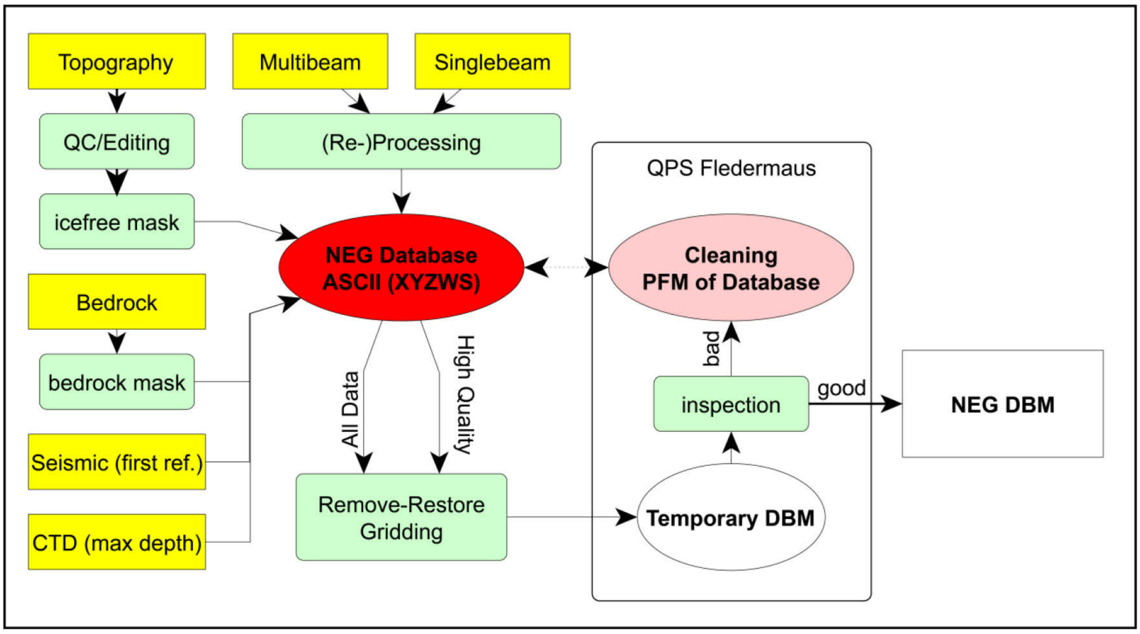

Figure 7.3: Scheme showing data-processing and gridding steps to produce the Northeast Greenland digital bathymetric model (NEG DBM). Yellow boxes represent data sources, green boxes are processing steps, and white boxes are the digital bathymetric models.

7.3.3 Gridding

The overall working scheme of the gridding process is shown in Figure 7.3. The XYZ ASCII files of all data sources form the data base of the NEG DBM. In addition to position and elevation (XYZ), a weighting value and a source identification number were assigned to each data point (XYZWS) to retain information on the data source. The DBM was calculated in a polar stereographic projection with latitude of origin at 70°N and the central meridian at 45°W (EPSG:3413—WGS 84 NSIDC sea ice polar stereographic north). It covers an area of approximately 400,000 km2 and includes the NEG continental shelf from ~74°N to 81.5°N.

The DBM was gridded with a multiresolution gridding algorithm which has also been used in other bathymetric compilations [*Arndt et al.*, 2013; *Hell and Jakobsson*, 2011; *Jakobsson et al.*, 2012b]. This technique produced a smooth interpolated surface in areas with sparse data, while retaining detailed information of the seafloor morphology, where data quality and density were sufficient. Two grid cell sizes were used: a 250 m × 250 m cell size was used as high resolution and 500 m 3 500 m cell size as low resolution. To minimize artifacts at the boundary between high and low-resolution areas, we used a bending algorithm [*Arndt et al.*, 2013] in a transition zone of 500 m. The resulting DBM was checked visually after gridding for artifacts in the QPS Fledermaus software. Checking the DBM and cleaning the database was repeated in an iterative process (Figure 7.3), until the DBM showed satisfactory results. During this process, further inferred contours were added in data gaps where the interpolation yielded unrealistic results in comparison to well-surveyed adjacent bathymetry or topography. Detailed information on the location of inferred contours can be obtained from the source identifier grid (Figure 7.2 and supporting information).

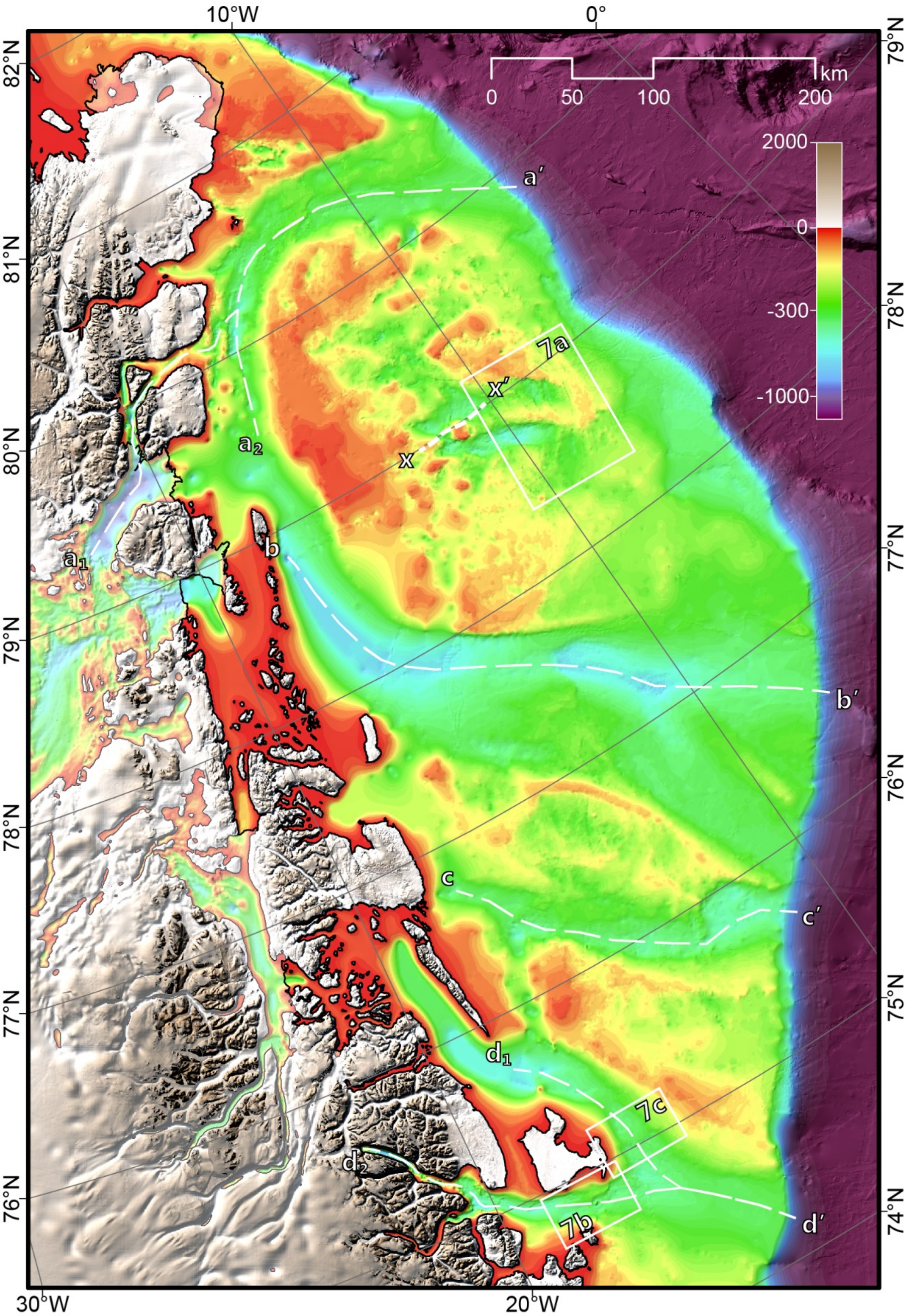

Figure 7.4: The new digital bathymetric model of the Northeast Greenland continental shelf based on the data shown in Table 7.1 and Figure 7.2. Black line shows the present-day coastline. White dashed lines show the locations of bathymetric profiles given in Figures 7.5 and 7.6 and the seismic line AWI-99080 in Figure 7.9.

7.4 Results

The resulting bathymetric model of the NEG continental shelf and adjacent areas is presented in Figure 7.4. In total, 18% of the grid cells on the NEG continental shelf (down to 1000 m) are constrained directly by depth measurements. These 18% can be broken down into: 9% constrained by multibeam data, 5% by singlebeam data, and 4% by other data such as seismic seafloor reflector and CTD maximum depths (Figure 7.2). Eighty-two percentages of the grid cells on the continental shelf remain unconstrained by depth measurements (Figure 7.2). Nearly 21% of the unconstrained grid cells are more than 5 km away from the nearest sounding, and 8% are more than 20 km away. Most of these unconstrained grid cells are located close to the coast, which has the lowest density sounding coverage of any location across the NEG continental shelf (Figure 7.2). At distances of less than 30 km from the NEG coast, only 8.6% of the grid cells are constrained directly by depth measurements.

7.4.1 Cross-Shelf Troughs

The new bathymetry model shows five prominent cross-shelf troughs which are deeper than the surrounding banks (Figure 7.4). From north to south, these are Westwind Trough, Norske Trough, Store Koldewey Trough, Dove Bugt Trough, and Hochstetterbugten Trough (Figure 7.1b). Together, the trough systems cover more than 40% of the NEG continental shelf with Norske Trough alone covering approximately 20% (Figure 7.4). The shallower shelf areas between the troughs have no names and hereafter are referred to as inter-trough areas. The area between Westwind Trough and Norske Trough is inter-trough area A (IT-A), the inter-trough area between Norske Trough and Store Koldewey Trough is inter-trough area B (IT-B), and the area between Store Koldewey Trough and Dove Bugt Trough is inter-trough area C (IT-C) (Figure 7.1).

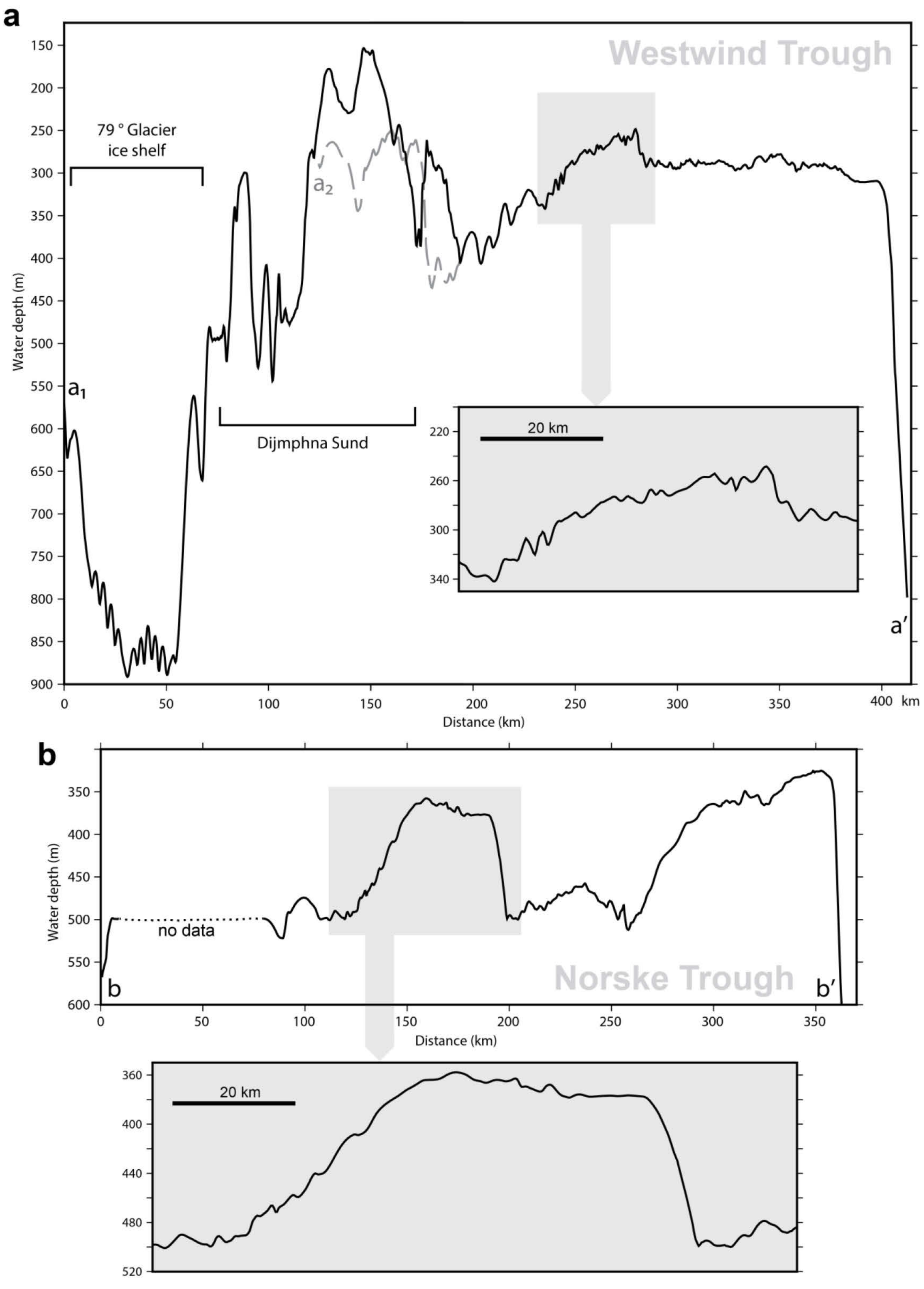

Figure 7.5: Bathymetric profiles of (a) Westwind Trough and (b) Norske Trough; grey insets are enlarged wedge-shaped bathymetric sills that we interpret as grounding-zone wedges; dotted line indicates that this part was not constraint by data. For locations, see Figure 7.4.

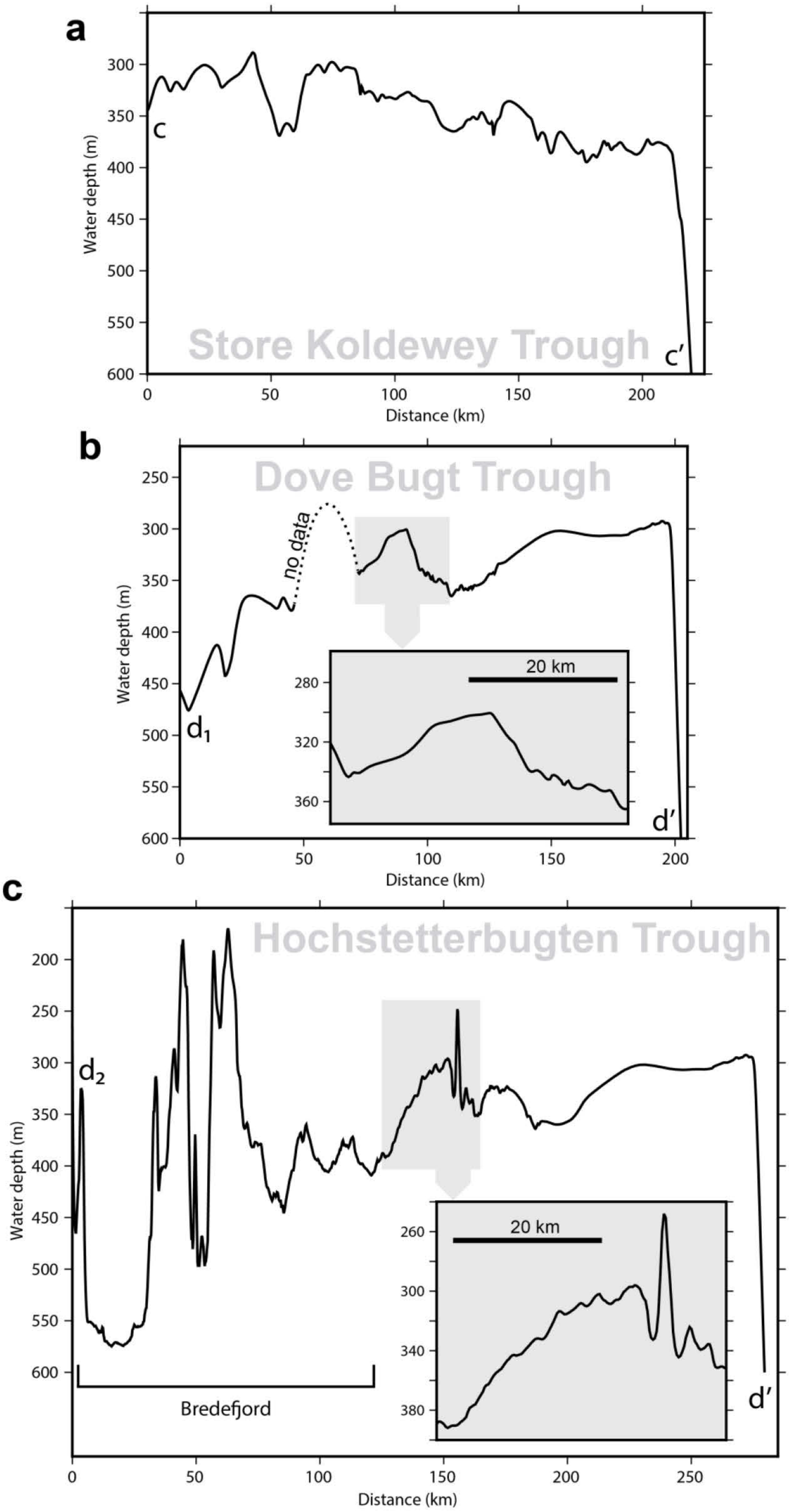

Figure 7.6: Bathymetric profiles of (a) Store Koldewey Trough, (b) Dove Bugt Trough, and (c) Hochstetterbugten Trough; grey insets are enlarged wedge-shaped bathymetric sills that we interpret as grounding-zone wedges; dotted line indicates that this part was not constraint by data. For location, see Figure 7.4.

7.4.1.1 Westwind Trough

Westwind Trough is about 300 km long with a median width of approximately 40 km. The centerline of Westwind Trough curves roughly 908 from north to east in direction (Figure 7.4). The edges of the trough are defined by ridges and banks on either side. On the inner shelf, an elongate ridge is present in the western part of the trough (80°N, 16.5°W). A cross section along Westwind Trough (Figure 7.4, a-a'; Figure 7.5a) shows that it has a reverse slope with a maximum water depth of more than 900 m underneath the ice shelf of 79°-Glacier and 300 m at the shelf edge. On the middle shelf, a wedge-shaped sill is present with a minimum water depth of 240 m at its easternmost position (kilometers 250–280 in Figure 7.5a). A sill at 160 m depth at the entrance of the Djimphna Sund fjord system is the shallowest part of the long profile.

7.4.1.2 Norske Trough

Norske Trough is 350 km long and its width increases from 35 km on the inner shelf to 90 km on the middle shelf and 200 km at the outer shelf (Figure 7.4). The centerline of Westwind Trough curves roughly 70° from a southward to a southeastward direction. Norske Trough has a reverse slope with 560 m maximum water depth at the inner shelf and 320 m at the shelf edge (Figure 7.5b). Close to the shelf edge, two shallower areas are present at 210 and 250 m water depth, respectively (Figure 7.4). On the middle shelf, a large 80 km long bathymetric sill is present where the maximum depth of the trough shallows from 490 to 360 m water depth (kilometers 120–200 in Figure 7.5b). Eastward of the sill, the edges of Norske Trough are defined by ridges (Figure 7.4 and 7.8). The ridge in the north is 50 km long and 30 m high. The ridge in the south is 170 km long and 100 m high.

7.4.1.3 Store Koldewey Trough

Store Koldewey Trough has a less pronounced trough morphology compared to the other four cross-shelf troughs (Figure 7.4). Its centerline is sinuous and oriented in a southeasterly direction over a length of 210 km. Its mean width is approximately 35 km. The cross section (Figure 7.4, c-c'; Figure 7.6a) shows that Store Koldewey Trough does not have a reverse slope but reaches its maximum depth at the shelf edge at 370 m water depth, shallowing to about 300 m on the inner shelf (Figure 7.8).

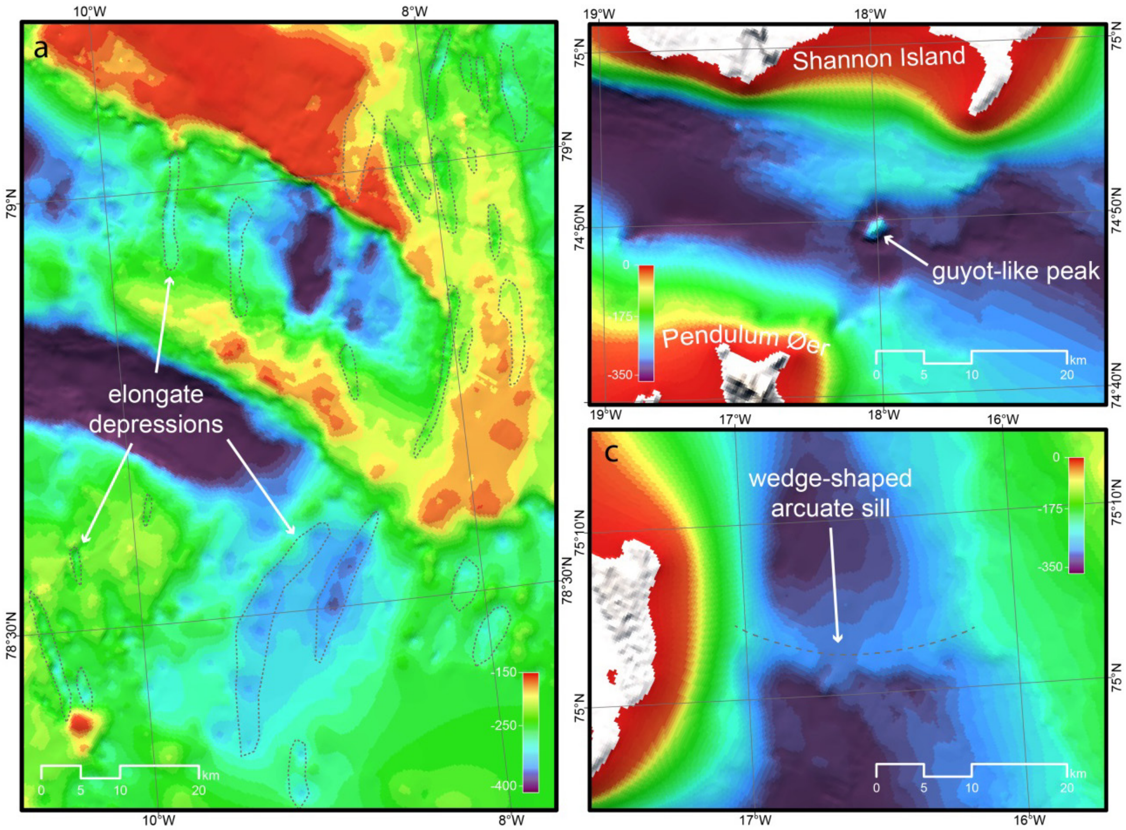

Figure 7.7: Detailed images of the Northeast Greenland bathymetry showing: (a) elongate depressions in inter-trough area A, (b) a guyot-like peak with a ring-shaped depression in Hochstetterbugten Trough, and (c) a wedge-shaped arcuate sill in Dove Bugt Trough. For locations, see Figure 7.4.

7.4.1.4 Dove Bugt Trough

Dove Bugt Trough trends southeastward until it merges with Hochstetterbugten Trough after about 120 km (Figure 7.4). The cross section (Figure 7.4, d-d'; Figure 7.6b) shows that Dove Bugt Trough has a reverse slope with a maximum water depth of about 490 m at the entrance to Dove Bugt and a minimum of about 300 m at the shelf edge. The northern limit of Dove Bugt Trough is defined by two banks with a ridge in between (Figures 7.4 and 7.8). The southern limit is defined by Shannon Island. A sill is present in Dove Bugt Trough (kilometers 70– 90 in Figure 7.6b). The sill has a relative elevation of about 40 m and has a wedge-like relief with a steeper slope in the offshore direction (Figure 7.6b). In plan view, the sill has an arcuate form (Figure 7.7c).

7.4.1.5 Hochstetterbugten Trough

Hochstetterbugten Trough is the continental shelf continuation of Bredefjord (Figure 7.4). On the inner shelf, the trough is still constrained by a mountainous terrain and islands to the north and south until it merges with Dove Bugt Trough east of Shannon

Island. Hochstetterbugten Trough has a reverse slope with a maximum depth on the inner shelf of 450 m water depth and more than 550 m in Bredefjord (Figure 7.6c). At the shelf break, the maximum depth is 300 m (Figure 7.6c). South of Shannon Island, a sill and a single peak are present in the trough (Figure 7.7b). The sill is 80 m high, reaching a minimum water depth of 300 m (Figure 7.6c). The top of the peak is relatively flat at a minimum depth of 250 m, with its flanks dropping abruptly up to 100 m into a ringshaped depression (Figure 7.7b).

7.4.2 Shoals and Banks

The Ob Bank in the very north of the study area is generally between 50 and 100 m deep (Figures 7.1b, 7.4, and 7.8). At its shallowest position, it reaches approximately 40 m in depth. Northwind Shoal is the shallowest part of IT-A with average depths ranging from 20 to 80 m. Banks with an average depth of approximately 100 m are present along the trough edges north (AWI Bank) and south (Belgica Bank) of Northwind Shoal (Figures 7.1b, 7.4, and 7.8). Both banks are interrupted by sinks with depth changes of up to 300 m on AWI Bank and 100 m on Belgica Bank. In IT-B no banks are present. Two banks are present in IT-C, one in the west and one in the southeast. The shallowest point of the westerly bank is at about 45 m water depth. The bank is separated from the Greenland coast by an approximately 15 km wide and 200 m deep channel connecting Store Koldewey Trough with Dove Bugt Trough. The southeasterly bank is on average at 100 m depth.

7.4.3 Undulating Seafloor

The DBM reveals undulating seafloor topography on the central part of IT-A with knolls, sinks, ridges and smaller banks at depths ranging from 80 to 440 m (Figures 7.4 and 7.8). The knolls are defined by a round shape of 10–15 km in diameter and are elevated by more than 100 m compared to the surrounding bathymetry. They appear mainly in the southwestern part of the central IT-A, but a single knoll is located in IT-B (77.4°N, 16.7°W). Features of similar size but not round in shape are present in the east and northeast of the central IT-A (close about 79.5°N, 10°W). They show similar elevation changes as the knolls, but, in contrast, are elongate in shape, have relatively

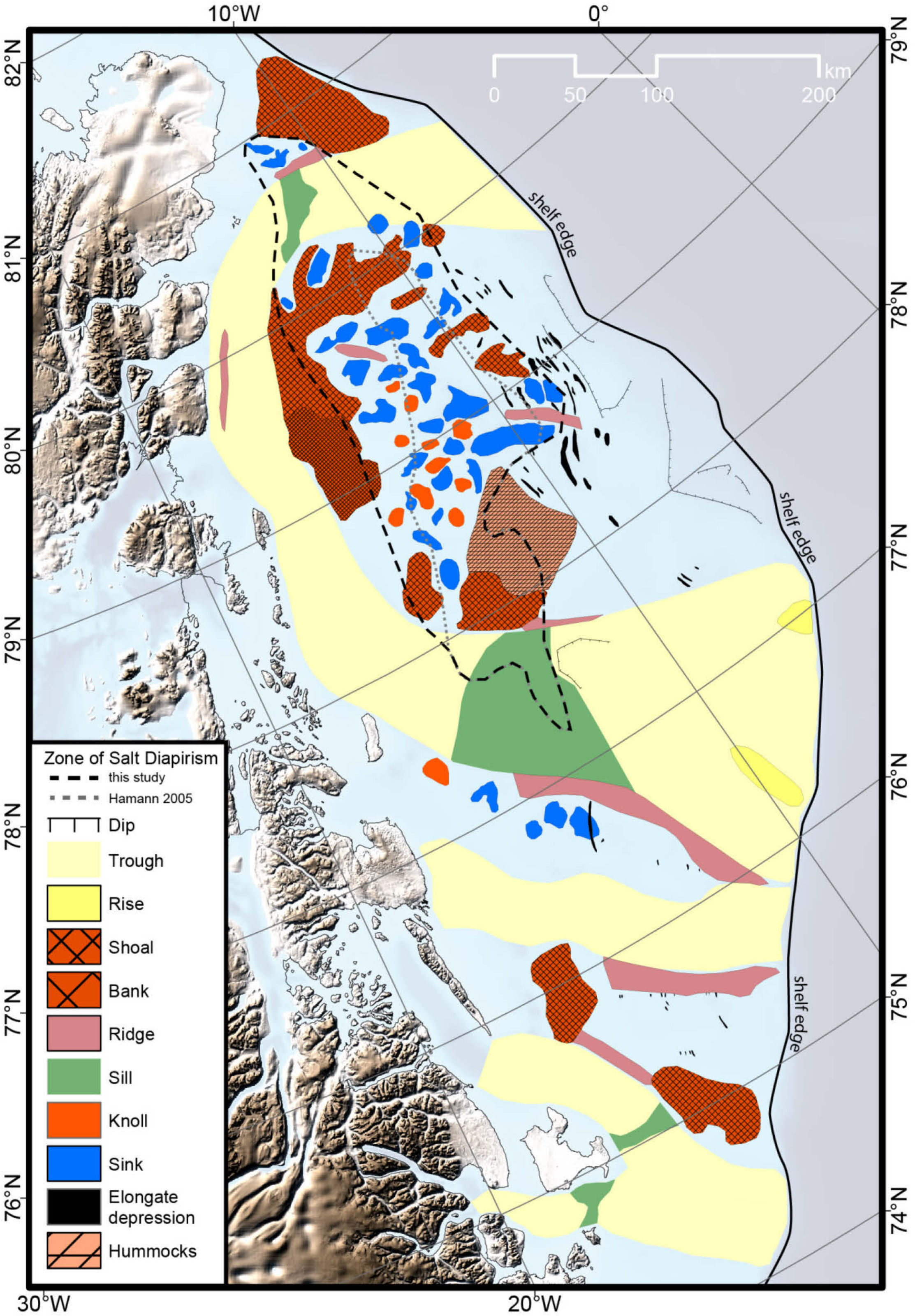

Figure 7.8: Schematic diagram of seafloor features on the Northeast Greenland continental shelf mapped from the digital bathymetric model.

flat tops and an average depth shallower than 100 m. For these reasons, we have classified them as banks rather than knolls (Figure 7.8).

Sinks are abundant from about 81°N to 76.5°N on the middle shelf (Figures 7.4 and 7.8). The bottom of the sinks varies from 200 to 440 m in depth. In the southern middle shelf part of IT-A (around 78.3°N, 12°W), a shallower (approximately 170 m average water depth) and less intensively undulating area is present (Figures 7.4 and 7.8). Instead of showing pronounced knolls and sinks, the seafloor here is hummocky with irregularly undulating elevation changes of about 30 m on average.

The interpreted multichannel seismic profile AWI-99080 crosscuts several knolls and sinks on the undulating seafloor in the central IT-A area (Figures 7.4 and 7.9 for location). The data show subsurface structures down to 2–3 km in depth. Two types of seismic unit can be distinguished in the profile. Type I units are vertically oriented bodies with irregular internal reflectors. Three such bodies are visible in the data; the second reaches the seafloor (Figure 7.9), whereas the other two are draped by Type II seismic units that, in contrast to Type I, have well-laminated internal reflectors. In the proximity of Type I seismic units, the reflectors of Type II units tend to bend upward with the distance between internal reflectors decreasing.

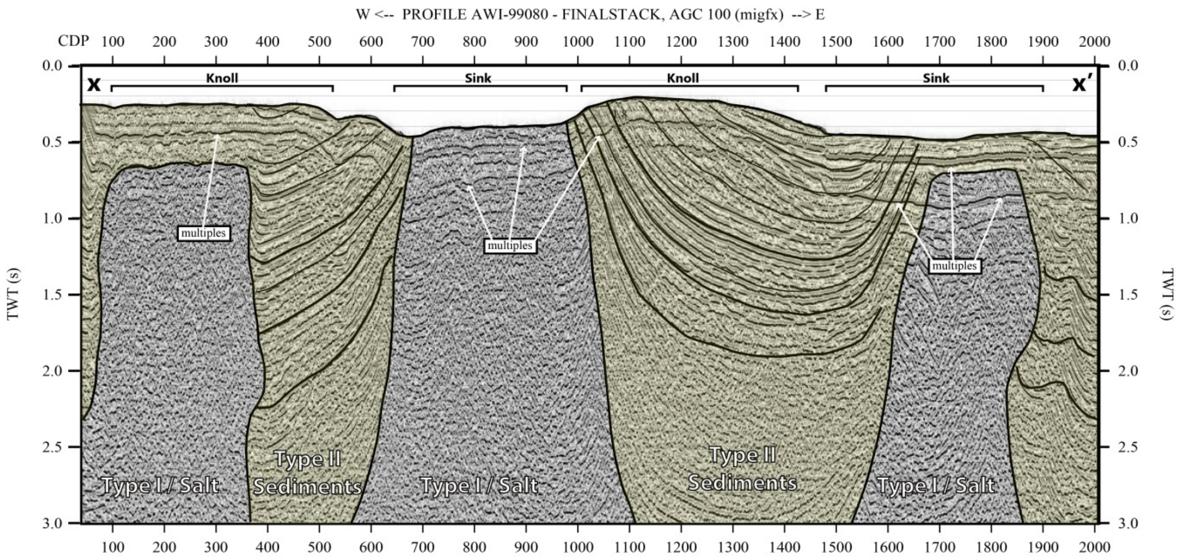

Figure 7.9: Seismic profile AWI-99080 crosscutting bathymetric knolls and sinks, showing that their formation is related to salt diapirism. For location, see Figure 7.4.

7.4.4 Middle Shelf Elongate Depressions

In a north-south strip on the eastern side of IT-A (between 10°W and 7°W), the NEG-DBM reveals the presence of elongate depressions (Figures 7.7a and 7.8). The depressions have a predominantly north-south orientation and often appear in close proximity to one another. They have U-shaped cross profiles. Compared to the adjacent seafloor, the depressions are on average 40 m deep with an average width of 1.5 km; ridges are present between depressions when they are located next to each other. Their maximum detected length is approximately 23 km. Accordingly, the minimum elongation ratio is approximately 1:15. Similar but much smaller elongate depressions are also present on the outer shelf of IT-B and IT-C (Figure 7.8). Hence, these elongate depressions are present from about 79°45'N to 75°15'N over a distance of approximately 500 km. No such features are detected in the cross-shelf troughs.

7.4.5 Fjords

Dijmphna Sund and Bredefjord (Figure 7.1) are the only coastal areas of the study area that are well covered by bathymetric soundings (Figure 7.2). In places, their depths are greater than 500 m. Most of the fjord bathymetry shows a relatively flat seafloor. Occasionally, however, their depth shallows abruptly to 100 m depth in Djimphna Sund and 150 m in Bredefjord within short distances. The other fjord systems are unconstrained by depth soundings, but the subaerial topography shows that they are surrounded mainly by the steep walls of adjacent mountains. In such locations, the fjords were modeled to 50 m water depth in the DBM with inferred contours (Figure 7.2).

The modern-day ice shelf of 79°-Glacier is located in a fjord (Nioghalvfjerdsfjorden; 79.5°N, 21°W) and is approximately 80 km long (Figure 7.4). The seafloor beneath the central part of the ice shelf is at about 900 m deep (Figure 7.5; 30–60 km), with an ice thickness of about 300 m and a water-filled cavity of about 600 m [*Mayer et al.*, 2000]. The northern ice front of 79°-Glacier terminates in Djimphna Sund at a maximum water depth of about 600 m. The eastern ice front is grounded on several ice rises and shows a shallower bathymetry with a maximum observed depth of about 250 m. The maximum depths of CTD stations, east of these ice rises (79.5°N, 19°W), show a deepening bathymetry. The next available depth information to the east is at 450 m water depth underneath the land-fast sea ice of the Norske Øer Ice Barrier (79.3°N, 17.5°W)

[*Wadhams et al.*, 2006]. These few depth constraints suggest a deep (>250 m) representation of this very sparsely mapped area. Hence, we added inferred contours to model this area accordingly. The depths offshore of other glacier margins (Zachariae Isstrøm, Storstrømmen, and L. Bistrup Bræ; Figure 7.1b) have been manually steered down offshore of the ice front to the next reliable bedrock elevation present close to the ice front position.

7.5 Discussion

7.5.1 Digital Bathymetric Model

The new DBM of the NEG continental shelf is based on the most comprehensive and up to date data base of bathymetric soundings and other depth information of this area (Table 1). This made it reasonable to select a grid cell size of 250 m × 250 m, which is twice that of IBCAO Version 3.0 [*Jakobsson et al.*, 2012b]. The number of artifacts in the data set has been limited as much as possible by the iterative cleaning, gridding and quality check steps (Figure 7.3). The combination of bathymetric data with bedrock topography data, instead of ice surface topography, and high-resolution land topography, has led to a smooth ocean-land transition in the DBM (Figure 7.4). In the new bathymetric model, submarine morphological features on the NEG continental shelf are now better resolved or revealed for the first time. Their description and interpretation improves our knowledge of processes taking place on the NEG continental shelf.

Despite the large data base of soundings, in some areas, data coverage is still sparse due mainly to year-round harsh sea-ice conditions linked to the cold East Greenland Current (Figure7. 1a). In these areas, the DBM suffers from reduced quality and reliability. This is most evident in areas close to the coast and in the vicinity of Norske Øer Ice Barrier (Figure 7.1), but also in a few parts of the continental shelf (Figure 7.2). The manually inferred contours attempt to give a realistic representation of the coastal bathymetry by estimating a continuation of the surrounding, better surveyed, bathymetry and topography. The inclusion of inferred contours at 50 m depth in major fjords based on neighboring steep fjord flanks yielded more realistic results than the otherwise <1 m deep fjords without manual steering. Nevertheless, we suggest that most of the fjords are probably several hundred meters deep, based on observations from elsewhere in Greenland [e.g. *Dowdeswell et al.*, 2010a; *Dowdeswell et al.*, 2014], and require further detailed surveys.

7.5.2 Past Ice Flow

High-resolution swath-bathymetric data revealed the presence of mega-scale glacial lineations and recessional moraines in the middle shelf region of Westwind Trough (Figure 7.10) [*Evans et al.*, 2009; *Winkelmann et al.*, 2010]. These glacial-sedimentary landforms are produced subglacially and ice marginally, respectively, and provided the first direct seafloor geomorphological evidence for the expansion and presence of a grounded Greenland Ice Sheet on the NEG continental shelf during the late Quaternary. Furthermore, the presence of MSGL constrained to shelf trough areas indicates that this ice cover contained fast flowing ice streams that preferentially drained through these troughs. A review by Funder et al. [2011], utilizing the evidence from these two papers, suggested that the LGM Greenland Ice Sheet extended at least to the middle continental shelf of NEG (Figure 7.10). However, Bennike and Björck [2002] proposed that the Greenland Ice Sheet extended to the outer shelf, based on radiocarbon dates indicating late onshore deglaciation. This view is further supported by investigations of shallow sedimentary rocks along the East Greenland margin, which are predominantly of glacial origin [*Berger and Jokat*, 2008; *Berger and Jokat*, 2009; *García et al.*, 2012; *Wilken and Mienert*, 2006]. Our new bathymetry reveals the presence of submarine features on the NEG continental shelf that we interpret to be formed by glacial processes. In addition, the presence of subglacial landforms and glacial sediments across the shoals and banks between troughs shows that they were probably influenced by grounded ice flow [*Evans et al.*, 2009] and may have served as base for local marine ice domes that laterally constrained the direction of past ice flow within the troughs.

7.5.2.1 Cross-Shelf Troughs

Cross-shelf troughs are characteristic features of glaciated continental shelves [*Batchelor and Dowdeswell*, 2014]. The reverse slopes observed in the bathymetry of Westwind Trough, Norske Trough, Dove Bugt Trough, and Hochstetterbugten Trough are similar to overdeepened troughs present in other formerly ice-covered regions [*Batchelor and Dowdeswell*, 2014; *Livingstone et al.*, 2012]. These troughs are suggested to be produced by high erosion rates beneath ice streams and rapid sediment transport to the ice-sheet margin during repeated glacial advances and retreats [*ten Brink and Schneider*, 1995]. Thus, this also suggests that the overdeepened troughs visible in the NEG bathymetry indicate ice-stream activity and subglacial erosion during multiple glaciations. Some of the ridges found on the edges of the glacial troughs are also similar in size and shape to lateral moraines found at the margins of other glacially eroded cross-shelf troughs [e.g. *Ottesen et al.*, 2005]. This similarity is most obvious for the two pronounced ridges in Norske Trough (Figures 7.4 and 7.10). Accordingly, we interpret these ridges as lateral moraines that were produced during one or multiple glaciations, probably including the LGM, at the lateral shear margins of former ice streams [*Ottesen et al.*, 2005; *Stokes and Clark*, 2002].

In contrast to the other troughs, Store Koldewey Trough has no reverse slope and the edges of the trough are not well pronounced (Figure 7.4). The ridge identified to the south of Store Koldewey Trough is broader and not as streamlined as those in the other troughs. The land topography implies that the interior ice-sheet basin-area draining into Store Koldewey Trough was much smaller than for the other troughs of the study area and that Store Koldewey Trough only served as a minor drainage path for the Greenland Ice Sheet (Figure 7.10). The mountain ranges between Germania Land and Storstrømmen Glacier (77.3°N, 21°W) provided a north to south trending obstacle for the Greenland Ice Sheet to drain in an eastward direction into Store Koldewey Trough (Figures 7.1b, 7.4, and 7.10). Instead, the north-south oriented fjord of Storstrømmen directs the outflow to Jøkelbugten in the north and Dove Bugt in the south (Figures 7.1b and 7.10). Thus, the drainage-basin area to Store Koldewey Trough is limited to Germania Land. The Germania Land topography suggests that major parts of its ice cover were drained to the north via Skærfjorden as a tributary to Norske Trough and to the south directly into Dove Bugt Trough (Figures 7.1b and 7.10), as also concluded from direct observations from Germania Land [*Landvik*, 1994]. Hence, we suggest that, in contrast to the other studied troughs of NEG with reverse slopes, Store Koldewey Trough probably was not eroded by an ice stream during multiple glaciations.

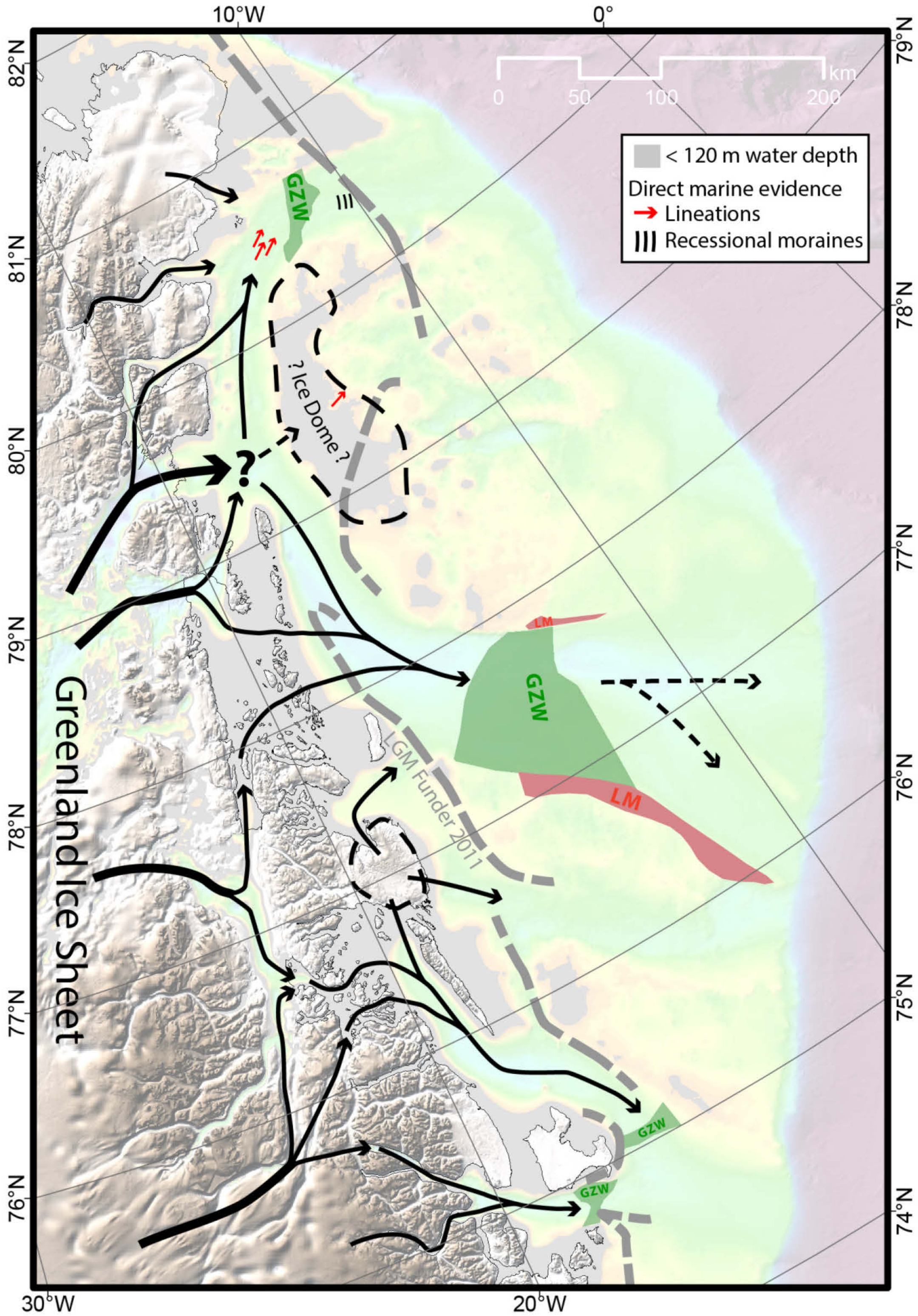

Figure 7.10: Interpretation of the paleo-ice flow on the Northeast Greenland shelf based on morphological features in the digital bathymetric model. Grounding-zone wedges (GZW, green) are located at similar distances from the modern-day fronts of marine-terminating outlet glaciers of the Greenland Ice Sheet. Lateral moraines (LM, red) are found at the sides of Norske Trough. Areas below 120 m water depth (grey) were above sea level at the LGM and could have supported an ice dome (black dashed line) built up on the shelf. The LGM ice extent across the shelf from Funder et al. [2011] is shown as grey dashed line.

7.5.2.2 Grounding-Zone Wedges

During still stands of the ice-sheet margin during regional deglacial retreat, the sediments transported to the terminus can build up sedimentary depositional centers, often referred to as grounding-zone wedges (GZWs) [e.g. *Batchelor and Dowdeswell*, 2015; *Dowdeswell and Fugelli*, 2012]. GZWs are asymmetrical, with a steeper ice-distal side and a longer but low-profile ice-proximal slope [e.g. *Ottesen et al.*, 2007]. Typically, they appear as subdued ridges perpendicular to the ice-flow direction over the entire width of the ice stream [e.g. *Batchelor and Dowdeswell*, 2015; *Jakobsson et al.*, 2012a]. The morphology of the bathymetric sills offshore of NEG shows great similarity to the typical morphology of GZWs (Figures 7.5a, 7.5b, 7.6b, 7.6c, and 7.7c). In addition, since they are located in glacial troughs, we interpret the sills in Westwind Trough, Norske Trough, Dove Bugt Trough, and Hochstetterbugten Trough as GZWs (Figure 7.10). All four GZWs are located on the middle shelf at a similar distance from the modern-day ice margin. Their locations are more or less in accordance with the proposed LGM position of the ice sheet at Westwind Trough, Dove Bugt Trough, and Hochstetterbugten Trough (Figure 7.10) [*Funder et al.*, 2011]. The GZW found in Norske Trough is further offshore compared to the proposed LGM ice-sheet margin. Batchelor and Dowdeswell [2015] mapped 10 buried or seafloor GZWs in Norske Trough from seismic data, including a seafloor GZW on the outer shelf. Nine buried or near-seafloor GZWs have also been mapped using seismic records from Store Koldewey Trough [*Batchelor and Dowdeswell*, 2015]. Hence, the LGM position around Norske Trough was probably located further offshore than suggested by Funder et al. [2011].

7.5.2.3 Local Marine Ice Dome

Tuppiaq Qeqertaa (Tobias Island), located on the western edge of Northwind Shoal about 70 km off the NEG coast (Figure 7.1), is today covered by a small ice cap that rises to 35 m above sea level [*Bennike et al.*, 2006]. The sea ice of the Norske Øer Ice Barrier develops each year around the island or around icebergs that ground in the shallow waters of Northwind Shoal [*Hughes et al.*, 2011]. The shallow areas of the NEG shelf are clearly important in the buildup of landfast sea-ice today and, thus, may have acted as areas of initial buildup of marine-based ice sheets in the past [*Berger and Jokat*, 2009]. During LGM, global sea level was approximately 120 m lower than today [*Rohling et al.*, 2009]. The DBM shows that large parts of the western IT-A are less than 120 m deep (Figure 7.10). Hence, under such conditions, the shoals and banks mapped on the DBM would have been emergent above sea level and could have served as bases of local marine ice dome, probably building up at the location of the modern-day small ice cap on Tobias Island (Figure 7.10).

Lavoie et al. [2015] investigated a bathymetric compilation around the Antarctic Peninsula and inferred the presence of seven local marine ice domes. These ice domes served as lateral constraints that guided the ice stream outlets. The planform of the Westwind Trough and Norske Trough centerlines indicates that ice flow draining across the shelf from the Greenland Ice Sheet was most likely redirected in a northward and southward direction around Northwind Shoal (Figure 7.10). Hence, we suggest that this redirection was probably constrained by an ice dome on NWS, similar to the ice domes suggested for the Antarctic Peninsula. Evans et al. [2009] showed that ice flow was active directly northeast of Northwind Shoal (Figure 7.10). Thus, assuming a complete redirection of the ice flow at Northwind Shoal as suggested by the trough morphology, the separate marine ice dome on the shoal was the source of this ice stream activity. Given an elevation above full-glacial sea level and an ice thickness large enough to initiate streaming ice, this ice dome could have harbored a significant contribution to sea level change. Using a rough calculation for ice dome thickness as used by Lavoie et al. [2015] with an estimated ice temperature of -20°C, a precipitation rate of ~150 mm a^{-1} [*Ohmura and Reeh*, 1991], and an ice dome radius of 40–50 km yields an approximate thickness of 900 m in center of the dome. Estimating a more moderate ice thickness of 500 m for the entire inter-trough areas (~100,000 km2) would yield an equivalent sea level rise of about 0.14 m; this contribution would clearly vary with the actual thickness and extent of glacier ice.

For verification of the ice dome presence, however, high-resolution bathymetric investigations of submarine glacial features in the area west of Northwind Shoal are necessary in order to determine if the ice flow from the Greenland Ice Sheet was crossing Northwind Shoal or if it was redirected into Westwind Trough and Norske Trough. However, the acquisition of such data has so far been impeded due to the persistence of the Norske Øer Ice Barrier.

7.5.2.4 Fjords

All fjord systems in our study area were covered by the Greenland Ice Sheet during the LGM and probably a number of previous glaciations, a pattern similar to that elsewhere in East Greenland [e.g. *Dowdeswell et al.*, 2010a; *Dowdeswell et al.*, 1994b; *Evans et al.*, 2002]. Thus, the deeply incised Dijmphna Sund and Bredefjord, as well as the other unsurveyed fjords in the area, are a result of glacial erosion from streaming ice that drained the expanded Greenland Ice Sheet during multiple Quaternary glaciations (Figure 7.10). Fjord systems can experience very high sediment accumulation rates, of up to 20 cm a21, when the ice is retreating, leading to sediment thicknesses of up to several hundred meters [e.g. *Hjelstuen et al.*, 2009]. Thus, we interpret the flat seafloor in parts of Dijmphna Sund and Bredefjord as the uppermost layer of postglacial sediments that partially filled the deeply incised glacially eroded fjords after deglaciation. Predominantly, these sediments were transported to the fjord by glaciers and released at the ice-sheet margin or transported by drifting icebergs as observed in the more southerly Scoresby Sund [*Dowdeswell et al.*, 1994a; *Julian A. Dowdeswell et al.*, 2000; *Ó Cofaigh et al.*, 2001; *Syvitski*, 1989]. However, it cannot be ruled out that the fjord sedimentary record also includes some fluvial and glacifluvial sediments that are transported along valleys in summer melting seasons in periods of a warmer climate and in modern conditions [*Hasholt*, 1996]. The steep rises and shallow intersections in fjord bathymetry are interpreted as bedrock outcrops [e.g. *Dowdeswell et al.*, 2014].

7.5.3 Water Mass Pathways

Satellite observations have revealed recent ice loss from marine-terminating glaciers in NEG [*Helm et al.*, 2014; *Khan et al.*, 2014]. Studies from elsewhere in Greenland and Antarctica have showed that the rate of ice loss by basal melting at marine-terminating glaciers is linked to the flow of warm water masses to the glacier that enhance basal melting, especially where a floating ice shelf or ice tongue is present [*Christoffersen et al.*, 2011; *Hellmer et al.*, 2012; *Holland et al.*, 2008; *Pritchard et al.*, 2012]. Warm Atlantic water, providing energy for basal melting, is also observed in several fjords around Greenland, including the 79°-Glacier [*Straneo et al.*, 2012]. The pathway of the water masses on the continental shelf is crucial for the temperature of this Atlantic water due to atmospheric heat loss and increased mixing with Polar Water at shallow locations [*Straneo et al.*, 2012]. Cross-shelf troughs with a reversed bathymetry have been demonstrated elsewhere to act as deep pathways that can direct warmer water into ice-shelf cavities, enhancing basal melting [*Hellmer et al.*, 2012; *Walker et al.*, 2007]. By contrast, bathymetric sills in a trough can also stabilize a retreating ice sheet in times of global warming by preventing the inflow of warmer water masses to the ice sheet margin [*Jenkins et al.*, 2010] and also by acting as pinning points and reducing iceberg production in relatively shallow water. Thus, the bathymetry of the cross-shelf troughs, fjords, and their sills is a key parameter for modeling the water mass exchange from the ocean to the glaciers and its impact on basal melting. The DBM reveals that all four major marine-terminating glaciers in the survey area (79°-Glacier, Zachariae Isstrøm, Storstrømmen, and L. Bistrup Bræ; Figure 7.1) are located at the western end of cross-shelf troughs with a reverse slope in bathymetry (Figure 7.4) that would allow the inflow of warm water to the ice front. Bathymetric sills in the troughs on the shelf and the fjord systems are obstacles in this pathway. The DBM defines these features and serves as an important morphological boundary condition for oceanographic modeling.

7.5.4 Halokinesis

The spatial distribution of knolls, sinks, and hummocky seafloor on the continental shelf of NEG (Figure 7.8) shows strong congruence to the previously mapped area of salt diapirism [*Hamann et al.*, 2005]. Seismic line AWI-99080 crosses knolls and sinks in the central IT-A area (Figure 7.4). We interpret acoustic unit Type I as uplifted salt structures (Figure 7.9). Occasionally, these salt structures crop out at the seafloor (Figure 7.9). Here they can be dissolved by seawater and form sinks. The sedimentary layers between the salt bodies (acoustic unit Type II) are synclinal in form and thin toward the salt bodies. The seafloor reflector of the seismic line demonstrates that the undulating seafloor topography in this area is influenced by the salt tectonics active beneath (Figure 7.9). Synclinal reflectors in the top sedimentary layers have also been identified in subbottom profiler data in the northern part of IT-A [*Evans et al.*, 2009]. These reflectors were linked to subaqueous sediment gravity flows at an ice-sheet margin or to glacitectonism of older unconsolidated sediments after an ice advance. The similarity of the top reflectors visible in the subbottom profiler data to those visible in the seismic data, however, suggests that both were caused by salt tectonics. Hence, we conclude that the undulating seafloor topography, where knolls, sinks, and hummocky seafloor were mapped from the DBM, is most probably related to salt diapirism active underneath. Accordingly, we suggest that the area of salt tectonic activity is larger than previously estimated at approximately 33,000 km2 (Figure 7.8), extending further to the northwest than the previously estimated area, which was based on a limited number of seismic lines (Figure 7.8) [*Hamann et al.*, 2005].

7.5.5 Elongate Depressions

The mainly north-south trending elongate depressions on the middle to outer shelf of NEG, illustrated in Figure 7.7a and mapped in Figure 7.8, were only detected in areas with relatively dense bathymetric data coverage (Figure 7.2). The reduced length of the more southerly elongate depressions is likely due to the lower coverage with high-resolution sounding data in that area. Here additional elongate depressions are probably present on the continental shelf but remain unresolved in the DBM.

The elongate depressions appear in basins filled with several kilometer-thick sediments [*Hamann et al.*, 2005]. They are located in the area of the north to south flowing EGC. While the major part of the EGC flows through the deeper western part of Fram Strait and along the continental slope, the EGC also flows over the middle to outer shelf of NEG at about 79°N and 8°W. Here a steady north to south water flow has been observed [*Bourke et al.*, 1987; *Budéus and Schneider*, 1995; *Rabe et al.*, 2009]. On the inner shelf, where no elongate depressions have been found, the currents are relatively less intense and show more fluctuations [*Bourke et al.*, 1987; *Budéus and Schneider*, 1995; *Wadhams et al.*, 2006]. The location of the elongate depressions could coincide with a full-glacial ice margin close to the shelf edge. If this is so, the depressions could have been formed by ice-marginal processes, possibly in combination with erosion caused by the EGC. The depressions may have formed: (a) between ice-marginal sedimentary deposition centers or are landforms produced by proglacial and submarginal glacitectonics, e.g., moraines or composite ridges [*Benn and Evans*, 2010] or (b) by a strengthened EGC that eroded sediments along a stable past ice margin, similar to moat structures at the base of continental slopes [*Rebesco et al.*, 2014]. The absence of elongate depressions in the cross-shelf troughs of NEG may be due to the presence of overconsolidated sediments, caused by ice flow in the troughs, that are less prone to erosional forces than noncompacted sediments. A systematic high-resolution bathymetric survey of the elongate depressions in combination of shallow seismic data acquisition across the depressions is needed to verify our interpretation.

7.5.6 Volcanic Remnants

The flat-topped peak at the bathymetric sill in Hochstetterbugten Trough south of Shannon Island is interpreted to be of volcanic origin (Figure 7.7b). The NEG volcanic province stretches from 75°N to 72°N of the continental shelf [*Hamann et al.*, 2005]. Eastern Shannon Island, 30 km north of the peak, and Pendulum Øer, 20 km south of the peak (Figure 7.7b), consist of basalts [*Henriksen*, 2003]. Voss et al. [2009] observed a significant seismic-velocity anomaly at the location of the peak. They also found no significant high-velocity lower crust which, in contrast, was observed further south, and that a positive magnetic anomaly is present at this location. They concluded that the observed surface basalts were related to a local volcanic event. We interpret the outcropping peak in the DBM as a remnant of this volcanic event. Eruption rates of the North Atlantic Igneous Province were highest between 56 and 55 Ma and later on were active only at the East Greenland margin between 66°N and 69°N [*Storey et al.*, 2007]. Assuming 55 Ma as the timing of the volcanic event, the guyot-like flat top of the peak at 250 m water depth is most probably a result of subsequent erosion by waves together with erosion by ice during glaciations.

7.6 Conclusions

The new DBM of the NEG continental shelf shown in Figure 7.4 has improved our knowledge of the shelf bathymetry compared to previous maps and models. The detailed grid allows the identification of seafloor features that have not been mapped previously or have had their shape insufficiently resolved. Nevertheless, the coverage map reveals that parts of the NEG shelf, especially close to the coast (Figure 7.2), are still not or only sparsely covered by soundings and additional data are needed to further improve our description and understanding of the NEG shelf.

The DBM reveals that the shape of the NEG continental shelf has been affected by a number of processes, including glacial erosion and deposition, salt tectonics (halokinesis), and past volcanism. The cross-shelf troughs were formed by glacial erosion by ice streams that drained an expanded Greenland Ice Sheet in full-glacial periods (Figure 7.10). Under modern conditions, these troughs act as potential pathways for relatively warm Atlantic waters to flow across the shelf to the margins of the marine-terminating glaciers and beneath any floating ice. Bathymetric sills (Figures 7.7c and 7.8), located in the cross-shelf troughs, are interpreted as depositional grounding-zone wedges that formed at the ice margin during phases of prolonged ice-sheet still stand (Figure 7.10), probably during deglaciation from the LGM. Salt tectonics formed the irregular seafloor on much of the middle shelf, represented by pronounced knolls, sinks, and hummocky areas (Figure 7.8). North-south trending elongate depressions have been mapped between the cross-shelf troughs on the middle to outer shelf (Figures 7.7a and 7.8). They are probably related to ice-marginal processes and ocean currents. In central Hochstetter Bugten Trough, a guyot-like remnant of a former volcano has been detected (Figure 7.7b), which is linked to a single volcanic event that probably occurred 55 Ma ago. The DBM can be obtained from http://dx.doi.org/10.1594/PANGAEA.849313.

7.7 Acknowledgments

We thank crew and scientists onboard of each data contributing cruise. We thank TGS for contributing depth information along their seismic lines. We thank Paul Dodd from the Norske Polar Institut, Martin Jakobsson from Stockholm University, and Fiamma Straneo from Woods Hole Oceanographic Institution for their contributions of echo sounder data. We thank Peter Wadhams who was chief scientist of JR106 and Autosub-II leg M365. We thank E. Domack and one anonymous reviewer for providing helpful comments on a previous version of this publication.

8. Ice sheet limits and retreat dynamics on the Northeast Greenland continental shelf during the last full-glacial period

Jan Erik Arndt[1], Wilfried Jokat[1], Boris Dorschel[1]

[1]*Alfred Wegener Institute Helmholtz Centre for Polar and Marine Research, Bremerhaven, Germany*

Submitted to *Quaternary Science Reviews*

Abstract

The modern-day Northeast Greenland ice stream drains about 16% of the Greenland Ice Sheet area via the marine terminating outlet glaciers 79°-Glacier and Zachariae Isstrøm into the North Atlantic. In glacial periods these glaciers extended onto the shelf via two cross shelf troughs (Westwind Trough, Norske Trough). However, the extent and subsequent retreat dynamics of this ice sheet system during its last maximum extent has so far been underestimated, mainly due to limited marine geophysical data coverage. Improved understanding of the past Greenland Ice Sheet extent and its response to a warming climate in this area is needed in order to verify its contribution to global sea-level rise and to constrain ice sheet models. We have investigated hydro-acoustic data acquired by R/V Polarstern on 20 marine research expeditions between 1985 and 2014 in order to reveal submarine glacial landforms. The mapped distribution and orientations of these landforms enabled us to establish a more comprehensive picture of the ice sheet dynamics during last full-glacial conditions. The Greenland Ice Sheet extended at least until the shelf break in both cross-shelf troughs, most likely during the Last Glacial Maximum (26.5-19 kyrs B.P.). In Westwind Trough, the ice retreat was highly variable. The Northeast Greenland Ice Stream fed the southern part and the rapid subsequent ice retreat was intermittent by slow stepwise retreat along a 100 km long section of the trough on the middle shelf. The northern part, fed by a different, smaller

drainage system, likely was not filled by a grounded ice stream until the shelf break, but terminated in form of an ice shelf with its grounding line located on the middle shelf. In Norske Trough, an ice shelf was formed after a first deglaciation phase that released tabular icebergs during its decay. Finally, a separate ice stream system was active in the inter-trough area between Westwind and Norske Trough, probably fed by a local ice dome. After deglaciation the seafloor was modified by icebergs, which predominantly drifted in north-south direction creating numerous iceberg ploughmarks down to 850 m water depth.

8.1 Introduction

The Greenland Ice Sheet is identified as one of the tipping elements in the Earth's climate system [*Lenton et al.*, 2008]. Recent changes observed in the Greenland Ice Sheet, however, need to be considered in the context of past Greenland Ice Sheet responses to a changing climate [*Vaughan et al.*, 2013]. High-resolution swath bathymetry data from formerly glaciated continental shelves have the potential to provide constraints for the extent and the retreat dynamics of former ice sheets by mapping submarine glacial landforms [*Jakobsson et al.*, 2014 and references therein; *Livingstone et al.*, 2012].

For the Northeast Greenland (NEG) continental shelf we processed and interpreted swath bathymetric data from Westwind Trough, Norske Trough, and their inter-trough area in order to reconstruct the past ice extent and its retreat dynamics (Figure 8.1). Important outlet glaciers in our research area are the 79°-Glacier and Zachariae Isstrøm, which are located at the landward end of the troughs mentioned above. These glaciers are fed by the NEG ice stream, which is the longest ice stream in Greenland reaching approximately 700 km inland [*Joughin et al.*, 2001]. Their drainage area sums up to approximately 16 % of the Greenland Ice Sheet [*Zwally et al.*, 2012]. Thus, their dynamics have and had major consequences for the mass balance of the entire Greenland Ice Sheet, especially when considering the vast ~300 km broad continental shelf might have completely been covered by an ice sheet [*Bennike and Björck*, 2002].

In the last review on past Greenland Ice Sheet extents, Funder et al. [2011] suggested a LGM extent on the middle shelf in Westwind Trough (~10° W), based on studies on submarine glacial landforms [*Evans et al.*, 2009; *Winkelmann et al.*, 2010], and a conceptual extent on the inner shelf for Norske Trough (~17° W). However, Funder et al. (2011) interpret this as a minimum extent since the previously available swath bathymetric data revealed submarine glacial landforms in Westwind Trough, but did not provide constraints on their eastern terminations [*Evans et al.*, 2009; *Winkelmann et al.*, 2010]. Furthermore, radiocarbon dates from the coastline of NEG indicate a late deglaciation (~9.3-9.7 kyrs) compared to deglaciation dates in the north and south (>10.2 kyrs) [*Bennike and Björck*, 2002]. Thus, Bennike and Björck [2002] supposed a grounded ice terminus at the continental shelf edge. However, marine evidence for this assumption has so far been missing.

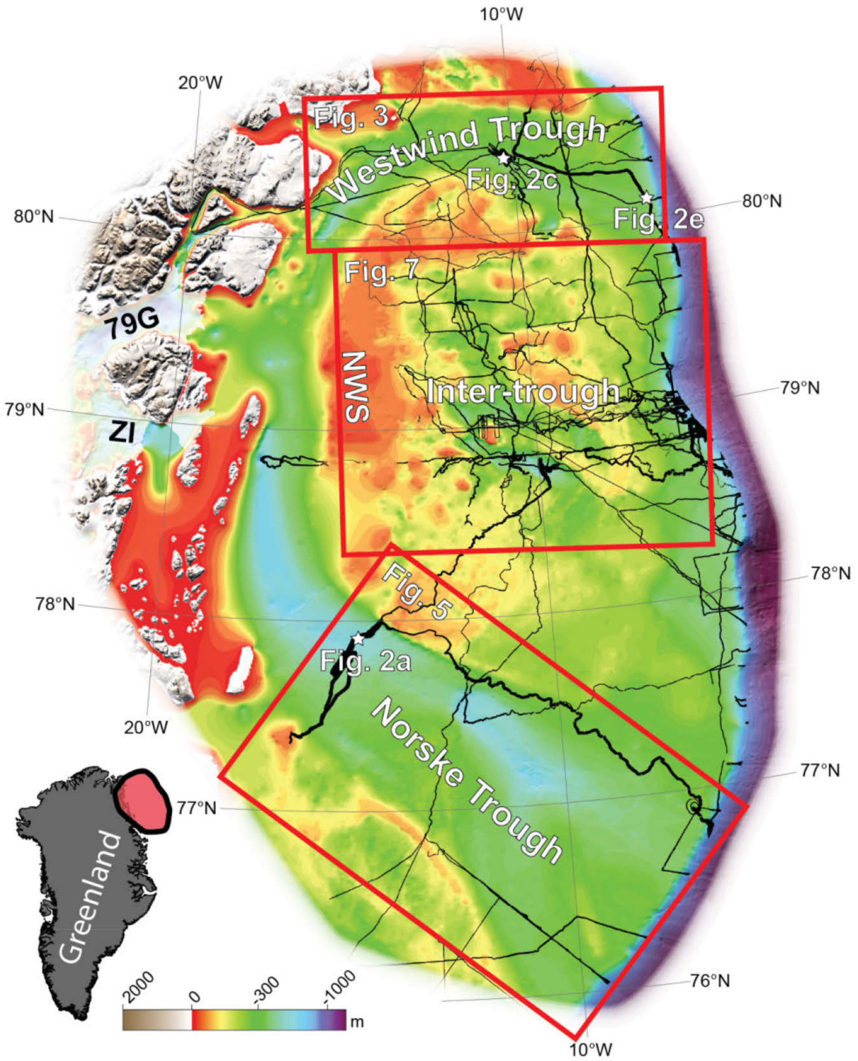

Figure 8.1: Bathymetry of the Northeast Greenland continental shelf [Arndt et al. 2015] with multibeam data coverage used in this study shown in black; 79G = 79°-Glacier; ZI = Zachariae Isstrøm

NEG is experiencing year-round harsh ice conditions as sea-ice from the Arctic Ocean is continuously exported via the East Greenland Current (EGC) through the western Fram Strait [*Aagaard and Coachman*, 1968]. This makes the area hardly accessible for research vessels and limits the availability of systematic marine geophysical data. Nevertheless, a new digital bathymetric model for the NEG shelf has been derived recently from available bathymetric data with a grid cell size of 250 × 250 m, thereby revealing past ice flow pathways and large scale glacial landforms, such as grounding-zone wedges and lateral moraines, on the middle shelf of both troughs [*Arndt et al.*, 2015]. Previous investigations of high resolution hydro-acoustic data (~20 m grid cell size) from single cruises revealed mega-scale glacial lineations and recessional moraines in Westwind Trough as well as more subtle lineations in the westernmost part of the inter-trough area [*Evans et al.*, 2009; *Winkelmann et al.*, 2010]. These submarine glacial landforms not only provided indications for the past ice extent but also indicate that ice retreat in Westwind Trough was highly variable and that fast flowing ice once also was present in the inter-trough area on Northwind Shoal. However, a more comprehensive reconstruction of the ice extent and retreat dynamics during the last deglaciation was impeded due to the limited amount of bathymetric data.

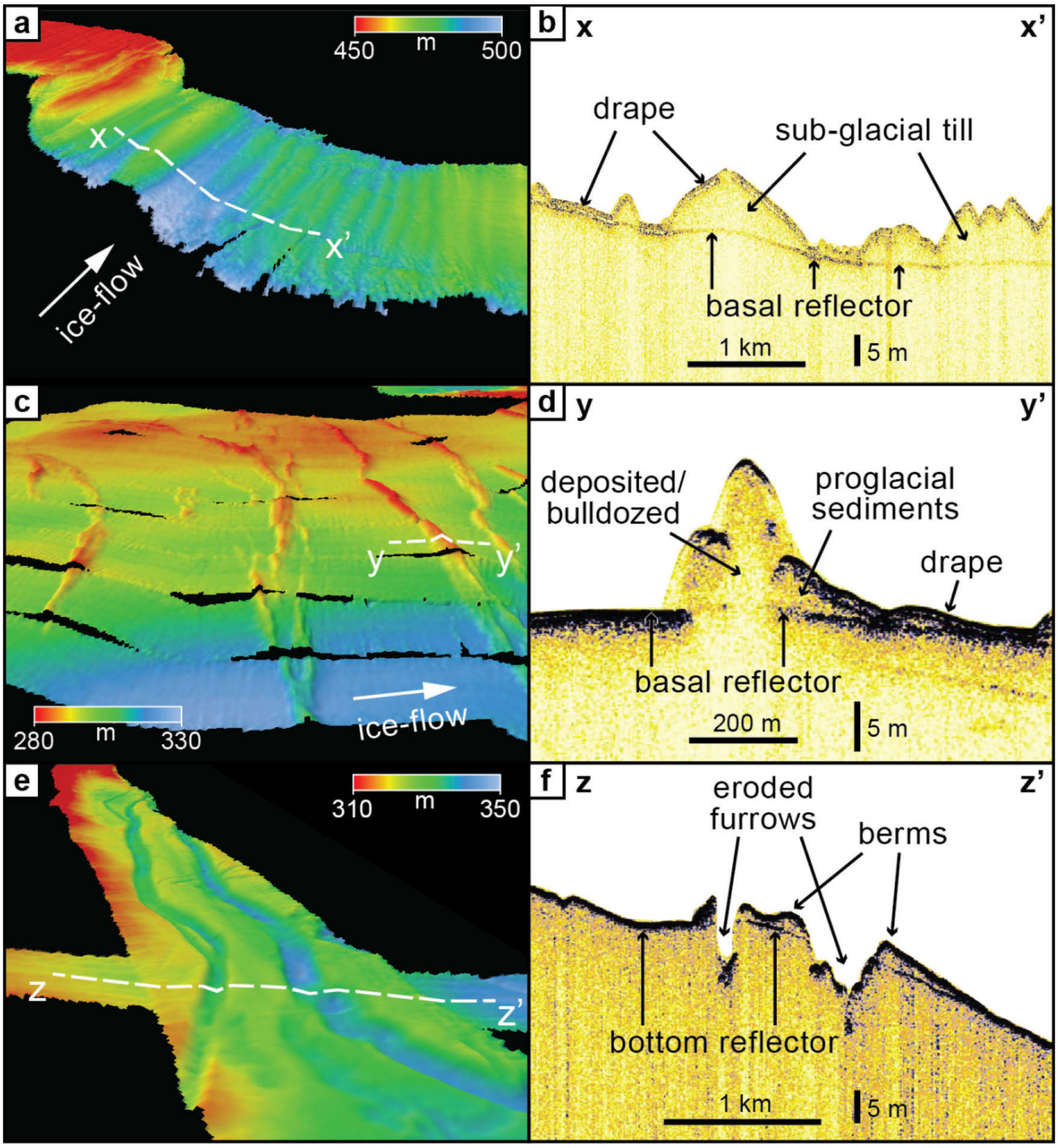

Figure 8.2: 3D-views and stratigraphy of mapped types of glacial landforms: glacial lineations (a, b), recessional moraines (c, d), iceberg ploughmarks (e, f)

Here, we present different sets of submarine glacial landforms visible in swath bathymetric data (Figure 8.2 a, c, and e). Subbottom profiler data have been used to resolve the subbottom stratigraphy of the identified landforms (Figure 8.2 b, d, and f). Our investigation gives first direct evidence for ice streaming activity in Norske Trough, for more intense ice streaming in the inter-trough area and for an extension of the Greenland Ice Sheet at least until the shelf break in Westwind and Norske Trough.

8.2 Data and Methods

Multibeam bathymetric data from 20 cruises of R/V Polarstern have been compiled for this study (Table 8.1, Figure 8.1). The data were acquired in between 1985 and 2014. In this time period, four different hull-mounted swath bathymetry systems were installed (Table 8.1). Accordingly, the data differ in accuracy, density and swath width. All data have been checked and reprocessed with CARIS and QPS Fledermaus. The data have been gridded at a grid cell size of 20 × 20 m with a weighted moving average gridding algorithm in QPS Fledermaus. Data examination and mapping of submarine glacial features were performed in ESRI ArcGIS and QPS Fledermaus.

Table 8.1: Swath bathymetric data and subbottom profiler data used in this study

Cruise ID	Year	Swath System	Subbottom Profiler
ARK-III/3	1985	Seabeam	
ARK-IV/1	1987	Seabeam	
ARK-IV/3	1987	Seabeam	
ARK-VII/1	1990	Hydrosweep DS1	
ARK-X/1	1994	Hydrosweep DS1	
ARK-XI/2	1995	Hydrosweep DS1	
ARK-XIII/3	1997	Hydrosweep DS1	×
ARK-XV/2	1999	Hydrosweep DS2	×
ARK-XVII/1	2001	Hydrosweep DS2	
ARK-XVIII/1	2002	Hydrosweep DS2	×
ARK-XVIII/2	2002	Hydrosweep DS2	
ARK-XIX/4a	2003	Hydrosweep DS2	×
ARK-XIX/4b	2003	Hydrosweep DS2	
ARK-XX/2	2004	Hydrosweep DS2	
ARK-XX/3	2004	Hydrosweep DS2	
ARK-XXIV/3	2009	Hydrosweep DS2	×
ARK-XXVII/1	2012	Hydrosweep DS3	
PS85 (ARK-XXVIII/2)	2014	Hydrosweep DS3	×
PS86 (ARK-XXVIII/3)	2014	Hydrosweep DS3	×
PS87 (ARK-XXVIII/3)	2014	Hydrosweep DS3	×

Sediment subbottom profiler data (PARASOUND) from 10 cruises of R/V Polarstern have been included (see Table 8.1). This system is using the parametric effect by sending two primary frequencies, usually at 18 and 23.5 kHz, that generate a secondary pulse of lower frequency, usually 5.5 kHz. Depending on the seafloor sediment type, the system can penetrate up to 100 m into the sediment. The vertical resolution of the system is approximately 30 cm.

8.3 Results and Interpretation

8.3.1 Distribution of submarine glacial landforms

For this study, we mapped landforms that we interpret as glacial lineations, recessional moraines and iceberg ploughmarks (Figure 8.2). Glacial lineations and more elongate mega-scale glacial lineations are formed by fast flowing ice into a sedimentary till layer at the base of an ice stream (Figure 8.2a and b) [e.g. *Clark*, 1993; *Dowdeswell et al.*, 2004; *Graham et al.*, 2009; *King et al.*, 2009; *Ó Cofaigh et al.*, 2002; *Ottesen et al.*, 2005]. Recessional moraines are formed at the ice stream margin by sub- and proglacial deposition during grounding line still stands or by bulldozed sediments during minor grounding line re-advances (Figure 8.2c and d) [*Golledge et al.*, 2008; *Winkelmann et al.*, 2010]. In terms of ice stream retreat behavior, the presence of glacial lineations is interpreted to be related to rapid retreat and the presence of recessional moraines is related to a slow and stepwise retreat [*Dowdeswell et al.*, 2008]. Iceberg ploughmarks are formed by keels of drifting grounded icebergs that scour into the uppermost sedimentary substrate of the seafloor (Figure 8.2e and f) [*Arndt et al.*, 2014; *Belderson et al.*, 1973; *Dowdeswell et al.*, 1993; *Jakobsson et al.*, 2010].

8.3.1.1 Westwind Trough

The distribution of submarine glacial landforms in Westwind Trough is shown in Figure 8.3. The easternmost occurrence of glacial lineations is directly at the shelf break (Figure 8.4f). Glacial lineations are also present in the southern part of the trough (Figure 8.3 and 8.4d). Subbottom profiler data across these lineations show no postglacial sedimentary layer or this layer is too thin to be resolved by the bottom penetrating data. (Figure 8.4e). The lineations were formed in an up to 8 m thick layer of basal till.

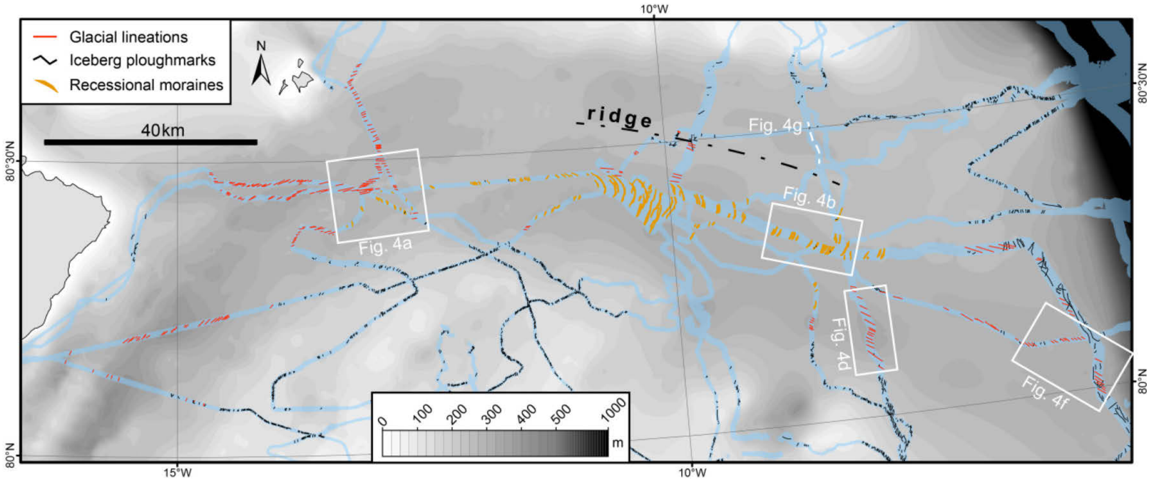

Figure 8.3: Mapped submarine glacial landforms in Westwind Trough. Glacial lineations on the inner and outer shelf indicate the presence of an ice stream and fast retreat. The set of recessional moraines on the middle shelf indicate a slow stepwise retreat in this area. The dash-dot line indicates the position of the ridge that separates the northern part of the trough from the southern part. Data coverage is shown in light blue.

The easternmost northern part of the trough has been intensely scoured by iceberg keels (Figure 8.3). The remaining northern part of the trough is relatively smooth and flat with only sparse appearance of iceberg ploughmarks (Figure 8.3). Subbottom profiler data of this area reveal that the deepest part of this area is covered by an approximately 3 m thick lentoid sedimentary fill on top of a flat basal reflector that thins towards shallower water (Figure 8.4g).

The southern part of the trough is characterized by a set of recessional moraines that are present in between 8°W and 13°W, thereby covering an area of ~1,100 km^2 (Figure 8.3, 4a and b). A thin drape of ~1 m or less is visible in between the moraines and indistinctly resolved on top of the moraines (Figure 8.4c). West and north of the innermost moraines, Westwind Trough is characterized by glacial lineations that align to the axis of the trough (Figure 8.3 and 8.4a).

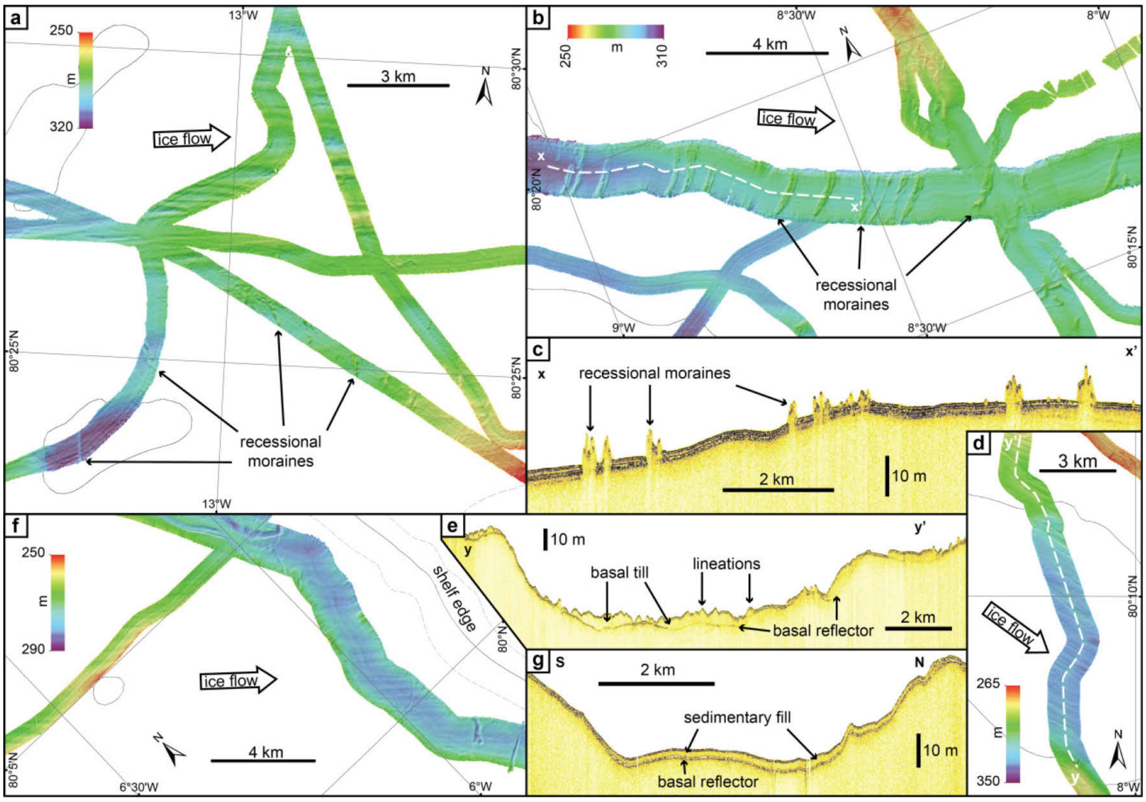

Figure 8.4: Swath bathymetry and sub-bottom profiler data from Westwind Trough, for locations see Figure 8.3. (a) Glacial lineations and recessional moraines on the inner shelf; (b, c) Easternmost mapped recessional moraines; (d, e) Pronounced glacial lineations in the southern part formed in basal till; (f) Glacial lineations close to the shelf break; (g) Sedimentary drape in the northern part of the trough.

8.3.1.2 Norske Trough

The distribution of submarine glacial landforms in Norske Trough is shown in Figure 8.5. Glacial lineations are present directly at the shelf break at about 300 m water depth in the northernmost part of the trough (Figure 8.6f). Subbottom profiles across the lineations reveal an up to 7 m thick acoustically transparent layer that can be interpreted as basal till (Figure 8.6e). The reflector at its base is relatively flat and continuous. The seafloor in the south does not show lineations, but is characterized by numerous iceberg ploughmarks (Figure 8.5).

Further landwards, iceberg ploughmarks with widths of up to 800 m and a flat bottom between its berms are mapped in a depth range from 260 to 300 m (Figure 8.5 and 8.6d). A set of mega-scale glacial lineations is mapped over a distance of approximately 70 km in the northern part west of 10°W (Figure 8.5 and 8.6b). More subtle lineations are also present north of the trough edge (Figure 8.5). The sparse multibeam data in the central trough show some ridges aligned in the axis of the troughs that we interpret as lineations (Figure 8.5). However, compared to the set of lineations present in the shallower northern part (Figure 8.6b) these are less distinct.

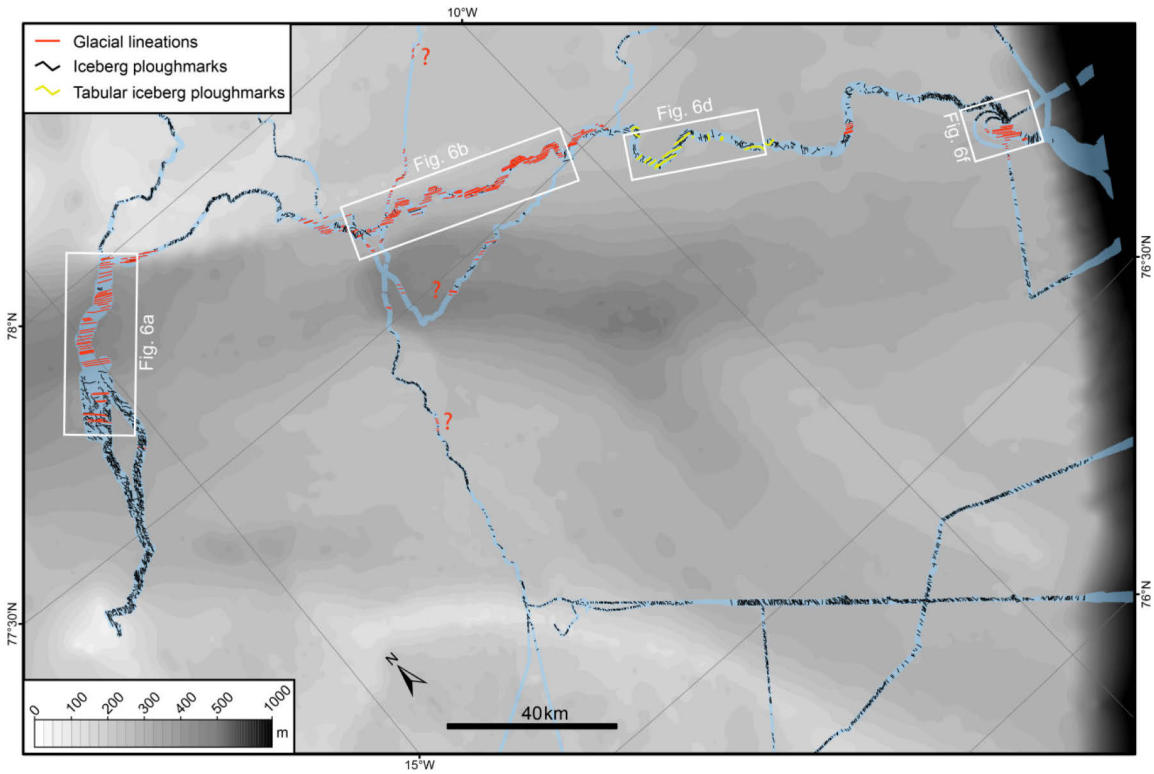

Figure 8.5: Mapped submarine glacial landforms in Norske Trough. The glacial lineations indicate the presence of an ice stream and fast retreat in this area. The tabular iceberg ploughmarks indicate that an ice shelf once was present during deglaciation. Note the large data gaps that limit a thorough investigation. Data coverage is shown in light blue.

Multibeam data of a trough transect at 15°W and 77°50'N show glacial lineations nearly over the entire width of the trough (Figure 8.6a). Their orientation is parallel to the axis of the trough. The lineations are up to 17 m in profile and are present from about 150 m at the northern trough edge down to 490 m in the trough center. The subbottom profiler data show that the lineations are formed in a basal till layer of about 10 m in average with an underlying flat basal reflector (Figure 8.6c). The lineations are draped by a thin postglacial sedimentary layer of ~1m thickness (Figure 8.2b). To the south the lineations are increasingly cross-cut by iceberg ploughmarks until the density of ploughmarks impeded the preservation of lineations (Figure 8.6a).

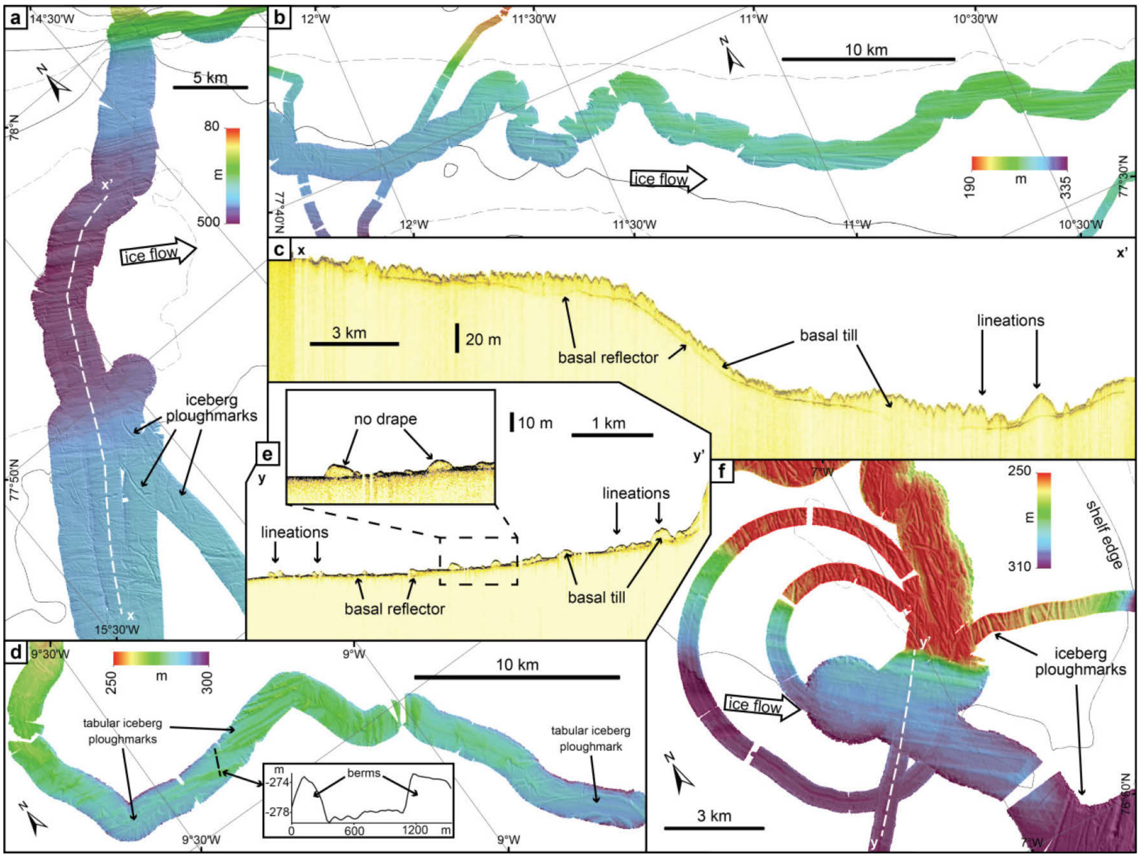

Figure 8.6: Swath bathymetry and sub-bottom profiler data from Norske Trough, for locations see Figure 8.5. (a, c) Pronounced glacial lineations formed in basal till on the inner shelf and iceberg ploughmarks on the southern part; (b) Tens of km long mega-scale glacial lineations at the northernmost part of the trough; (d) Tabular iceberg ploughmarks; (e, f) Glacial lineations at the shelf break in the northernmost part of the trough, note the iceberg sheltering function of the heavily reworked rise in the north.

8.3.1.3 Inter-trough area

The distribution of glacial landforms in the inter trough area is shown in Figure 8.7. Iceberg ploughmarks are abundant on the shallower parts and on the outer shelf of the inter-trough area (Figure 8.7 and 8.8a). Subbottom profiles across an intensely scoured area show how deep the upper sedimentary layer has been reworked (Figure 8.8b). Seafloor depressions of the inter-trough area are left widely undisturbed by ploughing icebergs, but occasionally glacial lineations could be detected here (Figure 8.7).

The westernmost set of lineations is located at 12.5°W and 79.5°N. These lineations strike southeastward and subbottom profiles reveal that the lineations are formed in a ~10 m thick layer of basal till (Figure 8.8c). In the deepest part, the lineations are covered by an up to 3 m thick sedimentary layer. This layer is thinning in shallower water until it is below the resolution of the subbottom profiler data. Beneath the prominent basal reflector, dipping strata is visible in several subbottom profiler sections

(Figure 8.8c and g), which represent inclined layers of sedimentary bedrock affected by uplifting salt diapirs [*Arndt et al.*, 2015]. To the southeast, further glacial lineations striking in the same direction are formed in a basal till layer (Figure 8.7, 8.8d and e). A thin lentoid sedimentary fill of ~2-3 m maximum thickness is visible in the deepest part on the lineations (Figure 8.8e). In a depression even further southeast, subtle lineations striking in similar direction are identified on its northern slope in ~250 m depth, but are absent in its center (9°W, 78.45°N, Figure 8.7). Subbottom profiles across this depression reveal two distinct lentoid layers of sedimentary fill, each up to ~3 m thick that are thinning in shallower waters until they are below data resolution (Figure 8.8i).

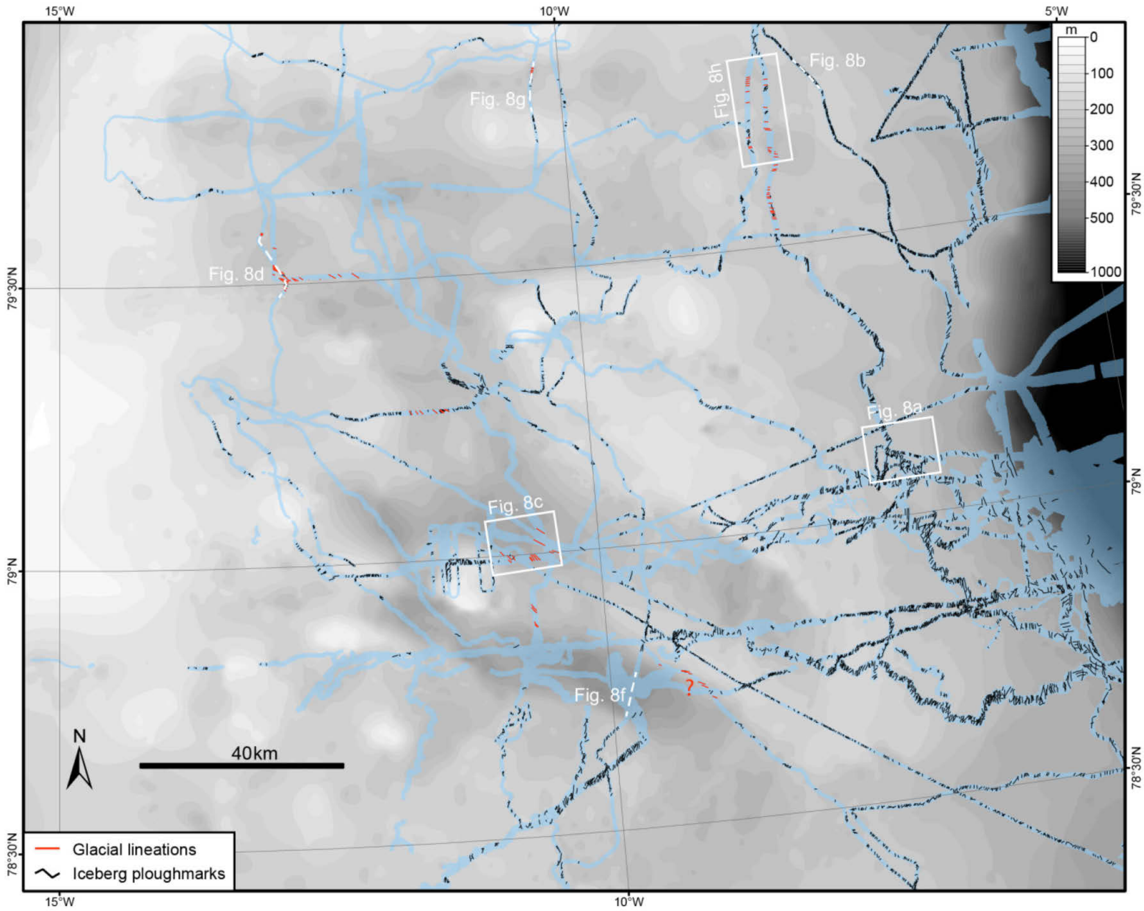

Figure 8.7: Mapped submarine glacial landforms in the inter-trough area. Shallow parts and the outer shelf are widely covered by iceberg ploughmarks. Glacial lineations are preserved in sinks and indicate an ice stream with an northern west-east flowing branch and a southern northwest-southeast flowing branch. Data coverage is shown in light blue.

Eastward oriented subtle lineations up to 2 m in cross section are present in the north and northeast of the inter-trough area (Figure 8.5 and 8.8h). A subbottom profile of the more westerly lineations reveals an acoustically transparent layer that we interpret as basal till, into which the lineations were formed (Fig 8.8g). In contrast, the lineations further to the east do not show such a basal till layer or this layer is too thin to be resolved by the subbottom profiler data (Fig. 8.8i).

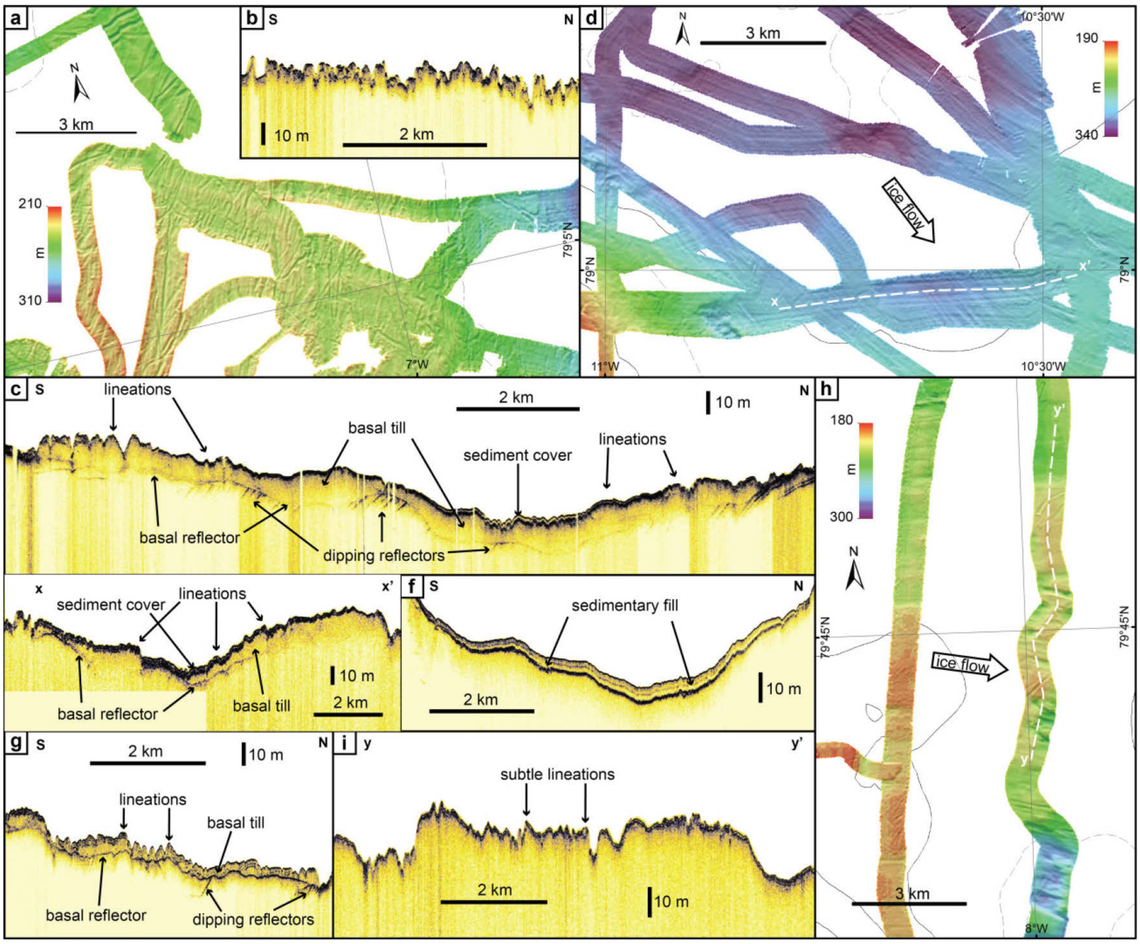

Figure 8.8: Swath bathymetry and sub-bottom profiler data from the inter-trough area, for locations see Figure 8.7. (a, b) Reworked seafloor from numerous iceberg ploughing events; (c, d, e, g) Glacial lineations located in different parts of the inter-trough area formed in basal till that indicate past fast flowing ice; (f) Thick postglacial sedimentary fill in a depression without glacial landforms; (g, h) Subtle lineations on the outer shelf, note the absence of basal till.

8.3.2 Iceberg Ploughmark orientation

The majority of the iceberg ploughmarks are NNE-SSW oriented (Figure 8.9a). We have subdivided their orientations into different classes depending on their depths and regional appearance (Figure 8.9b-n). In deeper waters, the predominant orientation turns counterclockwise (Figure 8.9c-f). The deepest ploughmark is found in 850 m water depth. The predominant ploughmark orientation of most regions is NNE-SSW (Figure 8.9g-n). The ploughmarks observed in the northern parts of Westwind Trough and Norske Trough (Area 3 and 7) are an exception of this trend. Iceberg ploughmarks located here do not show a significant trend in orientation but are rather randomly orientated (Figure 8.9i and m). Another exception are ploughmarks observed on the outer shelf north of Westwind Trough (Area 5). Here, a northwest north to southeast south orientation similar to the observation of ploughmark orientations in deeper waters (Figure 8.9k and f).

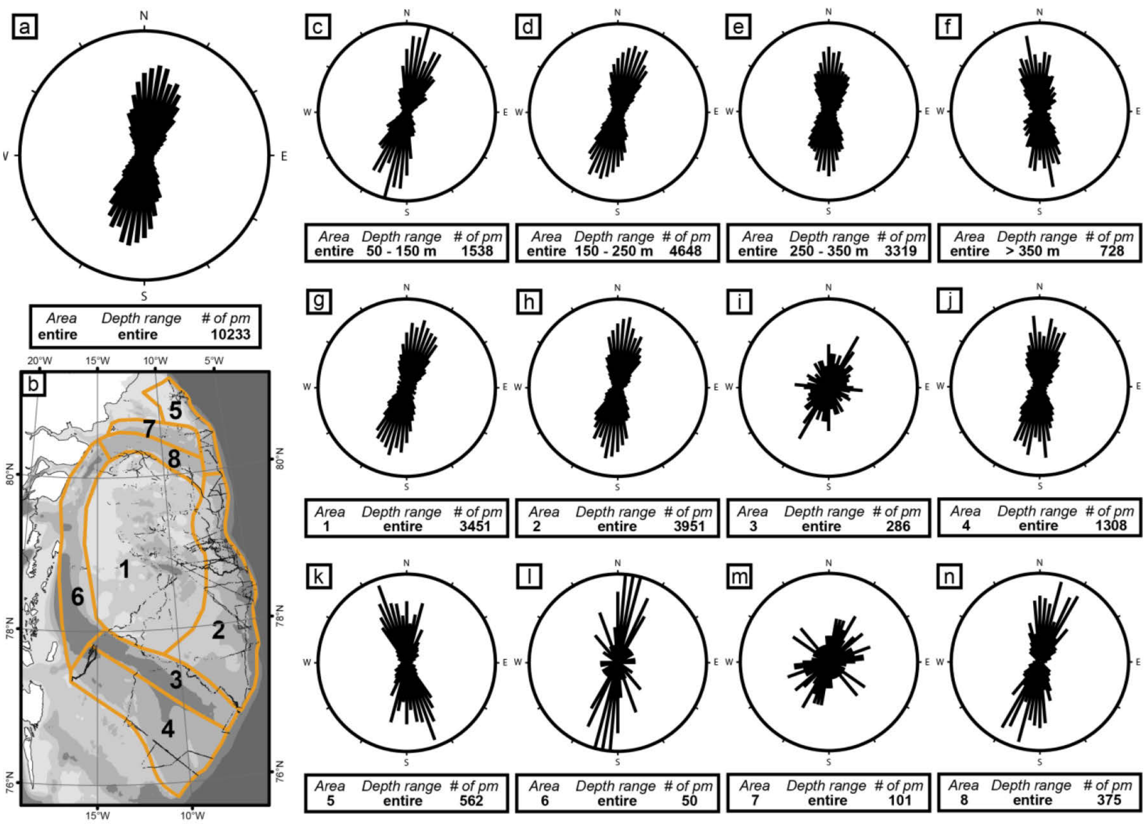

Figure 8.9: Iceberg ploughmark orientations in 5° steps for different areas and depth ranges. The diameter of the circles equals 10% of the observed orientations. (a) All orientations of ploughmarks; (b) Areas used as criteria, distribution of ploughmarks is shown in black; (c-f) Orientations for varying depth ranges; (g-n) Orientations for different areas.

8.4 Discussion

8.4.1 Reconstruction of past ice flow and retreat dynamics

The mapped glacial lineations and recessional moraines are directly linked to ice stream activity and thus provide information on the retreat behavior of ice streams during the last deglaciation [*Dowdeswell et al.*, 2008].

8.4.1.1 Westwind Trough

The mapped glacial landforms show that the fast-flowing ice stream in Westwind Trough was grounded until the continental shelf edge in the southern part at some point in the past (Figure 8.10a). The freshness of the outermost glacial lineations (Figure 8.4d and f) as well as the visual absence of postglacial sediments on top of the lineations (Figure 8.4e) suggests that this ice extent may have been present during the LGM (Figure 8.10b). The well-preserved lineations on the outer shelf indicate an initial phase of rapid deglaciation (Figure 8.10c), since any depositional features, such as grounding-zone wedges or moraines that would hint stand-still phases of the grounding zone, are absent.

In the northern part of Westwind Trough, no glacial lineations have been mapped (Figure 8.3). The flat featureless morphology, mapped in some parts of this area, is underlain by a relatively thick sedimentary fill in the deeper parts (Figure 8.4g). This fill probably has been sedimented after the last deglaciation and could have buried subtle glacial landforms. However, also the basal reflector does not show indications of lineations. Hence, a possible scenario is the absence of grounded ice in this area during the last maximum ice extent. Instead, the ice stream possibly rested on the grounding zone wedge that has been suggested in landward direction [*Arndt et al.*, 2015] and continued in the form of an ice shelf (Figure 8.10a).On the basis of the available data, however, we cannot entirely rule out the presence of grounded ice in the northern part of the trough, since large parts of this area are not mapped by multibeam data. Furthermore, iceberg ploughing on the outer shelf could have demolished any glacial landforms that would indicate the former presence of an ice sheet (Figure 8.5).

The recessional moraines located on the middle shelf indicate that a change in retreat behavior occurred in this section of the trough. A small portion of these moraines were already described by Winkelmann et al. [2010]. After a first phase of fast retreat on the outer shelf, the ice stream repeatedly halted in this area and the deglaciation speed slowed down (Figure 8.10c). We link this slow down to the trough morphology, as the trough bed changes its gradient from a more reverse gradient to a normal gradient, and, in addition, locally becomes even shallower in the trough section where moraines are observed [*Arndt et al.*, 2015]. This observation is in line with the numerical simulations that state unstable grounding zones on reverse bed slopes [*Schoof*, 2007]. Similar bed observations, corresponding to increased and reduced ice stream retreat speeds, have been observed for paleao-ice streams that flowed along other trough or fjord systems [*Briner et al.*, 2009; *J A Smith et al.*, 2011], but also in concurrent ice streams such as the Pine Island ice stream in Antarctica [*Jenkins et al.*, 2010]. Here, relatively warm (+1°C) Circumpolar Deep Water is upwelling onto the shelf and follows the cross shelf troughs towards the glacier cavity where it causes basal melting [*Jenkins et al.*, 2010]. The modern equivalent on the NEG continental shelf is relatively warm Atlantic water with potential for basal melting that is present on the inner shelf [*Straneo et al.*, 2012]. A similar upwelling process of Atlantic water in the past could have resulted in rapid retreat on the reverse-sloped sections of the NEG continental shelf. Contrasting this rapid response, a normal bed gradient rather triggered a slow grounding line retreat, thereby resulting in the deposition of recessional moraines within the southern trough sections, which characterizes a second phase of deglaciation in Westwind Trough (Figure 8.10d). The glacial lineations mapped on the reverse slope of the inner shelf rather indicate a fast grounding line retreat which we define as the final phase of deglaciation in Westwind trough.

As demonstrated above, the glacial landforms mapped within Westwind Trough indicate a deviating maximum extent and retreat behavior of the northern and southern portions of the trough. Ice flow reconstructions based on a bathymetric model show that the ice discharging trough Westwind Trough did not only originate from the NEG ice stream, but probably also derived from an ice drainage system through Ingolf Fjord further north (Figure 8.10a) [*Arndt et al.*, 2015]. The concurrent NEG ice stream reaches approximately 700 km inland and has one of the largest catchment areas in Greenland (274,220 km^2) [*Joughin et al.*, 2000; *Zwally et al.*, 2012]. The NEG area is characterized by the lowest precipitation and snow accumulation rates of Greenland [*Ohmura and Reeh*, 1991]. Therefore, we suggest that in the past the ice discharge through Ingolf Fjord and in the northern portion of Westwind Trough, which was likely fed by a smaller drainage system in the north, was smaller than the ice discharge in the southern portion, which was likely fed by the NEG ice stream. This difference in ice discharge between the northern and southern portions of Westwind Trough may explain the deviation in maximum extent and retreat behavior.

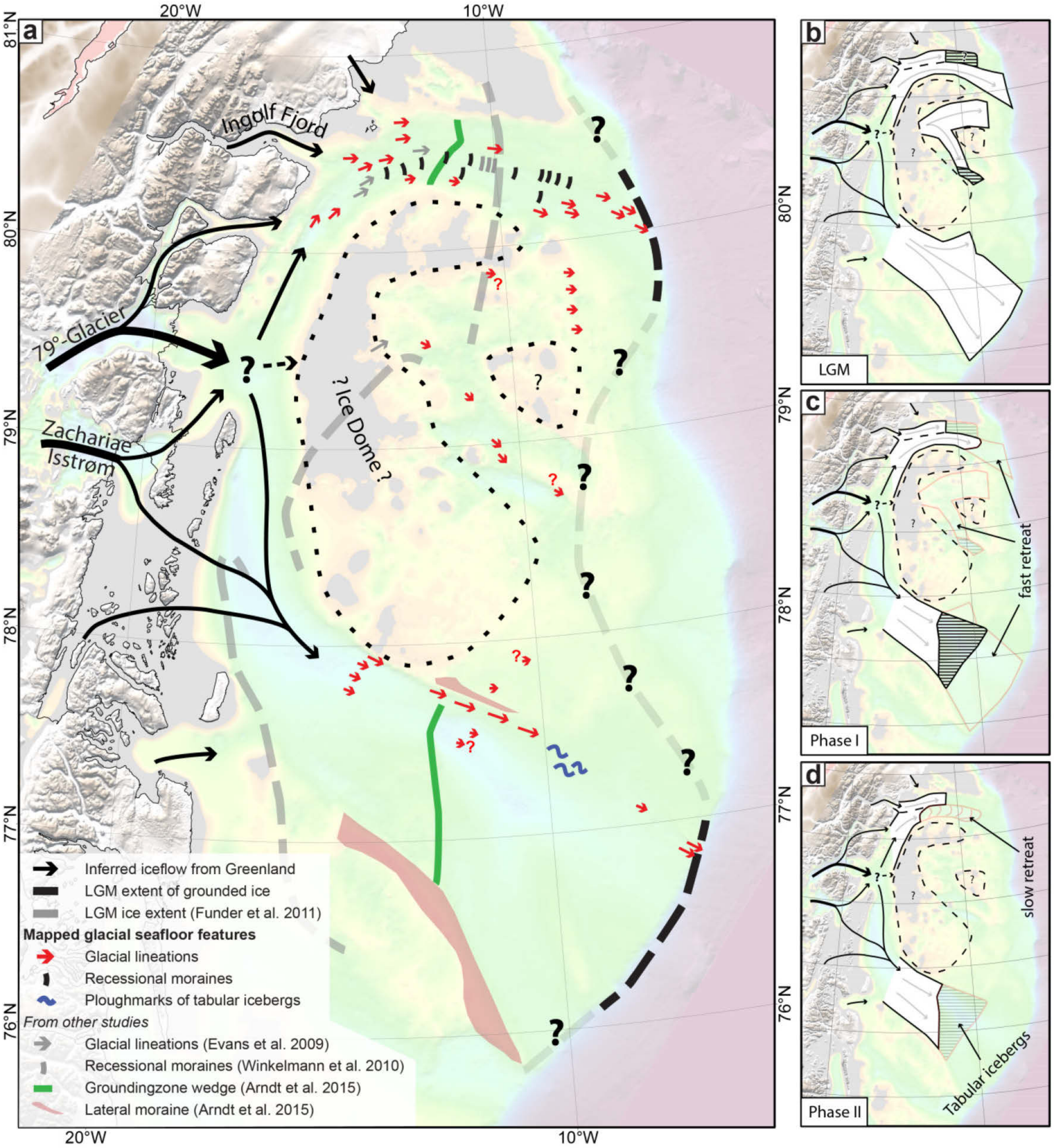

Figure 8.10: (a) Generalized overview of glacial seafloor features and new LGM extent of grounded ice, question marks on the outer shelf show locations where iceberg ploughmarks may have overprinted evidence of the maximum ice sheet extent, with inferred ice stream flow from the Greenland Ice Sheet (modified from Arndt et al. [2015]). (b, c, d) Reconstructed ice stream setting during (b) LGM, (c) a first phase of deglaciation, and (d) a second phase of deglaciation. The timing of deglaciation phases is not fixed and possibly occurred independently from each other in the three ice stream systems. Grounded ice streams are shown in white. Ice shelves are shown as hatched area. Deglaciated areas are shown semi-transparent with red outline.

8.4.1.2. Norske Trough

The lineations mapped throughout the entire northern part of Norske Trough are giving evidence for a grounded ice stream until the shelf break (Figure 8.10a). The freshness of the outermost lineations and the absence of a postglacial draping layer in subbottom profiler data suggest that the Greenland Ice Sheet may have reached this extent during the LGM (Figure 8.6c and 8.10b). The subtle lineations mapped in the deepest part of the trough further to the west, indicate that most probably the entire trough was filled by grounded ice. However, more swath bathymetric data of the deeper parts east of 13°W are needed to ensure correct interpretation of these seafloor landforms (Figure 8.5). The subtle lineations north of Norske Trough at 10.5°W and 77.9°N indicate that during maximum glaciation ice either have overflown the lateral moraine found at the northern edge of Norske Trough [*Arndt et al.*, 2015], or this lateral moraine has been deposited during a stage of deglaciation after its last maximum extent. We suggest the latter as otherwise the lateral moraine probably would have been removed by the overflowing ice stream (Figure 8.10b).

The iceberg ploughmarks with exceptional widths (Figure 8.6d) were very likely created by grounded tabular icebergs that typically have a flat bottom [*Kristensen et al.*, 1982]. Tabular icebergs are calved from floating ice shelves [*Dowdeswell and Bamber*, 2007]. The location of the tabular iceberg ploughmarks and the oceanographic setting give indications for their origin. The northern edge of Norske Trough continuously is shallower than the depths of the tabular iceberg ploughmarks. Thus, if they originated from outside Norske Trough they would have had to flow into the trough via the shelf break. From here, the icebergs would have had to drift approximately 90 km in northwest direction to arrive at the ploughmark locations. This direction, however, is in contrast to the observed dominant NNE-SSW direction of other icebergs. Even though palaeo-oceanographic currents could have been different, i.e. due to different sea level and ice extent on the shelf, the most likely iceberg drift direction for western Fram Strait is and was north to south [*Arndt et al.*, 2014; *Darby et al.*, 2002]. Subsequently, we suggest that these icebergs were calved from an ice shelf located in Norske Trough. A possible source is located ~70 km west of the ploughmarks. Here, a GZW has been suggested in the trough with a maximum depth of 390 m at its easternmost position (Figure 8.10a) [*Arndt et al.*, 2015]. This seems a plausible source for tabular icebergs with sufficient draft and size. The tabular icebergs could have been calved from this ice shelf during a second phase of deglaciation (Figure 8.10d). The calving of tabular icebergs could have either occurred continuously by single major calving events or at once during a rapid ice shelf breakup.

West of the proposed GZW, Norske Trough was entirely filled by an ice stream as indicated by the glacial lineations that were formed at its base (Figure 8.6a and c). Furthermore, these lineations suggest that after the disintegration of the ice shelf glacial retreat was relatively rapid. Even though only high resolution swath bathymetric data from one transect of the trough is available, most likely the inferred rapid glacial retreat has occurred at least 50 km west- and eastward. In this section, the trough bathymetry shows that the ice stream bed had a continuous reverse gradient [*Arndt et al.*, 2015], which is typically prone to fast retreat and the inflow of warmer water masses, as discussed for Westwind Trough [e.g. *Jenkins et al.*, 2010; *Schoof*, 2007].

In contrast to Westwind Trough, in Norske Trough no recessional moraines have been observed in the studied swath bathymetric data. This could indicate that the retreat pattern during deglaciation after the last maximum ice extent in Norske Trough differed from the retreat pattern in Westwind Trough and underlines that the retreat behavior is likely controlled by trough morphology rather than climate fluctuations.

8.4.1.3. Inter-trough area

The mapped lineations in the inter-trough area are traces for the distribution and flow direction of palaeo-ice streams in the area between Westwind Trough and Norske Trough (Figure 8.10a). Ice stream activity extended at least 100 km to the east and southeast and followed the complex pattern of sinks and depressions visible in the bathymetry [*Arndt et al.*, 2015]. The high density of iceberg ploughmarks on the outer shelf very likely has overprinted any seafloor relicts of an ice sheet presence until the shelf edge. Hence, the maximum extent of grounded ice remains unresolved for the inter-trough area as no landforms indication the ice sheet termination have been observed (Figure 8.10a).

The orientation of the mapped lineations indicates that both inter-trough ice streams originate from the same area at the northeastern part of NWS (Figure 8.10a). Here, glacial lineations have been described by Evans et al. [2009]. The ice streams where either a) fed by the NEG ice stream that overflowed NWS from west to east or b) they drained a separate ice dome that likely was located on NWS [*Arndt et al.*, 2015]. We favor the ice dome scenario since divergent ice flow around similar shallower parts of glaciated continental shelfs has been observed at the Antarctic Peninsula [*Lavoie et al.*, 2015] and the Norwegian continental margin [*Ottesen et al.*, 2005], which has been related to the presence of local marine ice domes. However, swath bathymetric data from west of NWS is needed to reveal glacial landforms that could indicate if ice flow from the Greenland Ice Sheet entirely diverged to the north into Westwind Trough and to the south into Norske Trough or if ice flow also continued across NWS to feed the ice stream system located in the inter-trough area.

East of NWS at about 11°W and 79.5°N, the ice stream diverged into a northern and a southern branch (Figure 8.10b). The area east of the ice flow divergence is shallower than 120 m and hence most likely was above sea level during maximum glaciations [*Rohling et al.*, 2009]. Possibly, also this area of the shelf was capped by an ice dome during glaciations, similar to the proposed ice dome on NWS, and accordingly constrained the divergent ice flow (Figure 8.10).

The thin, up to 3 m thick postglacial coverage on some of the lineations in the deepest parts most likely was deposited after the last maximum ice extent. Typically sedimentation rates on formerly glaciated continental shelves are highest during deglaciation (e.g. > 200 cm kyrs^{-1}) and are lower in inter-glacial periods (e.g. 1-3 cm kyrs^{-1}) [*Tore O. Vorren et al.*, 1984]. Estimating approximately 18 kyrs as timing for the onset of deglaciation after LGM in NEG [*Fleming and Lambeck*, 2004], the 3 m drape layer equals a linear sedimentation rate of 16.6 cm kyrs^{-1} which is reasonable in comparison to the typical sedimentation rates given above. The local differences in sediment thickness of the postglacial cover indicate sediment focusing into sinks and areas of deeper water, most likely induced by currents (e.g. the EGC). This highlights the spatial variability of postglacial sedimentation on top of the glacial landforms, the complexity of estimating the timing of glacial landform formation solely from a postglacial sediment layer and hence demands the need for geological constraints on the timing of landform formation.

8.4.2. Iceberg ploughmark orientations

Icebergs are steered by ocean currents and in addition by wind, waves, and sea-ice [*Death et al.*, 2006]. The curved and irregular trajectories of the ploughmarks are due to changing external forces (i.e. tidal currents), rotation and rolling of the icebergs [*Woodworth-Lynas et al.*, 1985]. The predominant orientation of the ploughmarks in north-south direction shows a strong correlation to the flow direction of the EGC [*Aagaard and Coachman*, 1968], that exports and exported icebergs from the Arctic Ocean via Fram Strait [*Darby et al.*, 2002]. This observation suggests that the EGC had this flow direction continuously since the last deglaciation of the shelf. The slight shift in orientation to NNW-SSE in the deeper parts and in the northern outer shelf area (Figure 8.9f and k) is supposed to be related to the SSE orientation of the shelf edge guiding the EGC along the shelf edge in this area. The maximum observed iceberg ploughmark depth of 850 m is well inside the depth range of iceberg ploughmarks that have been found elsewhere in and close to the Fram Strait [*Arndt et al.*, 2014; *Jakobsson et al.*, 2010].

The equal distribution of ploughmark orientations observed in the northern parts of Westwind Trough and Norske Trough (Figure 8.9i and m), which is in contrast to the predominant N-S orientation in the southern parts (Figure 8.9j and n), indicates that the ploughmarks found in the northern parts were not produced by icebergs transported in the EGC but instead resulted from icebergs with exceptional trajectories. The morphology of the east to west trending glacial troughs, with banks and ridges at their northern edge, sheltered the areas directly to their south from icebergs usually coming from northerly directions and impeded, or at least limited, overprinting of older glacial landforms (Figure 8.6a and f). A possible explanation for exceptional iceberg trajectories that led to ploughing events in these otherwise sheltered areas could be the presence of grounded ice on shallower areas of the continental shelf that temporarily could have redirected ocean currents.

8.5. Conclusions

We presented first geophysical evidence that the Northeast Greenland Ice Stream extended at least to the shelf break through Westwind Trough and Norske Trough (Figure 8.10a). This extent was most probably reached during the LGM. An at least 100 km long ice stream system was active in the inter-trough area. This ice stream system was most likely fed by an ice dome located on Northwind Shoal. The ice stream diverged into a northern and a southern branch, most probably constrained by another, smaller ice dome. The mapped submarine glacial features indicate that the speed and pattern of ice retreat was variable in the troughs and occurred in different phases during deglaciation (Figure 8.10b-d):

Westwind Trough:

Phase I - in the southern part, fast retreat from the shelf edge to about 8°W; in the northern part, possibly ice shelf decay.

Phase II - in the southern part, slow stepwise retreat to about 13°W; in the northern part, stabilization at grounding zone wedge with possibly ice shelf decay

Phase III - fast retreat into coastal areas in both parts

Norske Trough:

Phase I - fast grounding zone retreat from the shelf edge to stable position on the middle shelf at about 12°30'W and establishment of an ice shelf grounded at this location

Phase II - ice shelf decay with release of large tabular icebergs, possibly by single breakup event

Phase III - fast retreat into coastal areas

Inter-trough area:

Phase I - entirely fast retreat, no other indications found

These phases did not have to occur simultaneously. Dated cores are needed to constrain the timing of the retreat. After deglaciation the entire continental shelf, except from bathymetrically sheltered areas, was heavily disturbed by ploughing events of icebergs. These icebergs were pre-dominantly steered by the north to south flowing East Greenland Current.

8.6. Acknowledgments

We thank all captains, crews and scientists involved in collecting the data used in this study. We also thank J.P. Klages and F. Niessen (AWI) for providing comments on a preliminary draft of the manuscript.

9. Conclusions and Outlook

The Greenland Ice Sheet covered almost the entire NEG continental shelf during the LGM. At that time, Westwind Trough and Norske Trough were both filled by ice streams that reached at least until the shelf edge. These results confirm the suggested larger LGM ice extent from Bennike and Björck [2002] and significantly change the previous conceptual model of an ice sheet margin close to the coast.

The retreat dynamics of the Greenland Ice Sheet on the NEG continental shelf were spatially variable and have occurred in phases of rapid and slow retreat. The type of retreat shows strong correlation to the slope of the trough. Submarine glacial landforms indicative for slower and stepwise retreat are observed where no reverse slope is present in the trough. In parts of the troughs with reverse slope, landforms indicative of rapid retreat are observed. The mapped grounding zone wedges in four troughs, each located in a similar distance to the modern day ice margin, could indicate simultaneous grounding zone stabilization and the presence of paleo-ice shelves.

Due to the absence of dated cores on the NEG continental shelf, the timing of the ice retreat phases could only be roughly estimated based on their freshness in the swath bathymetric data and on observations of postglacial sedimentary layers on top of the submarine glacial landforms. Dated cores from the mapped submarine glacial landforms are needed to constrain the timing of the identified retreat phases and to resolve if the phases occurred synchronous or asynchronous in the different ice streams. A first step in this direction has been made during R/V Polarstern cruise PS93.1 in June 2015. Four gravity cores have been recovered from between the moraines located in Westwind Trough (Figure 9.1) to resolve the timing of the grounding line retreat in this sector.

Paleo-ice stream pathways on the NEG continental shelf are reconstructed based on a new digital bathymetric model and on submarine glacial landforms indicative for ice stream direction. Ice streams have been present in all cross-shelf troughs. The reconstruction suggests that local marine ice domes built up on shallow parts of the continental shelf. These ice domes could have harbored a significant contribution to sea-level change. An ice stream system with two ice stream branches is detected in the inter trough area between Westwind Trough and Norske Trough. This system was probably fed by an ice dome located on Northwind Shoal.

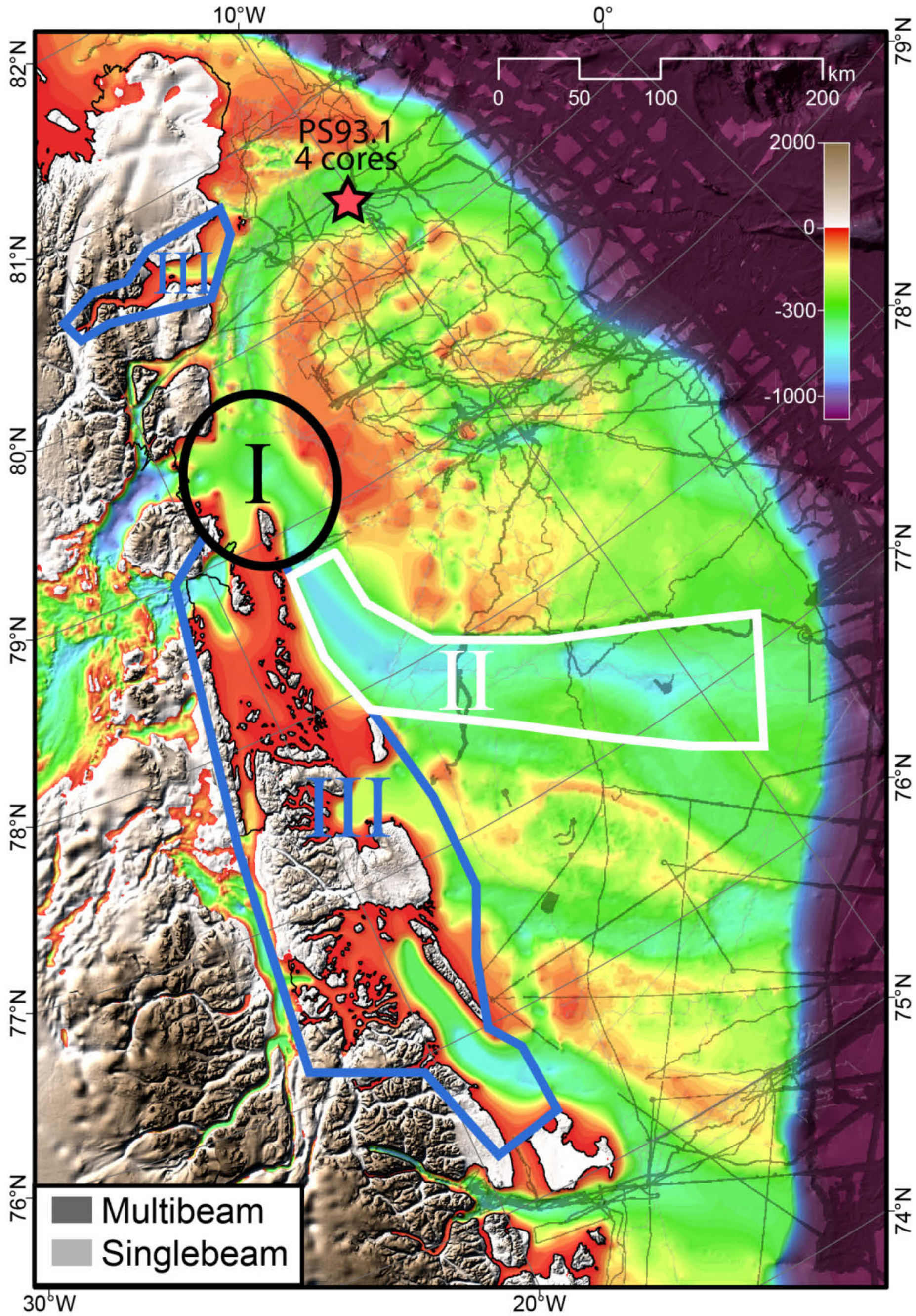

Figure 9.1: Bathymetric map of the Northeast Greenland continental shelf with core site of cruise PS93.1 and focus areas to acquire hydro-acoustic data in the future. Area I: Reveal if ice flow from Greenland continued onto Northwind Shoal. Area II: Ice Stream retreat dynamics in Norske Trough. Area III: Ice flow pathways, ice retreat dynamics, and water mass pathways in the unsurveyed coastal areas. Greyish overlay shows coverage with multibeam and singlebeam data.

Giant icebergs drifted southwards in Fram Strait, possibly during MIS 6 (190 to 130 kyrs B.P.). A fraction of the largest ones grounded on Hovgaard Ridge in a modern-day water depth of >1200 m and left behind six ploughmarks. The very deep iceberg drafts give a new constraint on paleo-ice sheet thickness at the calving line. Dated cores from the iceberg ploughmarks are necessary to give a more accurate timing of the giant iceberg export. Numerous iceberg ploughmarks in shallower depths are also mapped on the NEG continental shelf. Their dominant orientation is north to south, induced by the direction of the EGC. These traces of large iceberg export from the Arctic Ocean are indicating that a significant part of freshwater influx to the Greenland-Iceland-Norwegian Sea was facilitated by large icebergs during deglaciations and was effecting the NADW formation.

Large parts of the study area are still unmapped by hydro-acoustic systems. Subsequently, the complete distribution of submarine glacial landforms remains unknown. For an even more comprehensive reconstruction of ice stream pathways, their retreat dynamics and to further verify the pattern of iceberg ploughing events, more mapping efforts are needed. Complete mapping of the study area, however, will not be feasible within the next decades, at least for the scientific community. Nevertheless, focus areas for different research questions can be given (Figure 9.1). The central part of Norske Trough could yield important information to interpret the ice stream retreat dynamics that so far predominantly relies on data from the shallower northern part (Area II in Figure 9.1). The southern parts of the troughs as well as shallower parts of the inter trough areas most probably will not yield information on ice flow directions and retreat dynamics due to the higher rate of iceberg grounding and resulting perturbation of the seafloor. The coastal areas are nearly unmapped by hydro-acoustic systems. Data gathered in this area can yield valuable information to reconstruct the past glacial system and in addition is valuable to reveal possible pathways of water masses to marine terminating glaciers (Areas III in Figure 9.1). This is especially the case for the area west of Northwind Shoal (Area I in Figure 9.1). Here, swath bathymetric data most probably will instantly reveal if the NEG ice stream was entirely redirected to north and south direction into Westwind and Norske Trough or if ice flow continued across Northwind Shoal. This verify or respectively reject the theory of an ice dome located on Northwind Shoal that could have harbored a significant amount of ice above floatation with subsequent increase of sea level rise after its deglaciation.

Bibliography

Aagaard, K., and L. K. Coachman (1968), The East Greenland Current North of Denmark Strait: Part I, *Arctic*, 181-200.

Aagaard, K., and E. C. Carmack (1989), The role of sea ice and other fresh water in the Arctic circulation, *Journal of Geophysical Research: Oceans*, *94*(C10), 14485-14498, doi: 10.1029/JC094iC10p14485.

Arndt, J. E., F. Niessen, W. Jokat, and B. Dorschel (2014), Deep water paleo-iceberg scouring on top of Hovgaard Ridge–Arctic Ocean, *Geophysical Research Letters*, *41*(14), 5068-5074, doi: 10.1002/2014gl060267.

Arndt, J. E., W. Jokat, B. Dorschel, R. Myklebust, J. A. Dowdeswell, and J. Evans (2015), A new bathymetry of the Northeast Greenland continental shelf: Constraints on glacial and other processes, *Geochemistry, Geophysics, Geosystems*, *16*(10), 3733-3753, doi: 10.1002/2015GC005931.

Arndt, J. E., et al. (2013), The International Bathymetric Chart of the Southern Ocean (IBCSO) Version 1.0 - A new bathymetric compilation covering circum-Antarctic waters, *Geophysical Research Letters*, *40*, 3111-3117, doi: 10.1002/grl.50413.

Batchelor, C. L., and J. A. Dowdeswell (2013), The physiography of High Arctic cross-shelf troughs, *Quaternary Science Reviews*, *1*(29), doi: 10.1016/j.quascirev.2013.05.025.

Batchelor, C. L., and J. A. Dowdeswell (2014), The physiography of High Arctic cross-shelf troughs, *Quaternary Science Reviews*, *92*, 68-96, doi: 10.1016/j.quascirev.2013.05.025.

Batchelor, C. L., and J. A. Dowdeswell (2015), Ice-sheet grounding-zone wedges (GZWs) on high-latitude continental margins, *Mar. Geol.*, *363*, 65-92, doi: 10.1016/j.margeo.2015.02.001.

Belderson, R. H., N. H. Kenyon, and J. B. Wilson (1973), Iceberg plough marks in the northeast Atlantic *Palaeogeography, Palaeoclimatology, Palaeoecology*, *13*(3), 215-224.

Benn, D. I., and D. J. A. Evans (2010), *Glaciers & glaciation*, 2nd ed., Hodder Education, London.

Bennike, O., and A. Weidick (2001), Late Quaternary history around Nioghalvfjerdsfjorden and Jøkelbugten, North-East Greenland, *Boreas*, *30*(3), 205-227, doi: 10.1111/j.1502-3885.2001.tb01223.x.

Bennike, O., and S. Björck (2002), Chronology of the last recession of the Greenland Ice Sheet, *Journal of Quaternary Science*, *17*(3), 211-219, doi: 10.1002/jqs.670.

Bennike, O., N. Mikkelsen, R. Forsberg, and L. Hedenas (2006), Tuppiap Qeqertaa (Tobias Island): a newly discovered island off northeast Greenland, *Polar Record*, *42*(223), 309-314, doi: 10.1017/S003224740600550X.

Berger, D., and W. Jokat (2008), A seismic study along the East Greenland margin from 72°N to 77°N, *Geophysical Journal International*, *174*(2), 733-748, doi: 10.1111/j.1365-246X.2008.03794.x.

Berger, D., and W. Jokat (2009), Sediment deposition in the northern basins of the North Atlantic and characteristic variations in shelf sedimentation along the East Greenland margin, *Mar. Petrol. Geol.*, *26*(8), 1321-1337, doi: 10.1016/j.marpetgeo.2009.04.005.

Bischof, J., J. Koch, M. Kubisch, R. F. Spielhagen, and J. Thiede (1990), Nordic Seas surface ice drift reconstructions: evidence from ice rafted coal fragments during oxygen isotope stage 6, *Geological Society, London, Special Publications*, *53*(1), 235-251, doi: 10.1144/gsl.sp.1990.053.01.13.

Bourke, R. H., J. L. Newton, R. G. Paquette, and M. D. Tunnicliffe (1987), Circulation and water masses of the East Greenland shelf, *Journal of Geophysical Research: Oceans*, *92*(C7), 6729-6740, doi: 10.1029/JC092iC07p06729.

Bradley, R. S., and J. H. England (2008), The Younger Dryas and the Sea of Ancient Ice, *Quat. Res.*, *70*(1), 1-10, doi: 10.1016/j.yqres.2008.03.002.

Briner, J. P., A. C. Bini, and R. S. Anderson (2009), Rapid early Holocene retreat of a Laurentide outlet glacier through an Arctic fjord, *Nature Geosci*, *2*(7), 496-499, doi: 10.1038/ngeo556.

Broecker, W. S. (2010), *The Great Ocean Conveyor: Discovering the Trigger for Abrupt Climate Change*, 176 pp., Princeton University Press, Princeton.

Budéus, G., and W. Schneider (1995), On the hydrography of the Northeast Water Polynya, *Journal of Geophysical Research: Oceans*, *100*(C3), 4287-4299, doi: 10.1029/94jc02024.

Chen, C. T., and F. J. Millero (1977), Speed of sound in seawater at high pressures, *The Journal of the Acoustical Society of America*, *62*(5), 1129-1135, doi: 10.1121/1.381646.

Cherkis, N., and P. R. Vogt (1994), Regional Bathymetry of the Northern Norwegian - Greenland Sea, Naval Research Laboratory, Washington D.C.

Chopra, S., and K. Marfurt (2012), Seismic attribute expression of differential compaction, *The Leading Edge*, *31*(12), 1418-1422, doi: doi:10.1190/tle31121418.1.

Christoffersen, P., R. I. Mugford, K. J. Heywood, I. Joughin, J. A. Dowdeswell, J. P. M. Syvitski, A. Luckman, and T. J. Benham (2011), Warming of waters in an East Greenland fjord prior to glacier retreat: mechanisms and connection to large-scale atmospheric conditions, *The Cryosphere*, *5*(3), 701-714, doi: 10.5194/tc-5-701-2011.

Church, J. A., J. M. Gregory, N. J. White, S. M. Platten, and J. X. Mitrovica (2011), Understanding and projecting sea level change, *Oceanography*, *24*(2), 130-143, doi: 10.5670/oceanog.2011.33.

Clark, C. D. (1993), Mega-scale glacial lineations and cross-cutting ice-flow landforms, *Earth Surface Processes and Landforms*, *18*(1), 1-29, doi: 10.1002/esp.3290180102.

Darby, D. A., J. F. Bischof, R. F. Spielhagen, S. A. Marshall, and S. W. Herman (2002), Arctic ice export events and their potential impact on global climate during the late Pleistocene, *Paleoceanography*, *17*(2), 15-11-15-17, doi: 10.1029/2001pa000639.

de Jong, C. D., G. Lachapelle, S. Skone, and I. A. Elema (2002), *Hydrography*, Delft University Press, Delft.

Death, R., M. J. Siegert, G. R. Bigg, and M. R. Wadley (2006), Modelling iceberg trajectories, sedimentation rates and meltwater input to the ocean from the Eurasian Ice Sheet at the Last Glacial Maximum, *Palaeogeography, Palaeoclimatology, Palaeoecology*, *236*, 135-150, doi: 10.1016/j.palaeo.2005.11.040.

Dickens, W. A., A. G. C. Graham, J. A. Smith, J. A. Dowdeswell, R. D. Larter, C.-D. Hillenbrand, P. N. Trathan, J. E. Arndt, and G. Kuhn (2014), A new bathymetric compilation for the South Orkney Islands region, Antarctic Peninsula (49°–39°W to 64°–59°S): Insights into the glacial development of the continental shelf, *Geochemistry, Geophysics, Geosystems*, *15*(6), 2494-2514, doi: 10.1002/2014gc005323.

Dowdeswell, J. A., and J. L. Bamber (2007), Keel depths of modern Antarctic icebergs and implications for sea-floor scouring in the geological record, *Mar. Geol.*, *243*, 120-131, doi: 10.1016/j.margeo.2007.04.008.

Dowdeswell, J. A., and E. M. G. Fugelli (2012), The seismic architecture and geometry of grounding-zone wedges formed at the marine margins of past ice sheets, *Geological Society of America Bulletin*, doi: 10.1130/b30628.1.

Dowdeswell, J. A., R. J. Whittington, and P. Marienfeld (1994a), The origin of massive diamicton facies by iceberg rafting and scouring, Scoresby Sund, East Greenland, *Sedimentology*, *41*(1), 21-35, doi: 10.1111/j.1365-3091.1994.tb01390.x.

Dowdeswell, J. A., C. Ó. Cofaigh, and C. J. Pudsey (2004), Thickness and extent of the subglacial till layer beneath an Antarctic paleo–ice stream, *Geology*, *32*(1), 13-16, doi: 10.1130/g19864.1.

Dowdeswell, J. A., J. Evans, and C. Ó Cofaigh (2010a), Submarine landforms and shallow acoustic stratigraphy of a 400 km-long fjord-shelf-slope transect, Kangerlussuaq margin, East Greenland, *Quaternary Science Reviews*, *29*(25–26), 3359-3369, doi: 10.1016/j.quascirev.2010.06.006.

Dowdeswell, J. A., H. Villinger, R. J. Whittington, and P. Marienfeld (1993), Iceberg scouring in Scoresby Sund and on the East Greenland continental shelf, *Mar. Geol.*, *111*(1–2), 37-53, doi: 10.1016/0025-3227(93)90187-Z.

Dowdeswell, J. A., G. Uenzelmann-Neben, R. J. Whittington, and P. Marienfeld (1994b), The Late Quaternary sedimentary record in Scoresby Sund, East Greenland, *Boreas*, *23*(4), 294-310, doi: 10.1111/j.1502-3885.1994.tb00602.x.

Dowdeswell, J. A., D. Ottesen, J. Evans, C. O Cofaigh, and J. B. Anderson (2008), Submarine glacial landforms and rates of ice-stream collapse, *Geology*, *36*, 819-822, doi: 10.1130/G24808A.1

Dowdeswell, J. A., Whittington, Jennings, Andrews, Mackensen, and Marienfeld (2000), An origin for laminated glacimarine sediments through sea-ice build-up and suppressed iceberg rafting, *Sedimentology*, *47*(3), 557-576, doi: 10.1046/j.1365-3091.2000.00306.x.

Dowdeswell, J. A., K. A. Hogan, C. Ó Cofaigh, E. M. G. Fugelli, J. Evans, and R. Noormets (2014), Late Quaternary ice flow in a West Greenland fjord and cross-shelf trough system: submarine landforms from Rink Isbrae to Uummannaq shelf and slope, *Quaternary Science Reviews*, *92*, 292-309, doi: 10.1016/j.quascirev.2013.09.007.

Dowdeswell, J. A., et al. (2010b), High-resolution geophysical observations of the Yermak Plateau and northern Svalbard margin: implications for ice-sheet grounding and deep-keeled icebergs, *Quaternary Science Reviews*, *29*, 3518-3531, doi: 10.1016/j.quascirev.2010.06.002.

Ehlers, J., and P. L. Gibbard (2007), The extent and chronology of Cenozoic Global Glaciation, *Quaternary International*, *164–165*(0), 6-20, doi: 10.1016/j.quaint.2006.10.008.

Engen, Ø., J. I. Faleide, and T. K. Dyreng (2008), Opening of the Fram Strait gateway: A review of plate tectonic constraints, *Tectonophysics*, *450*(1–4), 51-69, doi: 10.1016/j.tecto.2008.01.002.

England, J. H., M. F. A. Furze, and J. P. Doupé (2009), Revision of the NW Laurentide Ice Sheet: implications for paleoclimate, the northeast extremity of Beringia, and Arctic Ocean sedimentation, *Quaternary Science Reviews*, *28*(17–18), 1573-1596, doi: http://dx.doi.org/10.1016/j.quascirev.2009.04.006.

England, J. H., N. Atkinson, J. Bednarski, A. S. Dyke, D. A. Hodgson, and C. Ó Cofaigh (2006), The Innuitian Ice Sheet: configuration, dynamics and chronology, *Quaternary Science Reviews*, *25*(7–8), 689-703, doi: http://dx.doi.org/10.1016/j.quascirev.2005.08.007.

Evans, J., C. Ó Cofaigh, J. A. Dowdeswell, and P. Wadhams (2009), Marine geophysical evidence for former expansion and flow of the Greenland Ice Sheet across the north-east Greenland continental shelf, *Journal of Quaternary Science*, *24*(3), 279-293, doi: 10.1002/jqs.1231.

Evans, J., J. A. Dowdeswell, H. Grobe, F. Niessen, R. Stein, H.-W. Hubberten, and R. J. Whittington (2002), Late Quaternary sedimentation in Kejser Franz Joseph Fjord and the continental margin of East Greenland, *Geological Society, London, Special Publications*, *203*(1), 149-179, doi: 10.1144/gsl.sp.2002.203.01.09.

Fieg, K., R. Gerdes, E. Fahrbach, A. Beszczynska-Möller, and U. Schauer (2010), Simulation of oceanic volume transports through Fram Strait 1995–2005, *Ocean Dynamics*, *60*(3), 491-502, doi: 10.1007/s10236-010-0263-9.

Fleming, K., and K. Lambeck (2004), Constraints on the Greenland Ice Sheet since the Last Glacial Maximum from sea-level observations and glacial-rebound models, *Quaternary Science Reviews*, *23*(9–10), 1053-1077, doi: 10.1016/j.quascirev.2003.11.001.

Flower, B. P. (1997), Overconsolidated section on the Yermak Plateau, Arctic Ocean: Ice sheet grounding prior to ca. 660 ka?, *Geology*, *25*(2), 147-150, doi: 10.1130/0091-7613(1997)025<0147:osotyp>2.3.co;2.

Funder, S., K. K. Kjeldsen, K. H. Kjær, and C. Ó Cofaigh (2011), The Greenland Ice Sheet During the Past 300,000 Years: A Review, in *Quaternary Glaciations - Extent and Chronology*, edited by J. Ehlers, P. L. Gibbard and P. D. Hughes, pp. 699-713, Elsevier, Amsterdam, The Netherlands.

García, M., J. A. Dowdeswell, G. Ercilla, and M. Jakobsson (2012), Recent glacially influenced sedimentary processes on the East Greenland continental slope and deep Greenland Basin, *Quaternary Science Reviews*, *49*, 64-81, doi: 10.1016/j.quascirev.2012.06.016.

Gebhardt, A. C., W. Jokat, F. Niessen, J. Matthiessen, W. H. Geissler, and H. W. Schenke (2011), Ice sheet grounding and iceberg plow marks on the northern and central Yermak Plateau revealed by geophysical data, *Quaternary Science Reviews*, *30*, 1726-1738, doi: 10.1016/j.quascirev.2011.03.016.

Golledge, N., E. Phillips, and British Geological Survey (2008), Sedimentology and architecture of De Geer moraines in the western Scottish Highlands, and implications for grounding-line glacier dynamics, *Sedimentary Geology*, *208*(1-2), 1-14, doi: 10.1016/j.sedgeo.2008.03.009.

Graham, A. G. C., F. O. Nitsche, and R. D. Larter (2011), An improved bathymetry compilation for the Bellingshausen Sea, Antarctica, to inform ice-sheet and ocean models, *The Cryosphere*, *5*, 95-106, doi: 10.5194/tc-5-95-2011.

Graham, A. G. C., R. D. Larter, K. Gohl, C.-D. Hillenbrand, J. A. Smith, and G. Kuhn (2009), Bedform signature of a West Antarctic palaeo-ice stream reveals a multi-temporal record of flow and substrate control, *Quaternary Science Reviews*, *28*, 2774-2793, doi: doi:10.1016/j.quascirev.2009.07.003.

Hamann, N. E., R. C. Whittaker, and L. Stemmerik (2005), Geological development of the Northeast Greenland Shelf, *Petroleum Geology Conference Series*, *6*, 887-902, doi: 10.1144/0060887.

Hasholt, B. (1996), Sediment transport in Greenland, in *Erosion and Sediment Yield: Global and Regional Perspectives*, edited by D. E. Walling and B. Webb, pp. 105-114, IAHS Press, Wallingford, UK.

Hell, B., and M. Jakobsson (2011), Gridding heterogeneuos bathymetric data sets with stacked continous curvature splines in tension, *Marine Geophysical Research*, *32*(4), 493-501, doi: 10.1007/s11001-011-9141-1.

Hellmer, H. H., F. Kauker, R. Timmermann, J. Determann, and J. Rae (2012), Twenty-first-century warming of a large Antarctic ice-shelf cavity by a redirected coastal current, *Nature*, *485*, 225-228, doi: 10.1038/nature11064.

Helm, V., A. Humbert, and H. Miller (2014), Elevation and elevation change of Greenland and Antarctica derived from CryoSat-2, *The Cryosphere*, *8*(4), 1539-1559, doi: 10.5194/tc-8-1539-2014.

Henriksen, N. (2003), Caledonian Orogen East Greenland 70° - 82° N, Geological Survey of Denmark and Greenland, Copenhagen.

Hjelstuen, B. O., H. Haflidason, H. P. Sejrup, and A. Lyså (2009), Sedimentary processes and depositional environments in glaciated fjord systems — Evidence from Nordfjord, Norway, *Mar. Geol.*, *258*(1–4), 88-99, doi: 10.1016/j.margeo.2008.11.010.

Holland, D. M., R. H. Thomas, B. de Young, M. H. Ribergaard, and B. Lyberth (2008), Acceleration of Jakobshavn Isbrae triggered by warm subsurface ocean waters, *Nature Geoscience*, *1*(10), 659-664, doi: 10.1038/ngeo316.

Howat, I. M., A. Negrete, and B. E. Smith (2014), The Greenland Ice Mapping Project (GIMP) land classification and surface elevation data sets, *The Cryosphere*, *8*(4), 1509-1518, doi: 10.5194/tc-8-1509-2014.

Hu, A., G. A. Meehl, B. L. Otto-Bliesner, C. Waelbroeck, W. Han, M.-F. Loutre, K. Lambeck, J. X. Mitrovica, and N. Rosenbloom (2010), Influence of Bering Strait flow and North Atlantic circulation on glacial sea-level changes, *Nature Geoscience*, *3*(2), 118-121, doi: 10.1038/ngeo729.

Hughes, N. E., J. P. Wilkinson, and P. Wadhams (2011), Multi-satellite sensor analysis of fast-ice development in the Norske Øer Ice Barrier, northeast Greenland, *Annals of Glaciology*, *52*(57), 151-160, doi: 10.3189/172756411795931633.

Jakobsson, M., C. Marcussen, and S. P. LOMROG (2008a), Lomonosov Ridge Off Greenland 2007 (LOMROG) - Cruise Report*Rep. ISBN 978-87-7871-238-7*, 122 pp, Geological Survey of Denmark and Greenland, Copenhagen.

Jakobsson, M., L. Polyak, M. Edwards, J. Kleman, and B. Coakley (2008b), Glacial geomorphology of the Central Arctic Ocean: the Chukchi Borderland and the Lomonosov Ridge, *Earth Surface Processes and Landforms*, *33*(4), 526-545, doi: 10.1002/esp.1667.

Jakobsson, M., J. B. Anderson, F. O. Nitsche, R. Gyllencreutz, A. E. Kirshner, N. Kirchner, M. O'Regan, R. Mohammad, and B. Eriksson (2012a), Ice sheet retreat dynamics inferred from glacial morphology of the central Pine Island Bay Trough, West Antarctica, *Quaternary Science Reviews*, doi: 10.1016/j.quascirev.2011.12.017.

Jakobsson, M., J. V. Gardner, P. R. Vogt, L. A. Mayer, A. Armstrong, J. Backman, R. Brennan, B. Calder, J. K. Hall, and B. Kraft (2005), Multibeam bathymetric and sediment profiler evidence for ice grounding on the Chukchi Borderland, Arctic Ocean, *Quat. Res.*, *63*(2), 150-160, doi: 10.1016/j.yqres.2004.12.004.

Jakobsson, M., et al. (2010), An Arctic Ocean ice shelf during MIS 6 constrained by new geophysical and geological data, *Quaternary Science Reviews*, *29*, 3505-3517, doi: 10.1016/j.quascirev.2010.03.015.

Jakobsson, M., et al. (2013), Arctic Ocean glacial history, *Quaternary Science Reviews*, 1-28, doi: 10.1016/j.quascirev.2013.07.033.

Jakobsson, M., et al. (2014), Arctic Ocean glacial history, *Quaternary Science Reviews*, *92*(0), 40-67, doi: 10.1016/j.quascirev.2013.07.033.

Jakobsson, M., et al. (2012b), The International Bathymetric Chart of the Arctic Ocean (IBCAO) Version 3.0, *Geophysical Research Letters*, *39*, doi: 10.1029/2012GL052219.

Jenkins, A., P. Dutrieux, S. S. Jacobs, S. McPhail, J. R. Perrett, A. T. Webb, and D. White (2010), Observations beneath Pine Island Glacier in West Antarctica and implications for its retreat, *Nature Geoscience*, *3*, 468-472, doi: 10.1038/NGEO890.

Johannessen, O. M. (1986), Brief Overview of the Physical Oceanography, in *The Nordic Seas*, edited by B. Hurdle, pp. 103-128, Springer New York.

Johnson, G. L., and O. B. Eckhoff (1966), Bathymetry of the north Greenland Sea, *Deep Sea Research and Oceanographic Abstracts*, *13*(6), 1161-1173, doi: 10.1016/0011-7471(66)90707-8.

Joughin, I., M. Fahnestock, D. MacAyeal, J. L. Bamber, and P. Gogineni (2001), Observation and analysis of ice flow in the largest Greenland ice stream, *Journal of Geophysical Research: Atmospheres*, *106*(D24), 34021-34034, doi: 10.1029/2001jd900087.

Joughin, I., B. E. Smith, I. M. Howat, T. Scambos, and T. Moon (2010), Greenland flow variability from ice-sheet-wide velocity mapping, *Journal of Glaciology*, *56*(197), 415-430, doi: 10.3189/002214310792447734.

Joughin, I. R., M. A. Fahnestock, and J. L. Bamber (2000), Ice flow in the northeast Greenland ice stream, *Annals of Glaciology*, *31*(1), 141-146, doi: 10.3189/172756400781820002.

Khan, S. A., et al. (2014), Sustained mass loss of the northeast Greenland ice sheet triggered by regional warming, *Nature Clim. Change*, *4*(4), 292-299, doi: 10.1038/nclimate2161.

King, E. C., R. C. A. Hindmarsh, and C. R. Stokes (2009), Formation of mega-scale glacial lineations observed beneath a West Antarctic ice stream, *Nature Geosci*, *2*(8), 585-588, doi: 10.1038/ngeo581.

Klenke, M., and H. W. Schenke (2002), A new bathymetric model for the central Fram Strait, *Marine Geophysical Researches*, *23*, 367-378, doi: 10.1023/A:1025764206736.

Knies, J., J. Matthiessen, A. Mackensen, R. Stein, C. Vogt, T. Frederichs, and S.-I. Nam (2007), Effects of Arctic freshwater forcing on thermohaline circulation during the Pleistocene, *Geology*, *35*(12), 1075-1078, doi: 10.1130/g23966a.1.

Knies, J., J. Matthiessen, C. Vogt, J. S. Laberg, B. O. Hjelstuen, M. Smelror, E. Larsen, K. Andreassen, T. Eidvin, and T. O. Vorren (2009), The Plio-Pleistocene glaciation of the Barents Sea–Svalbard region: a new model based on revised chronostratigraphy, *Quaternary Science Reviews*, *28*, 812-829, doi: 10.1016/j.quascirev.2008.12.002.

Kristensen, M., V. A. Squire, and S. C. Moore (1982), Tabular icebergs in ocean waves, *Nature*, *297*(5868), 669-671, doi: 10.1038/297669a0.

Kuijpers, A., and F. Werner (2007), Extremely deep-draft iceberg scouring in the glacial North Atlantic Ocean, *Geo-Marine Letters*, *27*(6), 383-389, doi: 10.1007/s00367-007-0059-1.

Kuijpers, A., F. Dalhoff, M. P. Brandt, P. Hümbs, T. Schott, and A. Zotova (2007), Giant iceberg plow marks at more than 1 km water depth offshore West Greenland, *Mar. Geol.*, *246*(1), 60-64, doi: 10.1016/j.margeo.2007.05.010.

Landvik, J. Y. (1994), The last glaciation of Germania Land and adjacent areas, northeast Greenland, *Journal of Quaternary Science*, *9*(1), 81-92, doi: 10.1002/jqs.3390090108.

Lavoie, C., et al. (2015), Configuration of the Northern Antarctic Peninsula Ice Sheet at LGM based on a new synthesis of seabed imagery, *The Cryosphere*, *9*(2), 613-629, doi: 10.5194/tc-9-613-2015.

Lenton, T. M., H. Held, E. Kriegler, J. W. Hall, W. Lucht, S. Rahmstorf, and H. J. Schellnhuber (2008), Tipping elements in the Earth's climate system, *Proceedings of the National Academy of Sciences*, *105*(6), 1786-1793, doi: 10.1073/pnas.0705414105.

Livingstone, S. J., C. Ó Cofaigh, C. R. Stokes, C.-D. Hillenbrand, A. Vieli, and S. S. R. Jamieson (2012), Antarctic palaeo-ice streams, *Earth-Science Reviews*, *111*(1–2), 90-128, doi: 10.1016/j.earscirev.2011.10.003.

Lurton, X. (2004), *An Introduction to Underwater Acoustics: Principles and Applications*, Springer-Verlag and Praxis Publishing, Chichester, UK.

Mayer, C., N. Reeh, F. Jung-Rothenhäusler, P. Huybrechts, and H. Oerter (2000), The subglacial cavity and implied dynamics under Nioghalvfjerdsfjorden Glacier, NE-Greenland, *Geophysical Research Letters*, *27*(15), 2289-2292, doi: 10.1029/2000gl011514.

Medwin, H. (1975), Speed of sound in water: A simple equation for realistic parameters, *The Journal of the Acoustical Society of America*, *58*(6), 1318-1319, doi: 10.1121/1.380790.

Mercer, J. H. (1970), A former ice sheet in the Arctic Ocean?, *Palaeogeography, Palaeoclimatology, Palaeoecology*, *8*(1), 19-27, doi: 10.1016/0031-0182(70)90076-3.

Moore, T. C. (2005), The Younger Dryas: From whence the fresh water?, *Paleoceanography*, *20*(4), PA4021, doi: 10.1029/2005pa001170.

Morlighem, M., E. Rignot, J. Mouginot, H. Seroussi, and E. Larour (2014), Deeply incised submarine glacial valleys beneath the Greenland ice sheet, *Nature Geoscience*, *7*(6), 418-422, doi: 10.1038/ngeo2167.

NASA Landsat Program (2000), L7CPF20000701_20000718_08 - Orthorectified, edited by Landsat7, USGS, Sioux Falls.

Niessen, F., et al. (2013), Repeated Pleistocene glaciation of the East Siberian continental margin, *Nature Geoscience*, *6*(10), 842-846, doi: 10.1038/ngeo1904.

Nitsche, F. O., S. S. Jacobs, R. D. Larter, and K. Gohl (2007), Bathymetry of the Amundsen Sea continental shelf: Implications for geology, oceanography, and glaciology, *Geochemistry Geophysics Geosystems*, *8*, Q10009, doi: 10.1029/2007GC001694.

Ó Cofaigh, C., J. A. Dowdeswell, and H. Grobe (2001), Holocene glacimarine sedimentation, inner Scoresby Sund, East Greenland: the influence of fast-flowing ice-sheet outlet glaciers, *Mar. Geol.*, *175*(1–4), 103-129, doi: 10.1016/S0025-3227(01)00117-7.

Ó Cofaigh, C., C. J. Pudsey, J. A. Dowdeswell, and P. Morris (2002), Evolution of subglacial bedforms along a paleo-ice stream, Antarctic Peninsula continental shelf, *Geophysical Research Letters*, *29*(8), 41-41-41-44, doi: 10.1029/2001gl014488.

O'Regan, M., M. Jakobsson, and N. Kirchner (2010), Glacial geological implications of overconsolidated sediments on the Lomonosov Ridge and Yermak Plateau, *Quaternary Science Reviews*, *29*(25–26), 3532-3544, doi: 10.1016/j.quascirev.2010.09.009.

Ohmura, A., and N. Reeh (1991), New precipitation and accumulation maps for Greenland, *Journal of Glaciology*, *37*(125), 140-148.

Ottesen, D., J. A. Dowdeswell, and L. Rise (2005), Submarine landforms and the reconstruction of fast-flowing ice streams within a large Quaternary ice sheet: The 2500-km-long Norwegian-Svalbard margin (57°–80°N), *GSA Bulletin*, *117*(5/6), B25577, doi: 10.1130/B25577.1.

Ottesen, D., J. A. Dowdeswell, J. Y. Landvik, and J. Mienert (2007), Dynamics of the Late Weichselian ice sheet on Svalbard inferred from high-resolution sea-floor morphology, *Boreas*, *36*(3), 286-306, doi: 10.1080/03009480701210378.

Perry, R. K., H. S. Fleming, N. Cherkis, R. H. Feden, and P. R. Vogt (1980), Bathymetry of the Norwegian-Greenland and western Barents seas, *Chart*, U.S. Naval Research Laboratory, Washington D.C.

Polyak, L., M. H. Edwards, B. J. Coakley, and M. Jakobsson (2001), Ice shelves in the Pleistocene Arctic Ocean inferred from glaciogenic deep-sea bedforms, *Nature*, *410*(6827), 453-457, doi: 10.1038/35068536.

Polyak, L., S. L. Forman, F. A. Herlihy, G. Ivanov, and P. Krinitsky (1997), Late Weichselian deglacial history of the Svyataya (Saint) Anna Trough, northern Kara Sea, Arctic Russia, *Mar. Geol.*, *143*(1–4), 169-188, doi: 10.1016/S0025-3227(97)00096-0.

Pritchard, H. D., S. R. M. Ligtenberg, H. A. Fricker, D. G. Vaughan, M. R. van den Broeke, and L. Padman (2012), Antarctic ice-sheet loss driven by basal melting of ice shelves, *Nature*, *484*, 502-505, doi: 10.1038/nature10968.

Rabe, B., U. Schauer, A. Mackensen, M. Karcher, E. Hansen, and A. Beszczynska-Möller (2009), Freshwater components and transports in the Fram Strait - recent observations and changes since the late 1990s, *Ocean Sci.*, *5*(3), 219-233, doi: 10.5194/os-5-219-2009.

Rabe, B., P. A. Dodd, E. Hansen, E. Falck, U. Schauer, A. Mackensen, A. Beszczynska-Møller, G. Kattner, E. J. Rohling, and K. Cox (2013), Liquid export of Arctic freshwater components through the Fram Strait 1998–2011, *Ocean Science*, *9*, 91-109, doi: 10.5194/os-9-91-2013.

Rebesco, M., F. J. Hernández-Molina, D. Van Rooij, and A. Wåhlin (2014), Contourites and associated sediments controlled by deep-water circulation processes: State-of-the-art and future considerations, *Mar. Geol.*, *352*, 111-154, doi: 10.1016/j.margeo.2014.03.011.

Rignot, E., and P. Kanagaratnam (2006), Changes in the Velocity Structure of the Greenland Ice Sheet, *Science*, *311*(5763), 986-990, doi: 10.1126/science.1121381.

Rohling, E. J., K. Grant, M. Bolshaw, A. P. Roberts, M. Siddall, C. Hemleben, and M. Kucera (2009), Antarctic temperature and global sea level closely coupled over the past five glacial cycles, *Nature Geoscience*, *2*(7), 500-504, doi: 10.1038/ngeo557.

Schauer, U., E. Fahrbach, S. Osterhus, and G. Rohardt (2004), Arctic warming through the Fram Strait: Oceanic heat transport from 3 years of measurements, *Journal of Geophysical Research: Oceans*, *109*(C6), C06026, doi: 10.1029/2003jc001823.

Schoof, C. (2007), Ice sheet grounding line dynamics: Steady states, stability, and hysteresis, *J. Geophys. Res.*, *112*, FS03S28, doi: 10.1029/2006JF000664.

Smith, J. A., C.-D. Hillenbrand, G. Kuhn, R. D. Larter, A. G. C. Graham, W. Ehrmann, S. G. Moreton, and M. Forwick (2011), Deglacial history of the West Antarctic Ice Sheet in the western Amundsen Sea Embayment, *Quaternary Science Reviews*, *30*(5-6), 488-505, doi: 10.1016/j.quascirev.2010.11.020.

Smith, W. H. F., and P. Wessel (1990), Gridding with continuous curvature splines in tension, *Geophysics*, *55*(3), 293-305, doi: 10.1190/1.1442837.

Stein, R., J. Matthießen, F. Niessen, A. Krylov, S.-I. Nam, and E. Bazhenova (2010), Towards a better (litho-) stratigraphy and reconstruction of Quaternary paleoenvironment in the Amerasian Basin (Arctic Ocean), *Polarforschung*, *79*(2), 97-121.

Stokes, C. R., and C. D. Clark (2002), Ice stream shear margin moraines, *Earth Surface Processes and Landforms*, *27*(5), 547-558, doi: 10.1002/esp.326.

Storey, M., R. A. Duncan, and C. Tegner (2007), Timing and duration of volcanism in the North Atlantic Igneous Province: Implications for geodynamics and links to the Iceland hotspot, *Chemical Geology*, *241*(3–4), 264-281, doi: 10.1016/j.chemgeo.2007.01.016.

Straneo, F., D. A. Sutherland, D. Holland, C. Gladish, G. S. Hamilton, H. L. Johnson, E. Rignot, Y. Xu, and M. Koppes (2012), Characteristics of ocean waters reaching Greenland's glaciers, *Annals of Glaciology*, *53*(60), 202, doi: 10.3189/2012AoG60A059.

Svendsen, J. I., et al. (2004), Late Quaternary ice sheet history of northern Eurasia, *Quaternary Science Reviews*, *23*(11–13), 1229-1271, doi: 10.1016/j.quascirev.2003.12.008.

Syvitski, J. P. M. (1989), On the deposition of sediment within glacier-influenced fjords: Oceanographic controls, *Mar. Geol.*, *85*(2–4), 301-329, doi: 10.1016/0025-3227(89)90158-8.

ten Brink, U. S., and C. Schneider (1995), Glacial morphology and depositional sequences of the Antarctic continental shelf, *Geology*, *23*(7), 580-584, doi: 10.1130/0091-7613(1995)023<0580:GMADSO>2.3.CO;2.

Tiedemann, R., M. Sarnthein, and N. J. Shackleton (1994), Astronomic timescale for the Pliocene Atlantic δ18O and dust flux records of Ocean Drilling Program Site 659, *Paleoceanography*, *9*(4), 619-638, doi: 10.1029/94pa00208.

Vaughan, D. G., et al. (2013), Observations: Cryosphere, in *Climate Change 2013: The Physical Science Basis. Contribution of Working Group I to the Fifth Assessment Report of the Intergovernmental Panel on Climate Change*, edited by T. F. Stocker, D. Qin, G.-K. Plattner, M. Tignor, S. K. Allen, J. Boschung, A. Nauels, Y. Xia, V. Bex and P. M. Midgley, pp. 317-382, Cambridge University Press, Cambridge, United Kingdom and New York, NY, USA.

Vorren, T. O., M. Hald, and E. Thomsen (1984), Quaternary sediments and environments on the continental shelf off northern Norway, *Mar. Geol.*, *57*(1–4), 229-257, doi: 10.1016/0025-3227(84)90201-9.

Vorren, T. O., M. Hald, M. Edvardsen, and O.-W. Lind-Hansen (1983), Glacigenic sediments and sedimentary environments on continental shelves: general principles with a case study from the Norwegian shelf, in *Glacial Deposits in northern Europe*, edited by J. Ehlers, Balkema, Rotterdam.

Voss, M., M. C. Schmidt-Aursch, and W. Jokat (2009), Variations in magmatic processes along the East Greenland volcanic margin, *Geophysical Journal International*, *177*(2), 755-782, doi: 10.1111/j.1365-246X.2009.04077.x.

Wadhams, P., J. P. Wilkinson, and S. D. McPhail (2006), A new view of the underside of Arctic sea ice, *Geophysical Research Letters*, *33*(4), L04501, doi: 10.1029/2005gl025131.

Walker, D. P., M. A. Brandon, A. Jenkins, J. T. Allen, J. A. Dowdeswell, and J. Evans (2007), Oceanic heat transport onto Amundsen Sea shelf through a submarine glacial trough, *Geophysical Research Letters*, *34*, L02602, doi: 10.1029/2006GL028154.

Weatherall, P., K. M. Marks, M. Jakobsson, T. Schmitt, S. Tani, J. E. Arndt, M. Rovere, D. Chayes, V. Ferrini, and R. Wigley (2015), A New Digital Bathymetric Model of the World's Oceans, *Earth and Space Science*, 2015EA000107, doi: 10.1002/2015ea000107.

Wessel, P., and W. H. F. Smith (1995), New Version of the Generic Mapping Tools, *EOS Transactions*, *76*(33), 329, doi: 10.1029/95EO00198.

Wilken, M., and J. Mienert (2006), Submarine glacigenic debris flows, deep-sea channels and past ice-stream behaviour of the East Greenland continental margin, *Quaternary Science Reviews*, *25*(7–8), 784-810, doi: 10.1016/j.quascirev.2005.06.004.

Winkelmann, D., W. Jokat, L. Jensen, and H.-W. Schenke (2010), Submarine end moraines on the continental shelf off NE Greenland - Implications for Lateglacial dynamics, *Quaternary Science Reviews*, *29*, 1069-1077, doi: 10.1016/j.quascirev.2010.02.002.

Wollenburg, I. (2012), Documentation of sediment core PS13/140-4, edited by P. R. f. M. Sediments, Alfred Wegener Institut.

Woodworth-Lynas, C. M. T., A. Simms, and C. M. Rendell (1985), Iceberg grounding and scouring on the Labrador Continental Shelf, *Cold Regions Science and Technology*, *10*(2), 163-186, doi: 10.1016/0165-232X(85)90028-X.

Zwally, H. J., M. B. Giovinetto, M. A. Beckley, and J. L. Saba (2012), Antarctic and Greenland Drainage Systems, edited by G. C. S. Laboratory, Greenbelt, USA.

Appendix

A Supplementary material, Deep water paleo-iceberg scouring on top of Hovgaard Ridge–Arctic Ocean

Supplementary material (2014GL059248):
Sub-bottom profiler data correlation from the Hovgaard Ridge crest to the proximity of drilling site ODP 908.

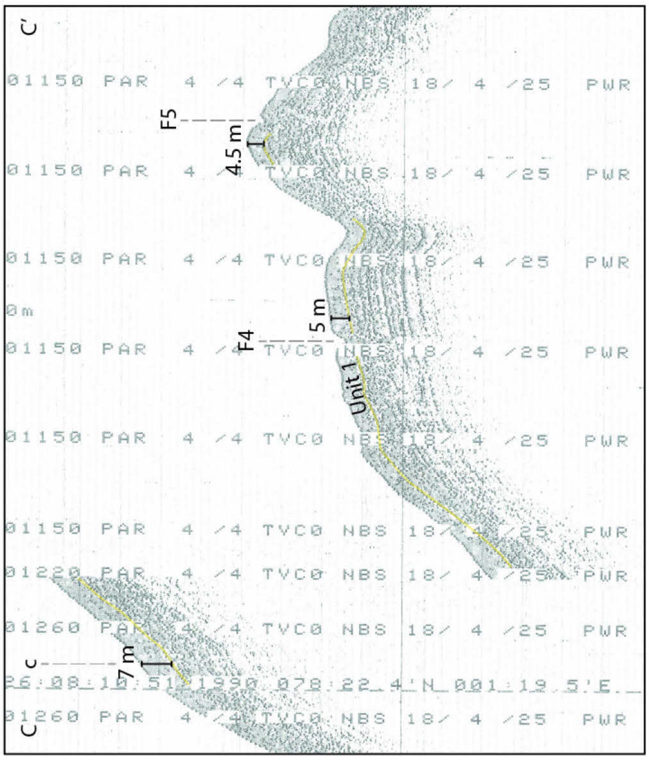

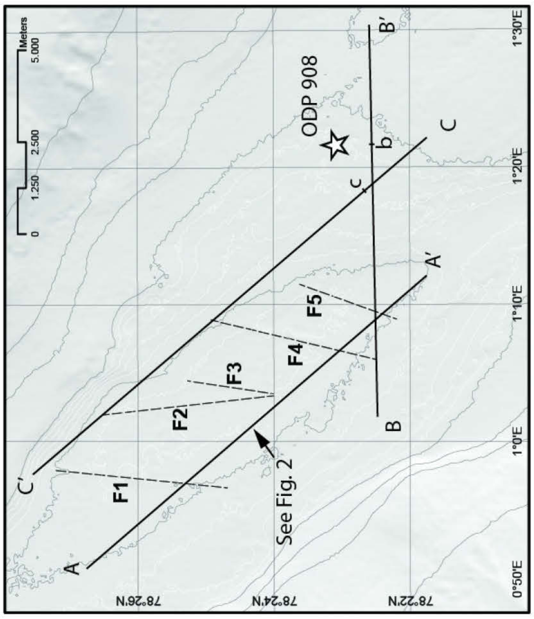

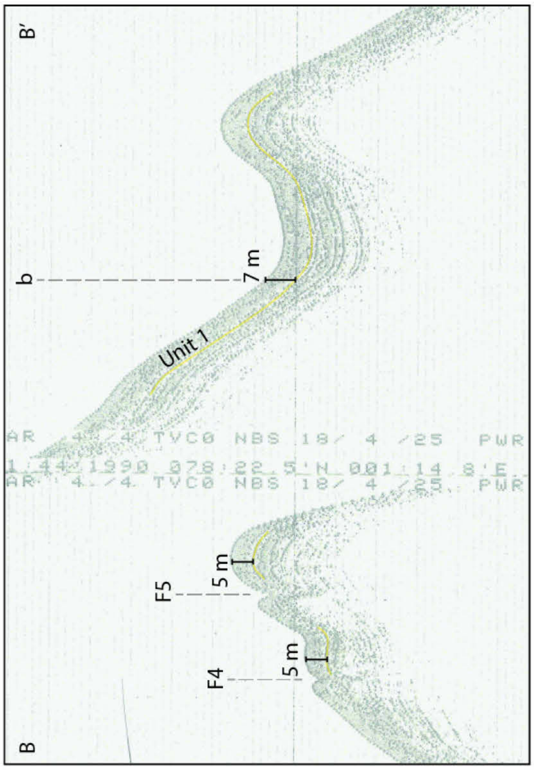

B Supporting Information, A new bathymetry of the Northeast Greenland continental shelf: Constraints on glacial and other processes

B.1

The NEG_DBM grid and the accompanying source identifier (SID) grid are available for download from: http://dx.doi.org/10.1594/PANGAEA.849313

When using the data please cite the reference paper (doi: 10.1002/2015GC005931)

B.2

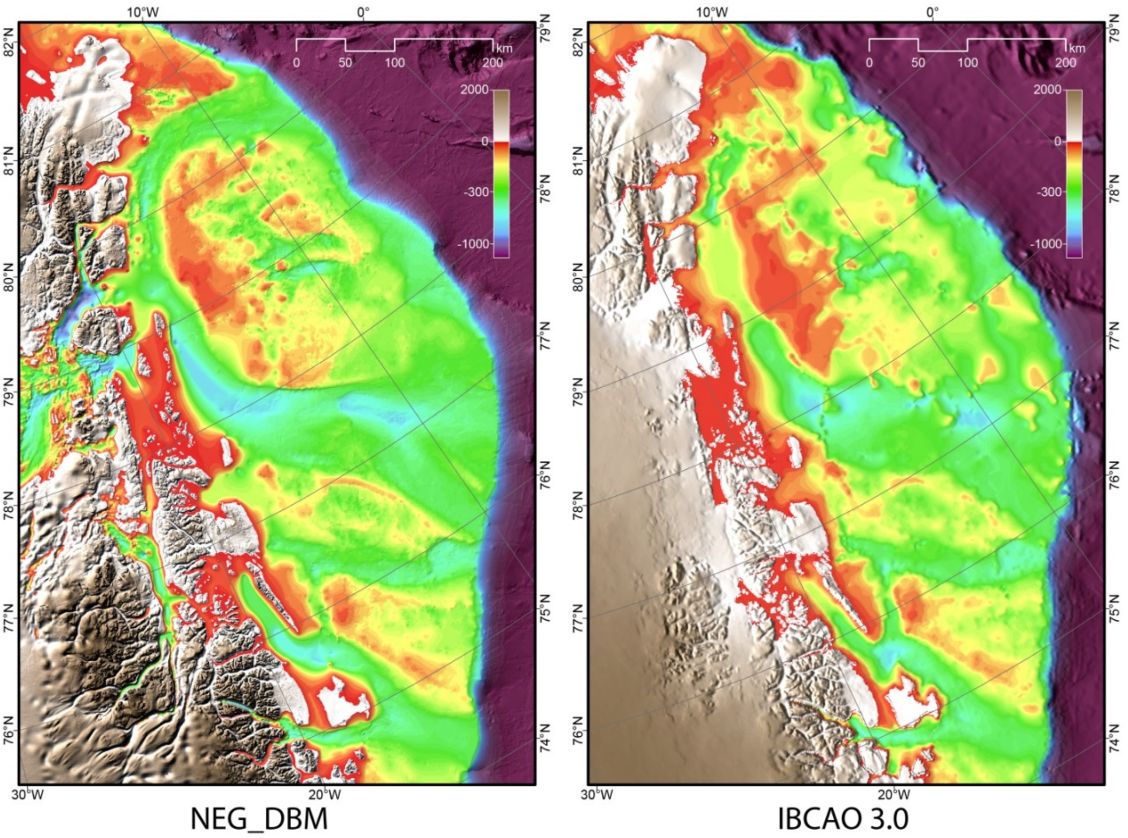

Figure B.0.1: Comparison of the NEG_DBM to the IBCAO V3.0 bathymetry; Note the large differences on the shelf and along the shelf edge especially north of 76°N.

B.3

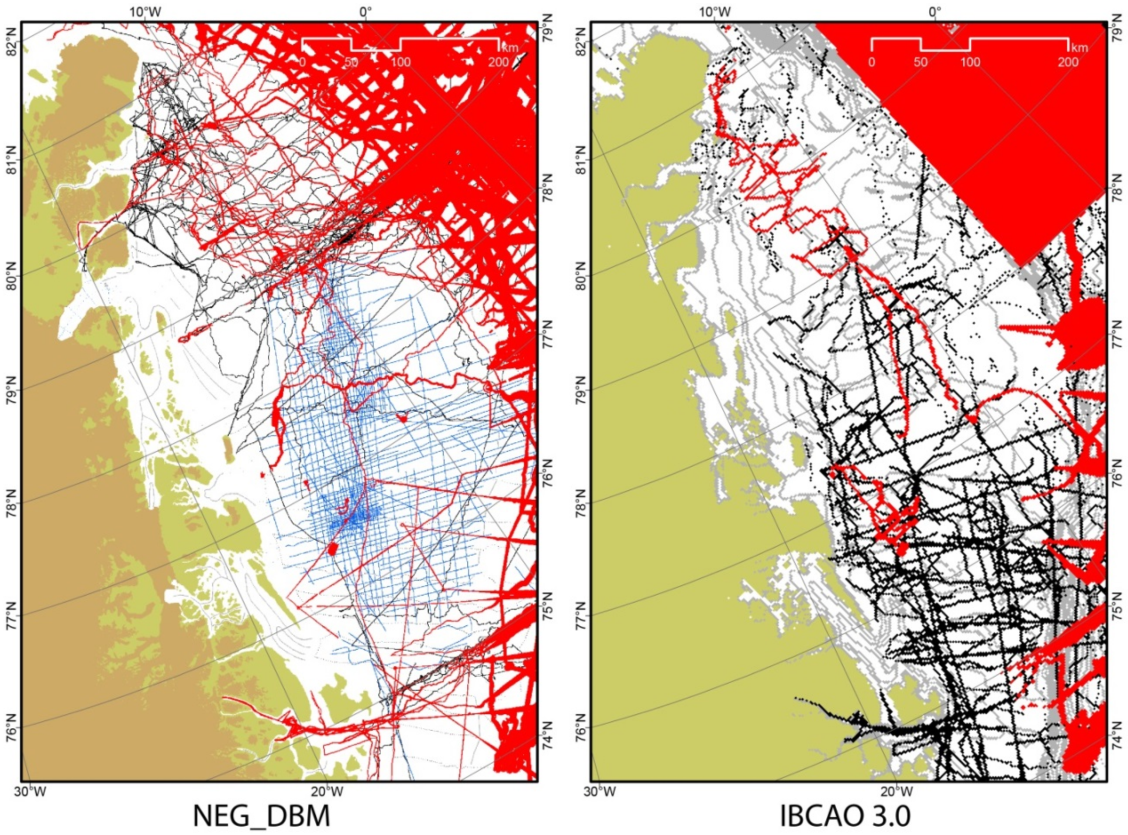

Figure B.0.2: Comparison of the NEG_DBM (500 m grid cell size) to the IBCAO V3.0 (2000 m grid cell size) source identifier grids (SID); Please note that due to the four times larger grid cell size, data coverage for IBCAO V3.0 appears up to 16 times larger; red = multibeam; black = singlebeam; grey = contours and inferred contours; blue = seismic first reflector; light green = topography; brown = under-ice topography

B.4

SID number	Data
21	FS Polarstern multibeam data
22	RV Oden multibeam data
23	RRV JC Ross multibeam data
31	FS Polarstern singlebeam data
32	Norske Polar Institut singlebeam data
33	Woods Hole Oceanographic Institut singlebeam data
34	U.S. Naval Research Laboratory singlebeam data
41	TGS-NOPEC first reflector picked from seismic data
42	Ice shelf seismic data
43	CTD maximum depths
44	Autosub-II data (digitized from publication)
51	Bedrock topography
52	Icefree topography
61	Inferred data for DBM steering

Danksagung

Ich danke Wilfried Jokat für die Ermöglichung meiner Promotion, der Begutachtung der Dissertationsschrift, sowie für die Betreuung meiner Promotion, inklusive der für ihn anstrengenden Gespräche mit einem Ingenieur.

Wolgang Bach danke ich für die Begutachtung dieser Doktorarbeit und den damit verbundenen Zeit- und Arbeitsaufwand.

Boris Dorschel danke ich für die Betreuung meiner Promotion und seines lockeren Tänzelns.

Hans Werner Schenke danke ich dafür, dass er es mir ursprünglich ermöglicht hat am AWI, sowie in der Meeresbodenvermessungs Gemeinde, Fuss zu fassen.

Zudem danke ich natürlich meinen Kollegen und Freunden die ich in meiner Zeit am AWI kennen lernen durfte, die mir die erforderliche Ablenkung oder gegebenenfalls auch Unterstützung während meiner Promotion und abseits davon ermöglicht haben.

Meinen Eltern, sowie meinen Brüdern danke ich für deren Grundvertrauen in alles was ich mache und für die Freiheit und Unterstützung dies auch zu tun.

Curriculum Vitae

Personal details:

Jan Erik Arndt
Alfred Wegenr Institute, Helmholtz Centre for Polar and Marine Research
Van-Ronzelen-Str. 2, 27568 Bremerhaven, Germany
Date of Birth: 18.2.1984, Nationality: German
Phone: +49 471 4831 1369, E-mail: Jan.Erik.Arndt@awi.de

Education:

09/2010	Diploma (comparable to Master) thesis
2003-2010	Study of geodesy at the Technical University of Darmstadt
1990 – 2003	School, graduated German "Abitur" (general qualification for university entrance)

Working Experience:

04/2013 – today	Research associate at Department of Geophysics, Alfred Wegener Institute, Helmholtz Centre for Polar and Marine Research and PhD candidate at University of Bremen; *Reconstructing the glacial history of the northeast Greenland continental shelf and adjacent waters using hydro-acoustic data, continuing Scientific Editor of the 'International Bathymetric Chart of the Southern Ocean (IBCSO)' project*
09/2011 – 03/2013	Research associate at Department of Geophysics, Alfred Wegener Institute, Helmholtz Centre for Polar and Marine Research; *Scientific Editor of the 'International Bathymetric Chart of the Southern Ocean (IBCSO)' project*
03/2011 – 08/2011	Sabbatical (travelling abroad)
09/2010 – 02/2011	Research associate at the Geodetic Institute, Technical University Darmstadt; *GIS analysis and map production for research projects and developing of a desktop GIS workshop*
11/2009 – 09/2010	Student assistant at the Geodetic Institute, Technical University Darmstadt; *independent GIS analysis and map production for research projects and teaching*
09/2008 – 07/2009	Student assistant at the Institute for physical Geodesy, Technical University Darmstadt; *independent programming in Java and Generic Mapping Tools (GMT)*

Publications:

ISI-Publications:

Arndt, J. E., Jokat, W., Boris Dorschel, B., Myklebust, R., Dowdeswell, J.A. and Evans, J. (2015) A new bathymetry of the Northeast Greenland continental shelf: constraints on glacial and other processes, *Geochemistry, Geophysics, Geosystems,* doi: 10.1002/2015GC005931

Weatherall, P., Marks, K. M., Jakobsson, M., Schmitt, T., Tani, S., **Arndt, J. E.,** Rovere, M., Chayes, D., Ferrini, V. and Wigley, R. (2015) A New Digital Bathymetric Model of the World's Oceans, *Earth and Space Science*, doi:10.1002/2015EA000107

Arndt, J. E., Niessen, F., Jokat, W. and Dorschel, B. (2014) Deep water paleo-iceberg scouring on top of Hovgaard Ridge–Arctic Ocean, *Geophysical Research Letters*, doi:10.1002/2014GL060267

Dorschel, B., Gutt, J., Piepenburg, D., Schröder, M. and **Arndt, J. E.** (2014) The influence of the geomorphological and sedimentological settings on the distribution of epibenthic assemblages on a flat topped hill on the over-deepened shelf of the western Weddell Sea (Southern Ocean), *Biogeosciences*, doi:10.5194/bg-11-3797-2014

Dickens, W. A., Graham, A. G. C., Smith, J. A., Dowdeswell, J. A., Larter, R. D., Hillenbrand, C. D., Trathan, P. N., **Arndt, J. E.** and Kuhn, G. (2014) A new bathymetric compilation for the South Orkney Islands region, Antarctic Peninsula (49°–39°W to 64°–59°S): Insights into the glacial development of the continental shelf, *Geochemistry, Geophysics, Geosystems*, doi:10.1002/2014gc005323

Gruetzner, J., Uenzelmann-Neben, G., Franke, D. and **Arndt, J. E.** (2014) Slowdown of Circumpolar Deepwater flow during the Late Neogene: Evidence from a mudwave field at the Argentine continental slope, *Geophysical Research Letters*, doi:10.1002/2014GL059581

Arndt, J. E., Schenke, H. W., Jakobsson, M., Nitsche, F. O., Buys, G., Goleby, B., Rebesco, M., Bohoyo, F., Hong, J., Black, J., Greku, R., Udintsev, G., Barrios, F., Reynoso-Peralta, W., Taisei, M. and Wigley, R. (2013) The International Bathymetric Chart of the Southern Ocean (IBCSO) Version 1.0 – A new bathymetric compilation covering circum-Antarctic waters, *Geophysical Research Letters*, doi:10.1002/grl.50413

ISI-Publications (submitted):

Arndt, J. E., Jokat, W., Boris Dorschel, B, Ice sheet limits and retreat dynamics on the Northeast Greenland continental shelf during the last full-glacial period, *Quaternary Science Reviews*

ISI-Publications (to be submitted):

Schaffer, J., Timmermann, R., **Arndt, J.E.**, Kristensen, S.S., Mayer, C., Morlighem, M. and Steinhage D., A global high-resolution data set of ice sheet topography and ocean bathymetry

Bohoyo, F., Larter, R.D., Galindo-Zaldívar, J., Leat, P.T., Maldonado, A., Tate, A.J., Flexas M.; Gowland, E.J.M., **Arndt, J.E.**, Dorschel, B., Kim, Y.D., Hong J.K., Livermore, R. A., Nitsche, F. , López-Martínez, J., Maestro, A.,Bermudez, O., and BATDRAKE team, BATDRAKE: The high-resolution bathymetry compilation of the Drake Passage (Antarctica), *Antarctic Science*

Peer-reviewed book contributions:

Arndt, J. E. and Forwick, M. (accepted) Deep-water iceberg ploughmarks on Hovgaard Ridge, Fram Strait, *Atlas of Submarine Glacial Landforms*, not published yet

Arndt, J. E. and Evans, J. (accepted) Glacial lineations and recessional moraines on the continental shelf of Northeast Greenland, *Atlas of Submarine Glacial Landforms*, not published yet

Conference contributions:

Talk - **Arndt, J. E**. , Jokat, W. and Dorschel, B., *Past and recent ice related impacts on the seafloor offshore Northeast Greenland*, 3P Arctic, Stavanger, 29 September 2015 - 2 October 2015

Poster - **Arndt, J.E.**, Bohoyo, F. And Dorschel, B., *IBCSO – Discovering Antarctica's present-day bathymetry*, XII ISAES, Goa, 13 July 2015 - 17 July 2015

Poster - Bohoyo, F., Larter, R. D., Galindo-Zaldívar, J., Leat, P., Maldonado, A., Tate, A. J., Flexas, M., Gowland, E., **Arndt, J. E**., Dorschel, B., Kim, Y., Hong, J. K., López-Martínez, J., Maestro, A., Bermudez, O. and Nitsche, F. O., *BATDRAKE V1.0: Multibeam bathymetry compilation of the Drake Passage (Antarctica-South America)*, XII ISAES, Goa, 13 July 2015 - 17 July 2015

Poster - **Arndt, J. E.**, Jokat, W. and Dorschel, B. *New insights on the glacial history of North-East Greenland from swath bathymetric data*, ICAM, Trondheim, 2 June 2015 - 5 June 2015

Poster - **Arndt, J. E.**, Jokat, W. and Dorschel, B. *Extensive ice stream activity on the North-East Greenland Continental Shelf*, European Geosciences Union General Assembly 2015, 12 April 2015 - 17 April 2015

Poster - Schaffer, J., Timmermann, R., Kanzow, T., **Arndt, J. E.**, Mayer, C. and Schauer, U., *Pathways of warm water to the Northeast Greenland outlet glaciers*, European Geosciences Union General Assembly 2015, Wien, Austria, 13 April 2015 - 17 April 2015

Talk - **Arndt, J. E.** et al., *New insights into the past glaciation of the northeast Greenland continental shelf*, AGU Fall Meeting, San Francisco, 15 December 2014 - 19 December 2014

Poster - Jensen, L., Dorschel, B., **Arndt, J. E.** and Jokat, W., *Southwest Indian Ocean Bathymetric Compilation (swIOBC)*, AGU 2014 Fall Meeting, San Francisco, California, 15 December 2014 - 19 December 2014

Poster - Wigley, R., Hassan, N., Chowdurry, M., Ranaweera, R., Le Sy, X., Runghen, H. and **Arndt, J. E**., *Nippon Foundation / GEBCO Indian Ocean Bathymetric Compilation Project*, AGU Fall Meeting, San Francisco, 15 December 2014 - 19 December 2014

Talk - Schaffer, J., Timmermann, R., **Arndt, J. E.**, Steinhage, D.and Kanzow, T., *RTopo-2: A global dataset of ice sheet topography, cavity geometry and ocean bathymetry to study ice-ocean interaction in Northeast Greenland*, REKLIM conference "Our Climate - Our Future", Berlin, Germany, 6 October 2014 - 9 October 2014

Co-Convenor – Session: *Mapping Antarctica and the Southern Ocean: ADMAP, BEDMAP, IBCSO and other activities*, SCAR Open Science Conference, Auckland, NZ, 25 August 2014 - 28 August 2014

Poster - **Arndt, J. E.** et al., *The International Bathymetric Chart of the Southern Ocean (IBCSO)*, SCAR Open Science Conference, Auckland, NZ, 25 August 2014 - 28 August 2014

Talk - **Arndt, J. E.** et al., IBCSO V1.0 – *New Bathymetry for the SCAR Community*, SACR 2014 Open Science Conference, Auckland, NZ, 25 August 2014 - 28 August 2014

Invited talk - Gruetzner, J., Uenzelmann-Neben, G., Franke, D. and **Arndt, J. E.**, *Cenozoic history of South Atlantic deep water circulation*, Colloquium of the DFG Priority Program SPP1375:South Atlantic Margin Processes and Links with onshore Evolution (SAMPLE), Bremerhaven, 3 June 2014 - 6 June 2014

Poster - Dickens, W. A., Graham, A. G. C., Smith, J. A., Dowdeswell, J. A., Larter, R. D., Hillenbrand, C. D., Trathan, P. N., **Arndt, J. E.** and Kuhn, G., *A new bathymetric compilation for the South Orkney Islands, Antarctic Peninsula (49°-39°W to 64°- 59°S): insights into the glacial development of the continental shelf*, European Geosciences Union General Assembly 2014, Vienna, 27 April 2014 - 2 May 2014

Talk - **Arndt, J. E.** et al., *IBCSO v1.0 - A new view on Antarctic bathymetry, GEBCO Science Day*, Venice, 8 October 2013 - 8 October 2013

Talk - **Arndt, J. E.** et al., *The International Bathymetric Chart of the Southern Ocean (IBCSO) – New 'classic' and lenticular Maps of Antarctica for Science and Outreach*, 26th International Cartographic Conference, Dresden, 26 August 2013 - 30 August 2013

Talk - **Arndt, J. E.** et al., *The International Bathymetric Chart of the Southern Ocean Version 1.0 – A new bathymetric compilation covering circum-Antarctic waters*, 25. Internationale Polartagung, Geomatikum, Hamburg, Germany, 17 March 2013 - 22 March 2013

Poster - **Arndt, J. E.** et al., *IBCSO v1 – The first release of the International Bathymetric Chart of the Southern Ocean*, AGU Fall Meeting 2012, San Francisco, 3 December 2012 - 7 December 2012

Poster - **Arndt, J. E.** et al., *The International Bathymetric Chart of the Southern Ocean – A new Map of Antarctica*, AGU Fall Meeting 2012, San Francisco, 3 December 2012 - 7 December 2012

Talk - **Arndt, J. E.** et al., *IBCSO v1 – A preview on Version 1 of the International Bathymetric Chart of the Southern Ocean*, XXXII SCAR Open Science Conference, Portland, Oregon, USA, 16 July 2012 - 19 July 2012

Poster - **Arndt, J. E.** et al., *The International Bathymetric Chart of the Southern Ocean IBCSO - Can we delete the last "White Spots" in Antarctica?*, AGU Fall Meeting, San Francisco, 5 December 2011 - 9 December 2011

Workshops and meetings:

04/2012 Work and Data Exchange Meeting for IBCSO V1.0 in Bremerhaven, Germany; *Meeting organization and chairing*

10/2013 Joint meeting of the Sub-Committee on Regional Undersea Mapping (SCRUM) and Technical Sub-Committee on Ocean Mapping (TSCOM) of GEBCO in Venice, Italy; *IBCSO status report*

05/2014 Second Indian Ocean Bathymetric Compilation (IOBC) Project Training Workshop in Kuala Lumpur, Malaysia; *invited to transfer knowledge from the IBCSO project to the IOBC*

12/2014 Joint meeting of the Sub-Committee on Regional Undersea Mapping (SCRUM) and Technical Sub-Committee on Ocean Mapping (TSCOM) of GEBCO in Mountain View, USA; *IBCSO status report*

02/2015 Work meeting of the BATDRAKE project: High Resolution bathymetry data in the Drake Passage (Antarctica) in Madrid, Spain; *invited to introduce the IBCSO gridding technique to BATDRAKE*

Expeditions:

- ANT-XXIX/8 (PS81), FS Polarstern, Cape Town – Cape Town, 9 November – 16 December 2013, group head of bathymetric data acquisition

- ARK-XXVIII/2 (PS85), FS Polarstern, Bremerhaven - Tromsø, 6 June – 3 July 2014, group head of bathymetric and subbottom profiler data acquisition

Student supervision:

Co-supervising of Geomatics master student Dhira M. Ahdiwijna from HafenCity University Hamburg (2014)